Boillot, G., Winterer, E. L., et al., 1988
*Proceedings of the Ocean Drilling Program, Scientific Results*, Vol. 103

# 22. CRETACEOUS RADIOLARIANS OF THE NORTH ATLANTIC OCEAN: ODP LEG 103 (SITES 638, 640, AND 641) AND DSDP LEGS 93 (SITE 603) AND 47B (SITE 398)[1]

J. Thurow, Institut und Museum für Geologie und Paläontologie, Universität Tübingen, Tübingen, Federal Republic of Germany

**ABSTRACT**

Radiolarians form a remarkable part of the fossil plankton for Cretaceous sediments of the North Atlantic. Selected sites with long-term sedimentary successions of deep facies were studied (ODP Leg 103 and DSDP Site 398 off northwest Spain and DSDP Site 603 off the east coast of the United States). Preservation of the radiolarian faunas is generally poor, and the faunal abundance and diversity reflect the diagenetic history of the host sediment rather than the original faunal productivity. Several exceptions include abundant and some well-preserved radiolarian faunas from lower Campanian, Cenomanian/Turonian boundary, upper Albian, lower Albian, and Barremian sediments. These increases in radiolarian abundance and preservation coincide with well-established Cretaceous oceanic events in the North Atlantic. Typical faunal associations of these sections are described, and faunal associations from the Cenomanian/Turonian Boundary Event are documented for the first time in the North Atlantic. The relationship of the radiolarian blooms with coeval oceanic events in the North Atlantic is also discussed.

## INTRODUCTION

Leg 103 of the Ocean Drilling Program (ODP) drilled a total of 15 holes on the Galicia Bank, along the northwest edge of the Iberian continental margin (Fig. 1). Four of the five sites drilled were devoted to the recovery of a continuous sedimentary record to document the timing of rifting for this part of the North Atlantic.

Sites 638, 639, and 641 form a transect through a tilted block and were drilled to obtain pre-, syn-, and post-rift sediments. The succession comprises an almost complete stratigraphic record from the Tithonian to lower Tertiary, according to foraminifer and nannofossil flora data. Except for the Upper Jurassic and lowermost Cretaceous, the depositional environment has characteristic deep-sea parameters (Moullade et al., this volume). The Cretaceous lithologic units are a time-controlled facies succession that is similar to the Atlantic formations established by Jansa et al. (1979). These formations are characterized by

Predominantly variegated claystones in the Upper Cretaceous (Plantagenet Formation)

A prominent biosiliceous black shale horizon at the Cenomanian/Turonian boundary (Herbin et al., 1986)

Cyclic sedimentation of black shales and grayish-greenish claystones in the upper Barremian to Albian (Hatteras Formation)

Light-colored nannofossil limestones with intercalations of dark calcareous mudstones.

Leg 103 drilled a thick pile of Valanginian/Hauterivian terrigenous sediments intercalated in the Blake-Bahama Formation, an arrangement similar to those reported from other North Atlantic sites (von Rad and Sarti, 1986). Stratigraphic gaps or condensed sections are recorded for the Cenomanian, Albian, and Barremian stages. In addition, the biostratigraphic resolution of the terrigenous sequence is not accurate. Remarkable radiolarian enrichments have been recorded in Lower Cretaceous sediments, whereas the Upper Cretaceous brown claystones are barren with respect to siliceous microfossils.

Site 398 (Fig. 1) of Deep Sea Drilling Program (DSDP) Leg 47B was drilled at the southern end of the Galicia margin, south of Vigo Seamount. Nearly 1000 m of Cretaceous (upper Hauterivian to Maestrichtian) sediment was recovered. Again, the sedimentary sequences are quite similar to the Atlantic formations of Jansa et al. (1979), and, as in the case of DSDP Sites 638 and 639, there is also a terrigenous influence in the upper Hauterivian/lower Barremian. Stratigraphic gaps occur between Campanian and Turonian and between upper Aptian/lower Albian sediments ("Site 398" chapter; Shipboard Scientific Party, 1979). Remarkable amounts of radiolarians were recovered in the Lower Cretaceous and sediments near the Cenomanian/Turonian boundary. The Upper Cretaceous brown claystones have not been studied in detail, but they are barren with respect to siliceous microfossils (Shipboard Scientific Party, 1979).

Site 603 of DSDP Leg 93 (Fig. 2) was drilled at the lower continental rise east of Cape Hatteras, North Carolina. Approximately 500 m of Cretaceous sediments was recovered, again with sedimentary successions similar to the Cretaceous Atlantic formations of Jansa et al. (1979). Like at Sites 638 and 639, a thick pile of terrigenous sediments is intercalated into the Hauterivian/Barremian sediments (Sarti and von Rad, 1987).

The biostratigraphic resolution is not as good as at Site 603. The "Site 603" chapter (Shipboard Scientific Party, 1987) documents a complete Upper Cretaceous stratigraphic record that could not be confirmed (Moullade et al., this volume). Parts of the Cenomanian are missing or are strongly condensed. The entire Lower Cretaceous may be represented, but the biostratigraphic control is not yet convincing.

Abundant radiolarians have been recovered in the lower Campanian and Turonian. The Lower Cretaceous lithologies, which compare well with those of the sites described in the preceding, have not been studied in detail, but thin-section studies and shipboard data (see the biostratigraphic summary in the "Site 603" chapter; Shipboard Scientific Party, 1987) reveal radiolarian faunas of Albian and Hauterivian/Barremian age.

Upper Cretaceous radiolarian-rich intervals in the North Atlantic are not well documented. Sanfilippo and Riedel (1976,

[1] Boillot, G., Winterer, E. L., et al., 1988. *Proc. ODP, Sci. Results*, 103: College Station, TX (Ocean Drilling Program).

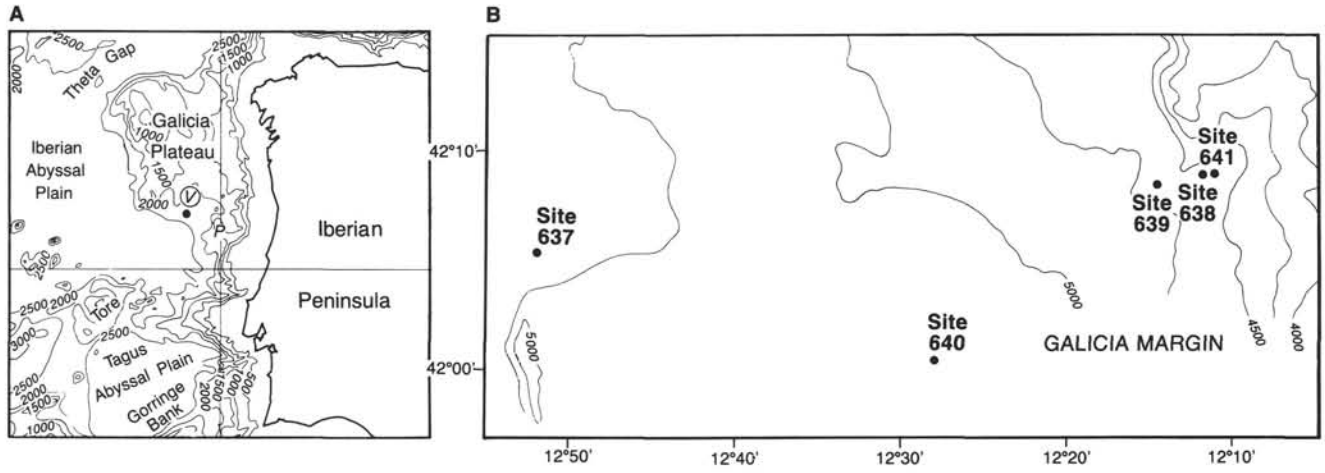


Figure 1. Location map of ODP Leg 103 and DSDP Leg 47B sites at the Galicia Bank/Vigo Seamount (V) region. Bathymetry in meters.

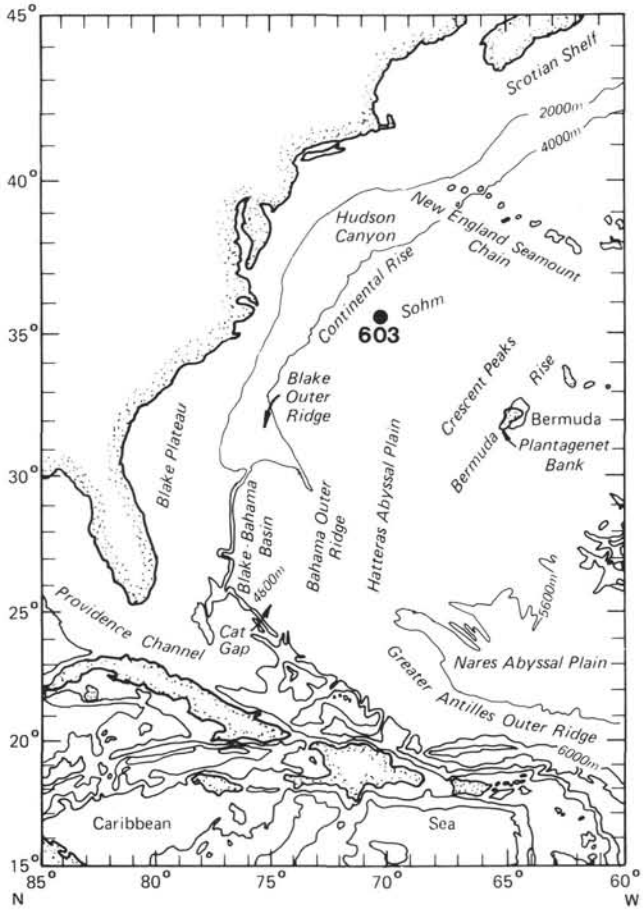


Figure 2. Location map of DSDP Site 603.

1985), Foreman (1977), Wolfart (1982), and Empson-Morin (1984) compiled Upper Cretaceous radiolarian occurrences from the North Atlantic based on DSDP data. However, the biostratigraphic control provided by calcareous planktonics (foraminifers and nannofossils) is generally poor. Well-preserved radiolarian faunas are rarely recorded, and they are usually of Campanian age, such as those off northwest Africa (Petrushevskaya and Kozlova, 1972; Foreman, 1978b) and in the Caribbean region (Pessagno, 1969; Foreman, 1973a; Sanfilippo and Riedel, 1976). Upper Cretaceous radiolarian occurrences in circum-North Atlantic onshore sections are commonly recorded, although abundance and preservation are poor, with the exception of the Caribbean occurrences. Most of these faunas are ascribed to the Campanian (Sanfilippo and Riedel, 1985).

Radiolarian associations from the Cenomanian/Turonian Boundary Event (CTBE) have never been documented from the North Atlantic, although strata deposited during this event are widely recorded at other locations (Müller et al., 1983, 1984; Herbin et al., 1986). Siliceous plankton faunas deposited during this event have been recorded from African coastal basins as well as from the alpine fold belts surrounding the western Mediterranean (Thurow et al. 1982; Kuhnt et al., 1986; Thurow and Kuhnt, 1986).

Radiolarian associations in the North Atlantic are better documented from Lower Cretaceous than from Upper Cretaceous DSDP sites (compilations in Foreman, 1977; Wolfart, 1982; Sanfilippo and Riedel, 1985) or from land sections in Europe and North Africa (e.g., Baumgartner, 1984). As Foreman (1977) pointed out, the radiolarian occurrences are not continuous in Lower Cretaceous sediments, and three major age distributions of radiolarians are usually distinguishable: a Late Jurassic to early Neocomian group (not considered in this chapter), a Hauterivian/Barremian group (widely represented in the samples from Sites 638 and 640), and an Albian/Cenomanian group (represented in samples from Sites 398 and 641).

## METHODS

Standard preparation methods used included the drying of samples, treatment with diluted HCl, sieving with a 63-$\mu$m sieve, and treatment with a mixture of $H_2O_2$ and chalk (to avoid oxidization of pyrite-replaced specimens). Many samples required final preparation with a detergent (REWOQUAT), followed by washing and squeezing of the sample through a flexible 63-$\mu$m nylon sieve formed like a sack. This procedure removed a large amount of the remaining secondarily silicified clay but may have also destroyed some of the more fragile skeletons. Nevertheless, despite the extensive number of preparation steps, many of the samples yielded radiolarian faunas too poorly preserved for biostratigraphic analyses. One explanation may be the presence of silica in the host sediment. Another problem is raised by the filling of pyrite-replaced skeletons, mainly with coarse calcite (Thurow, this volume), because processing of these samples is difficult and large parts of the fauna are destroyed. In general, faunal diversity within the pyritized radiolarian faunas is less than in those faunas with silica skeletons. Finally, in thin section, many samples exhibited grain sorting of radiolarians, indicating resedimentation or perhaps slight reworking of the fauna. Faunas that exhibit such phenomena are rarely considered in this paper.

Some samples from Cores 398D-110 through 398D-120 yielded rich faunas, but the preservation in many of the samples is so poor as to preclude consideration of these faunas in this study.

The preservation of radiolarians in each sample is defined as follows:

G = good—specimens show little or no surface dissolution and/or overgrowth
M-G = moderate-good (g-m = good-moderate)—specimens show some dissolution and/or overgrowth but not all species can be identified
M-P = moderate-poor (p-m = poor-moderate)—specimens show intermediate degrees of surface dissolution and/or overgrowth; although impaired, some identification of species is still possible
P = poor—specimens show a high degree of dissolution and/or overgrowth, with specific identification rare

The abundance of radiolarians calculated for 10 $cm^3$ in each sample is defined as follows:

Rare/few = present, but <100 specimens
Common = more than 100 specimens
Abundant = more than 500 specimens

Abundance was calculated without considering the preservation. In general, less than 10% of a fauna can be determined on a specific level. Furthermore, most of the determinable species have no stratigraphic value.

Selected samples with moderately to well-preserved radiolarians were studied under the scanning electron microscope (SEM), and the common faunal associations are documented in Plates 1–10. Studies under transmitted light were not possible because of skeletal pyrite replacement or the common occurrence of coarse zeolite steinkerns.

Species present in each sample from sites with sufficient radiolarians for Upper Cretaceous stratigraphic interpretation are tabulated in Tables 1 and 2. Tabulation of the species in each Lower Cretaceous sample would require study of the whole faunal association of each sample with the SEM, which was not possible in the time available and cannot be currently justified because of the poor preservation. (All Cretaceous samples that yielded comparable rich radiolarian associations are listed with their preservation mineralogy by Thurow, this volume.) However, such a study with a much broader sampling base, involving more sites, may be suitable for future research. Occurrence and abundance of Lower Cretaceous radiolarians from selected samples with well-preserved faunas are tabulated in Table 3. Occurrence is summarized in the text in general terms.

Age assignments of cores from Sites 398 and 603 and Leg 103, based on synthesis of calcareous nannoplankton and foraminifer assemblage data, are presented in Figure 3.

## Zonation

Previous studies of Cretaceous radiolarians have produced many preliminary zonations (Fig. 4), but well-documented Cretaceous sections containing known calcareous planktonics for biostratigraphic control are generally lacking. This may be one reason why there is no widely accepted zonation. Recently, Sanfilippo and Riedel (1985) and Schaaf (1985) presented updated modifications of previous zonations (Fig. 4). Although Schaaf's (1985) composite zonation is comparably fine, especially in the middle Cretaceous, occurrence data from both zonations were used because of the large amount of radiolarian-rich middle Cretaceous samples examined in this study. For reasons yet unknown, some index radiolarians were not observed in the material studied and others have different ranges; thus, the combined zonation of Sanfilippo and Riedel (1985) and Schaaf (1985) was modified in some parts.

Absolute age assignment for the different zones was difficult. No recent compilations with references to co-occurring planktonic organisms exist, and the various radiolarian studies use different time scales. In this report, Schaaf's (1985) age assignment is adapted, but it is worth noting that he fixed the Jurassic/Cretaceous boundary at 130 m.y., in contrast to the 144 m.y. date in the widely accepted DNAG time scale (Kent and Gradstein, 1985). The difference at the boundary between the Lower and Upper Cretaceous is only 2.5 m.y. (95 vs. 97.5 m.y., respectively).

However, in comparing the absolute age assignments given by Sanfilippo and Riedel (1985) and Schaaf (1985), there is a strong discrepancy in the age of several radiolarian zones. For example, the former authors place their *Staurosphaera septemporata* (*Cecrops septemporatus*) Zone in the lower to middle Valanginian, whereas the latter author gives a latest Valanginian/early Hauterivian age to his *C. septemporatus* Zone. Both zones are defined by the first occurrence (FO) of *C. septemporatus*.

The following is a summary of the zonation used in this report (Fig. 4):

The top of each zone is also defined by the base of the overlying zone (except in the Upper Cretaceous, where several gaps in the radiolarian record were observed), which coincides with the FO of each named species.

*Amphipyndax pseudoconolus* Zone

**Definition.** FO of *Amphipyndax pseudoconolus* (Pessagno, 1963).

**Age.** Santonian (Campanian, according to Sanfilippo and Riedel, 1985). No radiolarian record from the upper Turonian to the base of the Campanian.

*Crucella cachensis* Zone

**Definition.** FO of *Crucella cachensis* Pessagno, 1976.

**Age.** Latest Cenomanian/earliest Turonian, depending on the microfossil/macrofossil group used for calibration.

No radiolarian record in the lower and middle Cenomanian.

*Rhopalosyringium majuroensis* Zone

**Definition.** FO of *Rhopalosyringium majuroensis* Schaaf, 1981.

**Age.** Latest Albian.

**Remarks.** *R. majuroensis* was first found at Site 398 in upper Albian samples (according to foraminifer data; Müller et al., 1983, 1984). Schaaf (1985) described this species as having an FO in the middle Cenomanian, but he also figured specimens from Sample 398-63-6, 73–75 cm, which is of latest Albian age (Müller et al., 1983, 1984).

*Thanarla veneta* Zone

**Definition.** FO of *Thanarla veneta* (Squinabol, 1903).

**Age.** Late Albian.

*Pseudodictyomitra pseudomacrocephala* Zone

**Definition.** FO of *Pseudodictyomitra pseudomacrocephala* (Squinabol, 1903).

**Age.** Middle late Albian.

*Mita gracilis* Zone

**Definition.** FO of *Mita gracilis* (Squinabol, 1903).

**Age.** Base of late Albian.

*Holocryptocanium barbui* Zone

**Definition.** FO of *Holocryptocanium barbui* Dumitrica, 1970.

**Age.** Latest early Albian.

*Theoconus coronatus* Zone

**Definition.** FO of *Theoconus coronatus* Squinabol, 1904 (*Spongocapsula zamoraensis* Pessagno, 1976).

**Age.** Middle early Albian.

**Remarks.** *S. zamoraensis* Pessagno (1976) is regarded as a junior synonym of *T. coronatus* Squinabol (1904) in this chapter (see Appendix).

**Table 1. Occurrence and abundance of Upper Cretaceous radiolarians at Holes 603B and 641A.**

| Samples (interval in cm) | 25, CC | 26-1, 90–93 | 26-2, 90–93 | 26-3, 90–93 | 26, CC | 33-1, 48–52 | 33-1, 90–93 | 33-2, 90–93 | 33-3, 90–93 | 33, CC | 34-3, 90[a] | 35-1, 90–93[b] | 4X-1, 48–52 | 6X, CC (21–24) |
|---|---|---|---|---|---|---|---|---|---|---|---|---|---|---|
| *Acaeniotyle umbilicata* (Rüst) | | | | | | | | | · | | | | | |
| *Alievium gallowayi* (White) | ○ | • | • | • | · | sp. | | | | | | | | |
| *Alievium superbum* (Squinabol) | | | | | | | • | ○ | • | | | | | sp. |
| *Archaeospongoprunum* sp. div. | | | | | | | ○ | ○ | ● | | | | | |
| *Cavaspongia antelopensis* Pessagno | | | | | | | | ○ | · | | | | | |
| *Cavaspongia californiaensis* Pessagno | | | | | | | • | • | • | | | | | |
| "*Cenosphaera*" sp. | | | | | | | ○ | ○ | ○ | | | | | |
| *Conocaryomma universa* (Pessagno) | | | · | | | | · | • | • | | aff | | | |
| *Conocaryomma* cf. *C. universa* (Pessagno) | | | ○ | ○ | · | | | | | | | | | |
| *Crucella cachensis* Pessagno | | | | | | sp. | ● | ● | ● | | | | | |
| *Crucella espartoensis* Pessagno | ○ | • | • | • | | | | | | | | | | |
| *Crucella*(?) sp. A | ○ | • | • | • | ○ | | | | | | | | | |
| *Crucella* sp. B | ○ | • | • | ○ | ○ | | | | | | | | | |
| *Dumitricaia maxwellensis* Pessagno | | | | | | | ○ | • | • | | | | | |
| *Halesium quadratum* Pessagno | | | | | | | | | • | | | | | |
| *Halesium sexangulum* Pessagno | | | | | | | | | ○ | | | | | |
| *Orbiculiforma* sp. | | | | | | | ○ | • | ○ | | · | | | |
| *Patellula* sp. | ● | ● | · | ● | | · | ● | · | ● | | • | | | |
| *Patellula verteroensis* (Pessagno) | | ○ | | ○ | | | | | | | | | | |
| *Patulibracchium californensis* Pessagno | ? | | ○ | • | | | | sp. | sp. | | | | | |
| *Patulibracchium* cf. *davisi* Pessagno | | | sp. | | | | | · | ○ | | | | | |
| *Patulibracchium petroleumensis* Pessagno | | | | · | | | | | | | | | | |
| *Pseudoaulophacus floresensis* Pessagno | ○ | • | • | • | ○ | | | | | | | | | |
| *Pseudoaulophacus lenticulatus* (White) | | • | ○ | • | · | | | | | | | | | |
| *Pseudoaulophacus pargueraensis* Pessagno | · | ○ | ○ | ○ | · | | | | | | | | | |
| *Pseudoaulophacus putahensis* Pessagno | | | | | | | • | • | • | | | | | |
| *Pyramispongia glascockensis* Pessagno | | | | | | | • | ● | ● | | ○ | | | |
| *Amphipyndax pseudoconulus* (Pessagno) | | | | · | | | | | | | | | | |
| *Amphipyndax stocki* (Campell and Clark) | · | ○ | | · | | | | | | | | | | |
| *Archaeodictyomitra* cf. *A. lamellicostata* (Foreman) | · | ○ | ○ | ○ | | | | | ○ | | | | | |
| *Archaeodictyomitra* aff. *A. simplex* (Squinabol) | | | | | | | • | • | • | | | | | |
| *Clathropyrgus titthium* Riedel and Sanfilippo | · | | ○ | | | | | | | | | | | |
| *Cryptamphorella conara* (Foreman) | | | | ○ | | | | | ○ | | ? | | | |
| *Cryptamphorella macropora* Dumitrica | | ○ | | | | | | | | | | | | |
| *Dictyomitra formosa* Squinabol | ● | ● | • | ● | ● | sp. | | | | | | | | |
| *Dictyomitra* cf. *D. formosa* Foreman | · | | | | | ○ | | | · | | | | | |
| *Dictyomitra koslovae* s.l. | • | ● | • | ● | • | | | | | | | | | |
| *Eastonerius* sp. | | | · | | | | | | | | | | | |
| *Eucyrtidium*(?) sp. div. | • | ● | ● | ● | · | | | | | | | | | |
| *Heliocryptocapsa* sp. A | | ? | · | | | | | | | | | | | |
| *Hemicryptocapsa polyhedra* Dumitrica | | | | | | | | ○ | • | | | | | |
| *Neosciadiocapsa diabloensis* Pessagno | | | · | · | | | | | | | | | | |
| *Pseudodictyomitra nakesekoi* Taketani | | | | | | | ○ | ○ | ○ | | | | | |
| *Pseudodictyomitra pseudomacrocephala* (Squinabol) | | | | | | | • | • | • | | | | | |
| *Rhopalosyringium* sp. A | | | ○ | | | | | | | | | | | |
| *Sethocapsa* cf. *S. simplex* | | | | | | | | | | | | | · | |
| *Stichomitra* sp. | ○ | ○ | • | • | | | | | | | | | | |
| *Stichomitra communis* (Squinabol) | | | | | | | ○ | | • | | | | · | |
| *Thanarla*(?) sp. aff. *T. veneta* (Squinabol) | • | ○ | ○ | • | · | | | | | | | | | |
| *Theocampe tina* (Foreman) | | · | · | · | | | | | | | | | | |
| *Novixitus* sp. A | | | | · | | | | | | | | | | |
| *Novixitus* sp. B | | | | · | | | | | | | | | | |
| *Novixitus*(?) sp. div. | • | • | ○ | • | ○ | | | | | | | | | |
| *Xitus* sp. A | | | | | | | | | · | | | | | |
| *Xitus*(?) sp. div. | • | • | ○ | • | ○ | | | | | | | | | |
| *Afens liriodes* Riedel and Sanfilippo | • | • | ○ | ○ | ? | ○ | | | | | | | | |
| Abundance: · 1, ○—5, •—20, ● > 20 | a/m | a/m | a/m | a/p | c/p | f/p | c/p | c/m | c/m | f/p | r/p | a/p | | |

No age-diagnostic forms

No age-diagnostic forms

[a] Opaline preservation.
[b] Preserved in pyrite/quartz.

**Table 2. Occurrence and abundance of radiolarians around the CTBE interval in Hole 398D.**

| Samples (interval in cm) | 56-1, 112–116 | 56-2, 2–6 | 56-2, 10–12 | 56-2, 23–27 | 56-2, 32–36 | 56-2, 56–58 | 56-2, 73–77 | 56-2, 82–86 | 56-2, 98–102 | 56-2, 120–122 | 56-2, 139–143 | 56-3, 16–18 | 56-3, 43–47 | 56-3, 57–61 | 56-3, 145–149 |
|---|---|---|---|---|---|---|---|---|---|---|---|---|---|---|---|
| *Acanthocircus* sp. div. | ○ | • | | • | ○ | | ○ | | ○ | | ○ | | | | • |
| *Acaeniotyle umbilicata* (Rüst) | • | | | | | | | | | | | | ○ | ○ | • |
| *Acaeniotyle diaphorogona* Foreman | | | | | • | | ○ | ○ | | | | | ○ | | |
| *Acaeniotyle* sp. | | | | | | | | | | | | | ○ | | |
| *Alievium superbum* (Squinabol) | ○ | • | ● | • | | ● | ● | • | ○ | • | • | | • | • | |
| *Archaeospongoprunum cortinaensis* Pessagno | | | • | | | | | | | • | | | | • | |
| *Archaeospongoprunum* cf. *vascoensis* Pessagno | | | | | | | | | | | | | ○ | | |
| *Archaeospongoprunum* sp. div. | | | • | | • | • | | | | • | ○ | | ○ | ○ | |
| *Cavaspongia* sp. | | | | | | ○ | ○ | | | | | | | | |
| *Conocaryomma californiaensis* (Pessagno) | | | • | | | | | cf | • | | | | | | |
| *Conocaryomma universa* (Pessagno) | | | • | ○ | | ○ | | | | | | | | | |
| *Conocaryomma* sp. | ○ | | | | | | | | | | | | | | |
| *Crucella cachensis* Pessagno | aff. | ○ | ● | ○ | • | • | ● | ○ | ○ | | | | | | |
| *Crucella messinae* Pessagno | | | | | | | • | • | | ○ | • | cf | • | • | • |
| *Crucella* sp. | • | | | • | | | • | ○ | | ○ | | | | | |
| *Dumitricaia maxwellensis* Pessagno | | | ○ | | ○ | | | | | | | | | | |
| *Halesium quadratum* Pessagno | | | (p) | • | | | | | | | | | | | |
| *Halesium sexangulum* Pessagno | | • | | | | | | | | | | | | | |
| *Hexapyramis cretacea* Squinabol | | | | | | | | | | | | cf | | | ○ |
| *Orbiculiforma* sp. div. (incl. *O.* cf. *O. railensis* Pessagno) | ○ | | • | • | • | ○ | | • | • | ● | ● | | ● | ● | ● |
| *Patellula* sp. div. | ○ | | • | • | | ● | ● | • | | ● | • | | ● | ● | ● |
| *Paronella* sp. | | | | | | | | | | | ○ | | | • | ○ |
| *Patulibracchium* cf. *davisi* Pessagno | | | | | | | • | | | | | | | | |
| *Patulibracchium* sp. | • | • | • | • | | • | ○ | | ○ | ○ | • | ○ | ○ | ○ | • |
| *Pseudoaulophacus putahensis* Pessagno | • | • | ● | • | • | ○ | • | • | ○ | | | | cf. | (f) | (f) |
| *Pseudoaulophacus* sp. div. | ○ | | | | | | | ○ | ○ | | | | | | |
| *Pyramispongia glascockensis* Pessagno | | | ○ | | | • | | • | | ○ | | | | ○ | ○ |
| *Amphipyndax mediocris* (Tan Sin Hok) | | | | | | | | | | | | | • | | |
| *Archaeodictyomitra simplex* Pessagno | | | | | | | | | | • | ○ | | • | • | ○ |
| *Archaeodictyomitra squinaboli* Pessagno | • | ○ | • | | ○ | ○ | ○ | | | | | | | | |
| *Archaeodictyomitra* sp. | | | | ○ | | | | ○ | ○ | ○ | | | | | |
| *Cryptamphorella* sp. | ○ | • | • | • | | | | ○ | | | | | | | |
| *Dictyomitra formosa* Squinabol | ○ | | • | cf. | | | | | | | | | | | |
| *Eucyrtidium*(?) sp. div. | | ○ | ○ | • | | | | | | | | | ○ | | • |
| *Eusyringium spinosum* (Squinabol) | | | | | | | | | | | | | | • | • |
| *Hemicryptocapsa polyhedra* Dumitrica | | | | | | | | • | | | | | | | |
| *Hemicryptocapsa praepolyhedra* Dumitrica | | ○ | • | • | | | | | | | | | | • | |
| *Holocryptocanium* sp. | | | ● | • | | | | | | | ○ | | • | • | • |
| *Pseudodictyomitra carpatica* (Lozyniak) | | | | | | | | | | | cf. | | ● | • | ● |
| *Pseudodictyomitra nakasekoi* Taketani | ○ | | ○ | | | ○ | | | | • | ○ | | ○ | • | |
| *Pseudodictyomitra pseudomacrocephala* (Squinabol) | ○ | ○ | • | ○ | | • | • | ○ | ○ | ○ | ○ | | ● | ● | ○ |
| *Pseudodictyomitra* sp. | ○ | | | | ○ | | | | | | | | | | |
| *Rhopalosyringium* sp. | | | | | | | | | | | | | • | ○ | ○ |
| *Sethocapsa* sp. | | | | | | | | | | • | | | | | |
| *Squinabollum fossilis* (Squinabol) | | | | | | | | | | | | | | | ○ |
| *Stichomitra communis* (Squinabol) | | • | | • | | ○ | • | | ○ | • | • | ○ | ● | • | • |
| *Thanarla elegantissima* (Cita) | | | | | | | | | | | | | • | • | ● |
| *Thanarla veneta* (Squinabol) | | | ○ | • | ○ | ○ | ○ | ○ | | | | | ○ | ○ | |
| *Theoconus coronatus* (Squinabol) | | | | | | | | | | | • | • | ● | ● | ● |
| *Novixitus weyli* Schmidt-Effing | | | | | | | | | | ○ | • | • | • | ● | ● |
| *Xitus spicularius* (Aliev) | | | | | | | | | | • | | • | ○ | ○ | • |
| *Xitus* sp. B | | • | | | ○ | | • | | | | | | | | |
| *Ultranapora* sp. | • | | | | | | | | | | | | | | |
| "Large Spumellarians with four spines" | | | | | | | | | | | • | • | ○ | | • |
| Abundance: • 1, ○—5, •—20, ● >20 | c/m-p | a/m-p | a/m-p | a/m-p | f/p | a/m-p | c/m-p | c/m-p | r/p | a/m-p | c/p | c/m-p | a/m-p | a/m | c/p |

*Acaeniotyle umbilicata* Zone

**Definition.** Last appearance of Pantanellium lanceola (Parona, 1890), according to Foreman (1985). Last appearance of *Triactoma hybum* Foreman, 1975 according to Schaaf (1985).

**Age.** Late Aptian in the North Atlantic.

**Remarks.** Because of the lack of well-preserved Aptian faunas in the North Atlantic, the base of this zone is tentative.

*Stichocapsa euganea* Zone

**Definition.** FO of *Stichocapsa euganea* Squinabol, 1903.

**Age.** Early Aptian.

*Crolanium pythiae* Zone

**Definition.** FO of *Crolanium pythiae* Schaaf, 1981.

**Age.** Barremian.

**Table 3. Occurrence and abundance of Lower Cretaceous radiolarians from samples with well-preserved faunas at Sites 398, 638, 640, and 641.**

*Acaeniotyle diaphorogona* Foreman
*Acaeniotyle* sp. cf. *A. diaphorogona* Foreman
*Acaeniotyle umbilicata* (Rüst)
*Acaeniotyle* sp. A
*Acanthocircus dicranacanthos* (Squinabol)
*Acanthocircus* sp. cf. *A. dicranacanthos* (Squinabol)
*Acanthocircus trizonalis* (Rüst)
*Acanthocircus* sp.
*Alievium antiquum* Pessagno
*Alievium helenae* Schaaf
*Alievium superbum* (Squinabol)—"Cenomanian" form
*Alievium* sp. A
*Alievium* sp. C
*Amphipyndax mediocris* (Tan Sin Hok)
*Amphipyndax*(?) sp.
*Angulobracchia*(?) *portmanni* Baumgartner
*Archaeodictyomitra lacrimula* (Foreman)
*Archaeodictyomitra* sp. cf. *A. lamellicostata* (Foreman)
*Archaeodictyomitra pseudoscalaris* (Tan Sin Hok)
*Archaeodictyomitra puga* Schaaf
*Archaeodictyomitra* sp. cf. *A. puga* Schaaf
*Archaeodictyomitra simplex* Pessagno
*Archaeodictyomitra squinaboli* Pessagno
*Archaeodictyomitra vulgaris* Pessagno
*Archaeodictyomitra* sp. cf. *A. vulgaris* Pessagno
*Archaeodictyomitra* sp. A
*Archaeodictyomitra*(?) sp. B
*Archaeospongoprunum cortinaensis* Pessagno
*Archaeospongoprunum* sp. cf. *A. tehamaensis* Pessagno
*Cecrops septemporatus* (Parona)
*Conocaryomma lipmanae* (Pessagno)
*Conocaryomma* sp. aff. *C. lipmanae* (Pessagno)
*Conocaryomma universa* (Pessagno)
*Conocaryomma* sp. A
*Conocaryomma* (?) sp.
*Conosphaera tuberosa* Tan Sin Hok
*Crolanium pythiae* Schaaf
*Crolanium* sp. cf. *C. triquetrum* Pessagno
*Crucella messinae* Pessagno
*Crucella*(?) sp. C
*Crucella*(?) sp. D
*Cryptamphorella conara* (Foreman)
*Cryptamphorella* sp. cf. *C. conara*
*Cryptamphorella dumitricai* Schaaf
*Cryptamphorella* sp. A
*Cryptamphorella* sp. B
*Cyclastrum infundibuliforme* Rüst
*Cyrtocapsa* sp. cf. *C. grutterinki* Tan Sin Hok
*Dibolachras tytthopora* Foreman
*Dumitricaia maxwellensis* Pessagno
*Eucyrtis* sp. A
*Eusyringium spinosum* Squinabol
*Eusyringium* sp. cf. *E. spinosum* Squinabol
*Eusyringium* (?) *formanae* Taketani
*Godia*(?) sp. A
*Godia*(?) sp. B
*Godia*(?) sp. C
*Godia*(?) sp. E
*Godia*(?) sp. F
*Godia*(?) sp. G
*Halesium quadratum* Pessagno
*Halesium sexangulum* Pessagno
*Hemicryptocapsa* sp. cf. *H. polyhedra* Dumitrica
*Hemicryptocapsa* (?) sp. A
*Hexapyramis pantanelli* Squinabol
*Hexastylurus magnificus* (Squinabol)
*Holocryptocanium barbui* Dumitrica
*Holocryptocanium* sp. A
*Holocryptocanium* sp. B
*Holocryptocanium* sp. C
*Homosparonaella* (?) sp. A
*Mita gracilis* (Squinabol)
*Mita* sp. A
*Mita* sp. B
*Mita* sp. C
*Mita*(?) sp. D
*Mita*(?) sp. E

**Table 3 (continued).**

*Novixitus mclaugalini* Pessagno
*Novixitus weyli* Schmidt-Effing
*Novixitus* sp. C
*Orbiculiforma railensis* Pessagno
*Pantanellium lanceola* (Parona)
*Paronaella* sp. cf. *P. bandyi* Pessagno
*Paronaella* sp. A
*Paronaella* sp. B
*Paronaella* sp. C
*Parvicingula boesii* (Parona)
*Parvicingula malleola* (Aliev)
*Parvicingula*(?) sp.
*Patellula*(?) sp. B
*Patulibracchium* sp. cf. *P. davisi* Pessagno
*Podobursa triacantha* (Riechli)
*Podobursa tricola* Foreman
*Podobursa* sp. A
*Pseudoaulophacus putahensis* Pessagno
*Pseudoaulophacus* sp. B
*Pseudoaulophacus*(?) sp. C
*Pseudoaulophacus*(?) sp. B
*Pseudocrucella* sp. A
*Pseudocrucella* (?) sp. B
*Pseudocrucella* (?) sp. C
*Pseudodictyomitra carpatica* (Lozyniak)
*Pseudodictyomitra leptoconica* (Foreman) group
*Pseudodictyomitra lilyae* (Tan Sin Hok)
*Pseudodictyomitra lodogaensis* Pessagno
*Pseudodictyomitra pentacolaensis* Pessagno
*Pseudodictyomitra pseudomacrocephala* (Squinabol)
*Pseudodictyomitra* sp. cf. *P. pseudomacrocephala* (Squinabol)
*Pseudodyctyiomitra* cf. *P. vestalensis* Pessagno
*Pyramispongia glascockensis* Pessagno
*Rhopalosyringium majuroensis* Schaaf
*Rhopalosyringium* sp. A
*Rhopalosyringium* sp. B
*Rhopalosyringium* sp. C
*Sethocapsa orca* Foreman
*Sethocapsa* sp. A cf. *S. simplex*
*Sethocapsa trachyostraca* Foreman
*Sethocapsa uterculus* (Perona)
*Sethocapsa* sp. cf. *S. uterculus* (Parona)
*Sethocapsa*(?) sp. B
*Siphocampium*(?) *davidi* Schaaf
*Squinabollum fossilis* (Squinabol)
*Staurocyclia martini* (Rüst)
*Stichocapsa euganea* Squinabol
*Stichomitra communis* Squinabol
*Stichomitra* sp. cf. *S. communis* Squinabol
*Stichomitra*(?) sp. A
*Stichomitra*(?) sp. B
*Thanarla conica* (Aliev)
*Thanarla* sp. C aff. *T. conica* (Aliev)
*Thanarla*(?) sp. B aff. *T. conica* (Aliev)
*Thanarla elegantissima* (Cita)
*Thanarla pulchra* (Squinabol)
*Thanarla veneta* (Squinabol)
*Thanarla* sp. A
*Theocapsomma ancus* Foreman
*Theoconus coronatus* Squinabol group
*Theoconus* sp. cf. *T. coronatus* Squinabol
*Theocorys renzae* Schaaf
*Triactoma echoides* Foreman
*Triactoma hybum* Foreman
*Tritabe* sp. cf. *T. rhododactylus* Baumgartner
*Tritrabs* sp.
*Ultranapora durhami* Pessagno
*Ultranapora praespinifera*
*Vitorfus campbelli* Pessagno
*Vitorfus* ssp.
*Williriedellum* sp. aff. *V. carpathicum* Dumitrica
*Williriedellum gilkeyi* Dumitrica
*Williriedellum peterschmittae* Schaaf
*Williriedellum* sp. aff. *V. peterschmittae* Schaaf
*Williriedellum* sp. A
*Xitus alievi* (Foreman)
*Xitus* sp. A. cf. *Xitus alievi* (Foreman)
*Xitus plenus* Pessagno

| Age | Hole 398D | | Hole 603B | | Hole 638B | | Hole 640A | | Hole 641C | |
|---|---|---|---|---|---|---|---|---|---|---|
| | Section | Depth (mbsf) | Section | Depth (mbsf) | Section | Depth (mbsf) | Section | Depth (mbsf) | Section | Depth (mbsf) |
| Campanian | | | 25, CC<br>26, CC | 1056.5<br>1065.5 | | | | | | |
| Santonian | | | | | | | | | | |
| Coniacian | | | | | | | | | | |
| Turonian late | | | 33-1 | 1119.0 | | | | | | |
| Turonian early | 56-1<br>56-2 | 945.5<br>948.0 | 33-1<br>33-3 | 1119.0<br>1127.2 | | | | | | |
| Cenomanian late | 56-2<br>56-3 | 948.0<br>949.5 | 33, CC<br>35-1 | 1127.2<br>1137.5 | | | | | | |
| Cenomanian early | | | | | | | | | | |
| Albian late | 58-1<br>80-4 | 964.5<br>1202.0 | | | | | | | | |
| Albian early | 81-1<br>104-1 | 1202.0<br>1412.0 | | | | | | | 1-1<br>6-3 | 151.3<br>207.4 |
| Aptian late | 104-1<br>119-3 | 1412.0<br>1558.0 | | | | | | | 6-3<br>8-4 | 207.4<br>227.6 |
| Aptian early | 119-4<br>127-7 | 1558.0<br>1639.0 | | | | | | | 8-5<br>12-7 | 227.6<br>266.5 |
| Barremian late | 128-1<br>129-3 | 1639.0<br>1653.0 | | | 20-3<br>23-3 | 183.6<br>212.7 | | | 13-1<br>16-2 | 266.5<br>298.5 |
| Barremian early | 129-4<br>133-5 | 1653.0<br>1696.0 | | | 23-3<br>23-3 | 212.7<br>212.8 | 3-4<br>3, CC | 174.0<br>174.3 | | |
| Hauterivian late | 134-1<br>138-2 | 1696.0<br>1740.0 | | | 23-3<br>26-6 | 212.8<br>247.7 | 6-1<br>6, CC | 194.1<br>203.3 | | |
| Hauterivian early | | | | | 27-1<br>29-4 | 247.7<br>276.7 | | | | |
| Valanginian late | | | | | 30-1<br>31-2 | 276.7<br>288.2 | | | | |

Figure 3. Age assignments of cores from Holes 398D, 603B, 638B, 640A, and 641C, based on synthesis of calcareous nannofossil and foraminifer assemblage data (after Moullade et al., this volume; Shipboard Scientific Party, 1979, 1987).

*Dibolachras tytthopora* Zone

**Definition.** FO of *Dibolachras tytthopora* Foreman, 1973b.
**Age.** Late Hauterivian.

*Cecrops septemporatus* Zone

**Definition.** FO of *Cecrops septemporatus* (Parona, 1890) (= *Sphaerostylus septemporatus* Parona, 1890).
**Age.** Latest Valanginian/earliest Hauterivian.

*Sethocapsa trachyostraca* Zone

**Definition.** FO of *Sethocapsa trachyostraca* Foreman, 1973b.
**Age.** Late Valanginian.

## SITE 603

### Hole 603B

Radiolarians were recovered, extracted, and studied from samples of Upper Cretaceous black shales and variegated claystones from Hole 603B of DSDP Leg 93. Samples with abundant radiolarians are predominantly concentrated in the variegated claystones. These claystones can be divided into an upper part from Core 603B-24 to Section 603B-29-2, consisting of claystones with greenish gray layers mostly dominating over reddish brown layers, and a lower part of approximately Core 603B-33, consisting of pelagic greenish grayish claystones lacking any reddish brown color.

The preservation did not allow a statistical evaluation of the fauna, but the recovered specimens were sufficiently well preserved to resolve the biostratigraphy and provide pertinent paleoceanographic data for these radiolarian-rich intervals.

A first drilled interval of radiolarian-rich sediments is represented in Samples 603B-25, CC (90–93 cm), 603B-26-1, 90–93 cm, 603B-26-2, 90–93 cm, 603B-26-3, 90–93 cm, and Section 603B-26, CC. Radiolarians are common to abundant and generally poorly preserved, with diagenetic transformation into clinoptilolite. All of the samples, however, contain a small amount (<1% per 10 $cm^3$) of moderately to well-preserved specimens. Not all of the species are described, but many, especially nassellarians, are recorded by other workers in coeval strata, and some reliable stratigraphic markers can be discriminated. The most abundant forms belong to the genera *Dictyomitra* (*Dictyomitra formosa* and *Dictyomitra koslovae*), *Alievium* (*Alievium gallowayi*), and *Pseudoaulophacus* (*Pseudoaulophacus floresensis*, *Pseudoaulophacus lenticulatus*, and *Pseudoaulophacus parguераensis*). Other important stratigraphic forms include *Afens liriodes*, *Amphipyndax* cf. *pseudoconolus*, *Archaeodictyomitra lamellicostata*, *Clathropyrgus titthium*, *Theocampe tina*, and *Patulibracchium californiaensis* (Fig. 5 and Pls. 1 and 2).

Upper Cretaceous sections with radiolarians continuous throughout are rarely recorded; thus, the stratigraphic ranges of

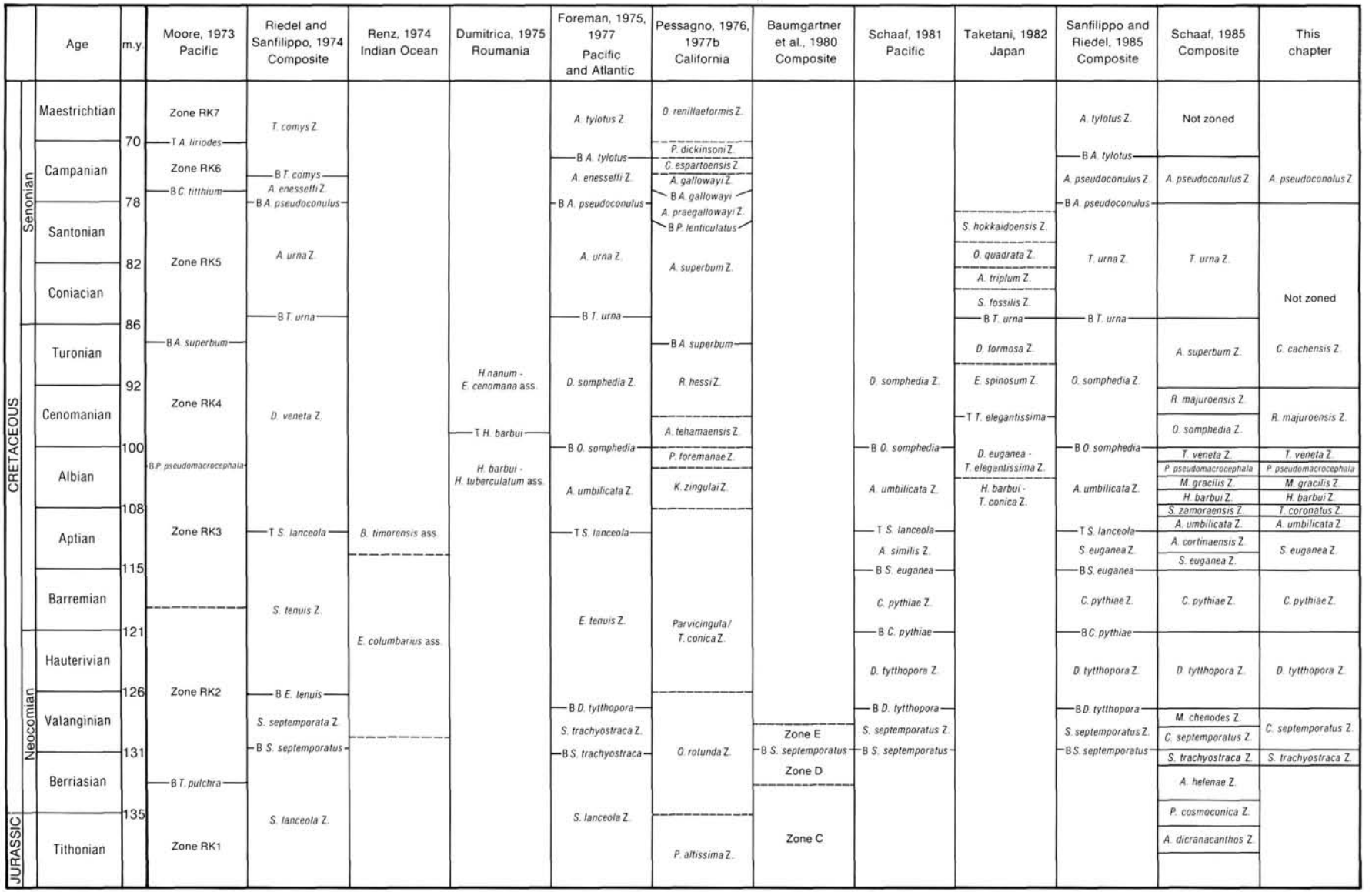


Figure 4. Compilation of radiolarian zonations (modified from Schaaf, 1985, and Sanfilippo and Riedel, 1985).

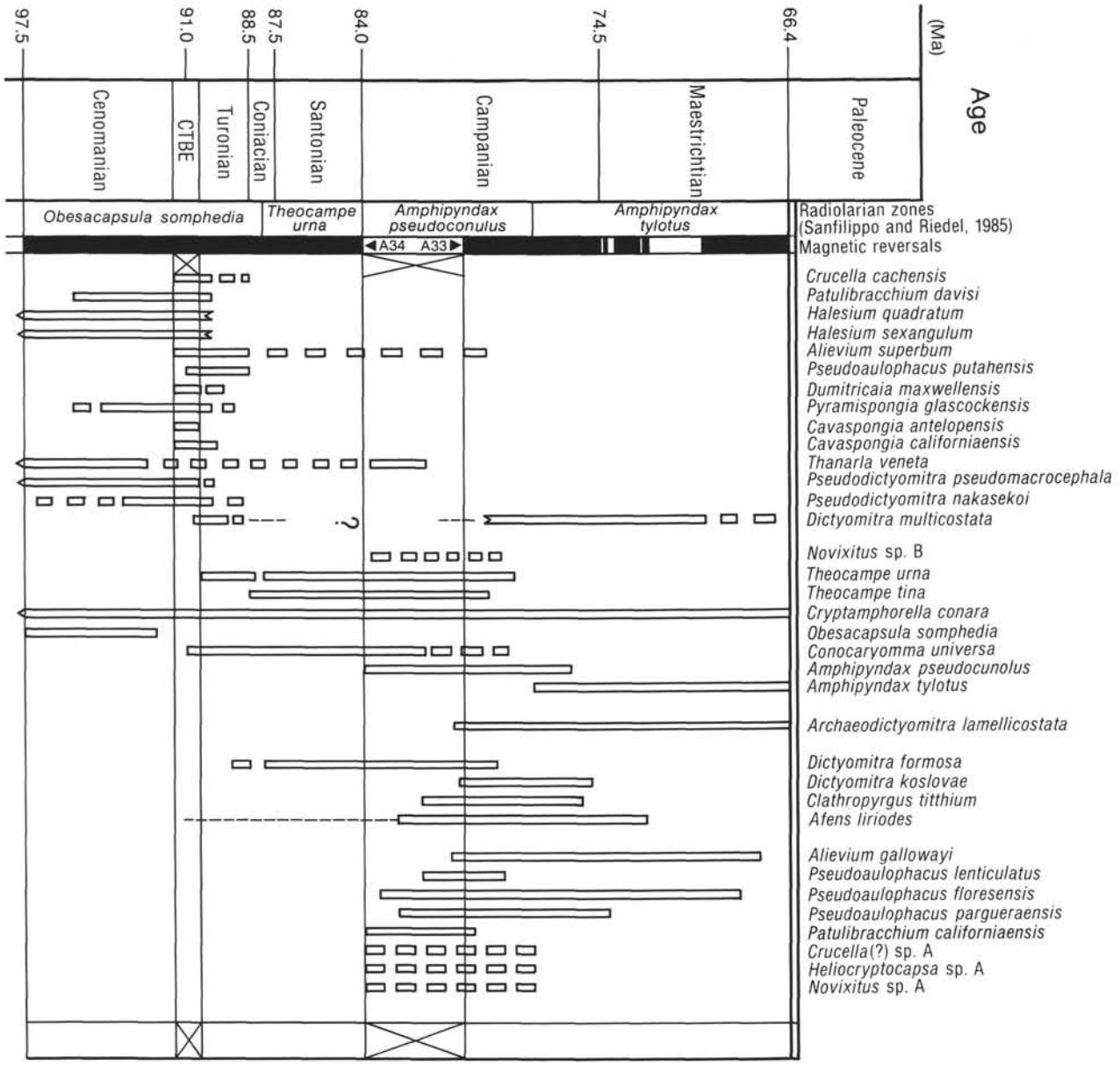


Figure 5. Composite range chart of Upper Cretaceous radiolarians. Most of the specimens have been identified in North Atlantic samples.

Upper Cretaceous species are not well established. But the co-occurrence of the forms listed above suggests, according to most authors (see also Moullade et al., this volume), a Campanian (probably early to middle Campanian) age for such a radiolarian association.

Sample 603B-33-1, 38–42 cm, from a quartz sandstone marks an important change in the sedimentation at Site 603. Shipboard scientists (Shipboard Scientific Party, 1987) fixed the boundary between their lithologic Units III (= Plantagenet Formation) and IV (= Hatteras Formation) at this level. The sample contains rare and poorly preserved (replaced by clinoptilolite) radiolarians. *A. liriodes*, *Alievium* sp., *Crucella* sp. (with a large lacuna in the central part), *Patellula* sp., and some poorly preserved *Dictyomitra* ssp. can be distinguished. The age of this sample is uncertain. *A. liriodes* would indicate a Campanian age, but Sanfilippo and Riedel (1985) recently reported *A. liriodes* from Turonian strata in northern Italy. *Crucella* sp. with a large lacuna in the central area is either *Crucella cachensis* (Turonian) or *Crucella espartoensis* (Santonian/Campanian). *Alievium* sp. is common in the Upper Cretaceous, and *Patellula* sp. is a long-ranging form.

Present knowledge of radiolarians would suggest a Turonian age for this sample, which would set the lithologic boundary between the Plantagenet Formation and the Hatteras Formation above the CTBE, which is rather unlikely. This sample most probably contains the youngest radiolarian fauna present in the underlying suite of radiolarian-rich sediments. The sample is most probably a mixture of the youngest Turonian clay and the overlying detrital layer of unknown age (older than Campanian).

A second interval of radiolarian-rich sedimentation occurs below 42 cm in Section 603B-33-1. The sequence consists of dark greenish gray and greenish black claystones with the ap-

pearance of the first true black shales. Samples 603B-33-1, 90–93 cm, 603B-33-2, 90–93 cm, and 603B-33-3, 90–93 cm, contain common to abundant, poor to moderately preserved, and clinoptilolite-replaced radiolarians (Table 1). The most characteristic form is *C. cachensis*. Additional species of stratigraphic importance include *Alievium superbum*, *Pseudoaulophacus putahensis*, *Cavaspongia antelopensis*, *Cavaspongia californiaensis*, *Pyramispongia glascockensis*, *Dumitricaia maxwellensis*, *Pseudodictyomitra nakasekoi*, and *P. pseudomacrocephala* (Pls. 1–3).

The radiolarian association in the second interval is the characteristic fauna of the CTBE (Thurow et al., 1982; Thurow and Kuhnt, 1986). This event is always characterized by a strong biosiliceous component. A calibration of mid-Cretaceous radiolarians with planktonic foraminifers (Thurow et al., 1982; Kuhnt et al., 1986) reveals that species such as *C. antelopensis*, *C. californiaensis*, or *C. cachensis* never occur together with the keeled planktonic foraminifer genera *Rotalipora*, which becomes extinct in the uppermost Cenomanian. Observed specimens of *C. cachensis* always display an elevated and prominent central area that characterizes species from the deeper part of the *C. cachensis* partial range Zone. The FO of this form is always coeval with the onset of the *Whiteinella aprica* Zone (planktonic foraminifer), which marks the chronologically less precisely fixed Cenomanian/Turonian boundary. On the other hand, none of the species known to have late Turonian FOs is present (e.g., *Thanarla urna*); therefore, an early Turonian age is suggested for this interval. This age assignment is in good accordance with the dinoflagellate data (Herbin et al., 1987). Dinoflagellate cysts in Sample 603B-33, CC (1 cm), suggest a late Cenomanian/early Turonian age immediately below the radiolarian-rich interval.

Cores 603B-35 and 603B-34 (black shales) and Section 603B-33, CC, (greenish claystone) contain rare, generally poorly—but sometimes moderately—preserved radiolarians. Most of the specimens are not determinable to either a specific or generic level. The two samples studied from the black shale interval (603B-35-1, 90–93 cm, and 603B-34-3, 90 cm) contain only a few age-diagnostic forms, which is also true for Section 603B-33, CC (transition from the black shales to the overlying greenish zeolitic claystones). In Sample 603-34-3, 90 cm, *Holocryptocanium* aff. *barbui*, *Conocaryomma* aff. *universa*, *P. glascockensis*, *P. putahensis*, and *Patellula* sp. can be distinguished. This association is not very common, but *P. glascockensis* is recorded from Cenomanian to middle Turonian sediments, whereas *P. putahensis* s.s. never occurs before the CTBE. A late Cenomanian/early Turonian age is likely for this interval.

## SITE 398

### Hole 398D

Based on Sigal's (1979) compilation, which provides an overview of abundance, preservation, and skeletal mineralogy of Lower to middle Cretaceous faunas found at Site 398, and listings in Basov et al. (1979) and Schaaf (1985), radiolarian-rich intervals of Barremian to Turonian age were sampled. The Upper Cretaceous brownish claystones at this site were not considered. According to the "Site 398" chapter (Shipboard Scientific Party, 1979), they are devoid of radiolarians.

To allow direct comparison with the radiolarian-rich intervals studied at other sites, the faunal description is presented in three parts that reflect the three radiolarian-rich intervals. The Upper Cretaceous interval from Samples 398D-56-1, 112–116 cm, to 398D-56-3, 145–149 cm, comprises the CTBE. The other two intervals, in the thick upper Lower Cretaceous (Albian) sequence from Cores 398D-58 to 398D-104, are the result of radiolarian-rich sedimentation or enhanced preservation and contain moderately to well-preserved faunas. The second interval is upper to uppermost Albian, from Samples 398D-62-1, 57–61 cm, to 398D-63-6, 90–94 cm. The third interval is the upper part of the middle Albian, from Samples 398-71-4, 36–40 cm, to 398D-75-2, 37–40 cm.

Below these intervals down to the bottom of the hole, concentrations of radiolarians are common, but the quality of preservation decreases downhole and the faunas are generally too poorly preserved for biostratigraphic analysis.

#### *Upper Cretaceous (CTBE): Samples 398D-56-1, 112–116 cm, to 398D-56-3, 145–149 cm*

Fifteen samples were studied from this interval, and the results are presented in Table 2. Radiolarians are common but, in general, poorly preserved. The poor preservation does not allow a statistical evaluation of the fauna, but enough specimens are sufficiently preserved for biostratigraphic analysis. The samples compare well in faunal composition, and differences reflect preservation rather than primary faunal composition.

Biostratigraphically important species include *A. superbum*, *P. putahensis*, *Cavaspongia* sp., *P. glascockensis*, *Archaeodictyomitra simplex*, *Archaeodictyomitra squinaboli*, *D. formosa*, *Novixitus weyli*, *Pseudodictyomitra carpatica*, *P. nakasekoi*, *Thanarla elegantissima*, *Thanarla veneta*, and *T. coronatus*. This association is characteristic of the fauna around the CTBE (Fig. 5).

The most important marker species for this time, *C. cachensis*, first occurs in Sample 398D-56-2, 98–102 cm. This form is used as the marker for the onset of the CTBE (Thurow et al., 1982), and its FO coincides with the latest Cenomanian extinction of the foraminifer genus *Rotalipora*, which is followed by the onset of the *Whiteinella archaeocretacea* Zone. This zone includes the chronologically less precise Cenomanian/Turonian boundary. Several species are not influenced by this event, including *D. maxwellensis*, *Halesium quadratum*, *Halesium sexangulum*, *P. glascockensis*, and *P. pseudomacrocephala*. But this event is also reflected in the disappearance of *P. carpatica*, *T. elegantissima*, and *T. coronatus* and the appearance of *A. superbum* s.s., *C. cachensis*, *Conocaryomma universa*, *A. squinaboli*, and *D. formosa*.

It is worth noting that the species that is always a common element in a typical CTBE radiolarian association, *D. maxwellensis*, is rare. The presence of *A. superbum* s.s.[2], which has its FO together with *C. cachensis* in other occurrences of the CTBE interval, is known prior to Sample 398D-56-3, 57–61 cm. *P. putahensis* s.s. is found together equally with the first *C. cachensis* in onshore CTBE outcrops. In Samples 398D-56-3, 43–47 cm, and 398D-56-3, 57–61 cm, both forms occur together with the planktonic foraminifer *Rotalipora cushmani* (which suggests a late Cenomanian age), some centimeters below the FO of *C. cachensis* (Table 2). Because planktonic foraminifers in this interval are found generally within detrital (resedimented?) layers in the claystones, their biostratigraphic value is impaired. The preceding samples may show a mixed fauna of autochthonous and allochthonous plankton. However, the samples are not older than late Cenomanian.

It is obvious from comparison of the radiolarian inventory of the Site 398 CTBE interval with well-documented onshore CTBE assemblages (Kuhnt et al., 1986; Thurow and Kuhnt, 1986; Thurow, 1987 [Tethyan and Atlantic realms]; Pessagno, 1976 [California]) that the diversity at Site 398 is lower. One

[2] *A. superbum* is first described from a sample of latest Albian age at Site 398 (Schaaf, 1985). However, reexamination of this interval (Core 398D-63) reveals that although the specimens described as *A. superbum* are, without a doubt, closely related to *A. superbum*, they do not show all of the characteristics of the type species. The FO of true specimens of *A. superbum* (*A. superbum* s.s.) is around the Cenomanian/Turonian boundary.

possible explanation for the lower diversity is that the missing species have fragile skeletons (e.g., *Neosciadiacapsidae*) that were destroyed during diagenesis.

### *Lower Cretaceous*

One hundred thirty samples were prepared from Lower Cretaceous strata at Site 398, including the dark grayish-greenish and black claystones low in $CaCO_3$ and the more calcareous layers at the base of the sequence. Only a few samples were really barren, with most of them revealing common to abundant radiolarians with varying preservation. Whereas poor preservation is the rule in the lower part of the sequence, moderately to well-preserved faunas occur in the upper part (except for Cores 398D-57 through 398D-61, which are barren with respect to radiolarians, representing the uppermost Albian and lower Cenomanian, according to calcareous plankton).

#### *Upper Albian: Samples 398D-62-1, 57–61 cm, to 398D-63-6, 90–94 cm*

The 10 samples from the interval from Samples 398D-62-1, 57–61 cm, through 398D-63-6, 90–94 cm, contain abundant and well-preserved radiolarians. SEM observation reveals that the surfaces of the specimens are slightly dissolved or broken by the crystallization of clinoptilolite inside the skeleton. However, the radiolarian faunas in this interval are abundant, diverse, and well preserved, a rare exception to the unfavorable habitat presented by the Atlantic Ocean for radiolarians at that time.

The faunas are dominated by species of the genera *Pseudodictyomitra* Pessagno 1977b (compare with Pl. 3, Figs. 11–17), *Novixitus* Pessagno 1977b, *Xitus* Pessagno 1977b, *Mita* Pessagno 1977b, *Thanarla* Pessagno 1977b, *Orbiculiforma* Pessagno 1973, emend. Pessagno 1976, and *Patellula* Petrushevskaya and Kozlova 1972, emend. Empson-Morin 1981. Common and well-known species are *M. gracilis*, *P. pseudomacrocephala*, *Xitus alievi*, *N. weyli*, *Stichomitra communis*, *Amphipyndax mediocris*, *T. elegantissima*, and *T. veneta*. Less common are *T. coronatus*, *H. barbui*, *Cryptamphorella conara*, *Eusyringium spinosum*, *Sethocapsa*(?) *simplex*, and *Squinabollum fossilis*.

These forms are recorded from Albian/Cenomanian strata. A comparison with the zonal scheme reveals that they can be ascribed to the *A. umbilicata* Zone of Schaaf (1985). Compared with the subzones defined by Schaaf (1985), the co-occurrence of *A. umbilicata*, *T. coronatus*, *H. barbui*, *M. gracilis*, *P. pseudomacrocephala*, and *T. veneta* is noteworthy. The FO of these marker species defines their nominate subzones (Schaaf, 1985) within the *A. umbilicata* Zone of Schaaf (1985) (Fig. 4). The occurrence of *T. veneta* indicates a latest Albian age. On the other hand, the common occurrence of *R. majuroensis* and the lack of *Obesacapsula somphedia* would suggest the upper part of the *O. somphedia* Zone/*R. majuroensis* Subzone of Schaaf (1985), which is of late Cenomanian age. However, the co-occurring planktonic foraminifers from this interval ascribe a latest Albian age.

The samples from Core 398D-64 to Sections 4 and 5 of Core 398D-71 contain few to abundant, rather poorly preserved radiolarians (see Thurow, this volume) that are highly similar to the following faunal association. These samples are not considered in this chapter.

A second radiolarian peak was found in the upper Albian, from Samples 398-71-4, 36–40 cm, to 398D-75-2, 37–40 cm. The overall composition of the fauna is similar to the association described for the preceding interval, but the poorer preservation decreases the biostratigraphic potential of the samples. Common faunal elements within each sample include the following: *A. metacryst*, *A. simplex*, *Cyrtocapsa perspicua*, *H. barbui*, *M. gracilis* (Pl. 3, Fig. 2; and the forms figured by Schaaf, 1985, p. 110–111, figs. 5a–5c, H), *N. weyli* (rare), *Pseudodictyomitra* group without *P. pseudomacrocephala*, *Rhopalosyringium* sp. (see Pl. 4, Fig. 17), *Sethocapsa* cf. *S. simplex* (Pl. 4, Fig. 23), *T. coronatus* (rare), *Napora* sp., *Xitus alievi* and *Xitus spicularius* (both rare), cryptothoracic nassellarians (as figured in Pl. 4, Figs. 24 and 26), *Acaeniotyle diaphorogona*, *A. umbilicata*, *Acaeniotyle* sp. (Pl. 6, Fig. 2), *Alievium antiquum*, *Alievium* sp. (Pl. 5, Fig. 12), *Archaeospongoprunum cortinaensis*, *Conocaryomma* sp., *Crucella messinae*, *Hexapyramis pantanellii*, *Paronaella* sp. (Pl. 6, Fig. 8), *Patellula* ssp., *Patulibracchium* sp. aff. *P. grapevinensis*, and *Pseudoaulophacus* ssp. (Pl. 5, Figs. 14 and 14A).

Nonsilicified samples within this interval have also fragments of *Hagiastrids*, *Neosciadiocapsids*, and *Acanthocircus* ssp. in common.

A careful check for the index species of the subzones within the *A. umbilicata* Zone of Schaaf (1985) found *A. umbilicata*, *T. coronatus* (rare), *H. barbui*, and *M. gracilis*. The co-occurrence of these forms characterizes the base of the upper Albian (*M. gracilis* Zone), which is in accordance with the age of calcareous planktonics within this interval (Sigal, 1979).

Below this interval, only a few samples revealed abundant and sufficiently preserved radiolarians (see Thurow, this volume).

The overall faunal composition of Samples 398-77-3, 37–41 cm, to 398D-102-1, 134–138 cm, is comparable to that described from the overlying interval. All samples contain some elements in common, although not all of the distinctive species are present in all samples. The more common (and unfortunately, not yet age diagnostic) species include *Godia*(?) ssp., *Patellula* ssp., *Orbiculiforma* ssp., numerous undescribed *Pseudoaulophacids*, numerous fragments of *Hagiastrids*, *H. pantanellii*, *A. diaphorogona*, *A. umbilicata*, *A. metacryst*, *Archaeospongoprunum* ssp., *Halesium* cf. *H. sexangulum* (Pl. 6, Fig. 4), *Patulibracchium* sp., *Pseudodictyomitra* ssp., *Sethocapsa* cf. *S. simplex*, *Napora* sp., *X. alievi*, *X. spicularius*, and unknown nassellarians gen. et sp. indet. 6 (Pl. 4, Fig. 24). The upper part of this interval has common *Conocaryomma* sp., *C. conara*, *H. barbui*, *M. gracilis*, *Sethocapsa* cf. *S. simplex*, and *S. communis*.

A check for the subzone marker species in this interval revealed that *C. conara* s.s. and *H. barbui* s.s. have their FOs in Sample 398-89-4, 66–70 cm. *M. gracilis* and *P. pseudomacrocephala* are lacking. The indicated *H. barbui* Zone is not older than late early Albian.

The *Parvicingula malleola* group, which Schaaf (1981, 1985) described from the lower Aptian, occurs downhole from Sample 398-97-4, 61–65 cm. All of the other species Schaaf (1981, 1985) described as characteristic of an Aptian association are lacking; therefore, a younger age is possible.

Downhole from Sample 398D-100-3, 148–150 cm, the faunal composition changes, and the occurrence of *S. euganea*, *Acanthocircus trizonalis*, *A. cortinaensis*, *Dicroa* sp. A Foreman, 1975, and *Eucyrtis* aff. *E. tenuis* indicates an Aptian age, which is roughly coincident with the calcareous plankton age (base of the Albian).

The faunal association in Samples 398D-100-5, 34–41 cm, 398D-101-5, 98–102 cm, and 398D-102-1, 134–138 cm, is almost identical to that of Sample 398D-100-3, 148–150 cm. In Sample 398D-100-5, 34–41 cm, *Triactoma* cf. *T. echoides*, and *Emiluvia*(?) sp. also occur. The absence of *A. cortinaensis* and the common occurrence of *S. euganea* might suggest a slightly older age. *X. alievi*, which has been recorded from strata not younger than middle Aptian, occurs in Sample 398D-101-5, 98–102 cm. The last sample with determinable specimens (Sample 398D-102-1, 134–138 cm) contains *Staurocyclia martini*, *S. euganea*, and *X. alievi*, which are characteristic of the *S. euganea* Zone (lower to middle Aptian). This age assignment based on the radiolarian fauna is in disagreement with that from the cal-

careous plankton, which suggest the base of the Albian. However, studied upper Lower Cretaceous sections are not numerous, and the ranges are not well-established. The quite similar faunal composition in Samples 398D-77-3, 37–41 cm, to 398D-102-1, 134–138 cm, is easily explained by the high sedimentation rate during the early to middle Albian at this site.

## SITE 641

### Hole 641A

Twenty samples from this hole were studied, but only two samples (103-641A-4X-1, 48–52 cm, and 103-641A-6X, CC [21–24 cm]) contain rare and poorly preserved radiolarians.

Two radiolarians were found in Sample 103-641A-4X-1, 48–52 cm: *S. fossilis* (Squinabol) (Pl. 4, Fig. 21) and a nassellarian that is generally named *S. communis* Squinabol (Pl. 4, Fig. 10). *S. fossilis* is recorded from the upper Albian to the top of the upper Turonian in Japan, and *S. communis* is common in mid-Cretaceous sediments of southern Europe, northwest Africa, and at Site 398. However, the stratigraphic ranges of both forms are not well established; therefore, the precise age of the sample remains uncertain. Furthermore, the rarity (two specimens) and preservation of the radiolarians in a sedimentary environment that is generally devoid of siliceous microfossils suggests that these specimens may be derived from a small lithoclast.

A zeolite-replaced, and therefore doubtful, *Alievium* sp. with a domed pillowlike shape was found in Sample 103-641A-6X, CC (21–24 cm), of the black shale. Such forms have their FO approximately at the base of the Turonian.

### Hole 641C

Eighty samples from this site were studied. Radiolarians are common throughout the sequence, sometimes abundant in the upper part, and less common in the lower part. They are replaced by quartz or opal-CT in most samples and are poor to moderately preserved. Certain fauna may show replacement of the skeleton by pyrite or pyrite overgrowths. Coarse zeolite casts are abundant, and from Core 103-641C-10R downhole, radiolarians are commonly replaced by pyrite.

Shipboard scientists ("Site 641" chapter; Boillot, Winterer, et al., 1987) divided the sedimentary sequence into several subunits, but only the deepest unit, lithologic Unit VI (Core 103-641C-11R to Section 103-641C-16R, CC), contains a distinct radiolarian fauna. This unit broadly corresponds to lithologic Subunit IIA at Site 638, and the radiolarian faunas compare well, except for the exclusive replacement by pyrite.

The radiolarians can be used to divide the upper part of the sequence into two biostratigraphic intervals. An upper interval from Samples 103-641C-1R-1, 36–38 cm, to 103-641C-3R-5, 8–12 cm, is characterized by greenish gray and black, homogeneous and laminated claystones and is rich in radiolarians, some of which are moderately preserved. Several of the radiolarians are of biostratigraphic importance, which allows age assignment for this interval. The faunas of this interval broadly correspond to those of Subunit IVb at Site 398 (Cores 398-79 to 398-102), which roughly represents the lower and middle Albian. Common surface dissolution of the silica-preserved radiolarian tests precludes a precise age determination and a statistical evaluation at the present.

Calcareous plankton are not common in the interval recovered at Site 641, but nannofossil data (Applegate and Bergen, this volume) suggest either a late early Albian or early late Albian age. There is no general difference in radiolarian abundance and preservation between the greenish gray and black claystones. Several samples contain a remarkable amount of siliceous sponge debris (Thurow, this volume).

The faunal composition of each sample within this interval is similar, and differences reflect variation in preservation rather than primary diversity fluctuations. Characteristic species for this interval are *A. diaphorogona*, *A. umbilicata*, *Acaeniotyle* sp. with four spines, *A. antiquum*, *Archaeospongoprunum tehamaensis, Archaeospongoprunum* ssp., *C. messinae*, *Crucella* sp., *Godia*(?) ssp., *H. pantanellii*, *Paronaella* ssp., fragments of *Hagiastrids*, *A. metacryst*, *A. simplex*, *E. spinosum* (see Pl. 4, Figs. 18 and 20), *M. gracilis*, *N. weyli*, *Pseudodictyomitra lodogaensis*, *Rhopalosyringium* aff. *R. obiraensis*, *Sethocapsa* cf. *S. simplex*, *S. communis*, *Napora* sp., and *X. spicularius*.

The faunal composition indicates an Albian age for the interval. This age is confirmed by the common occurrence of *M. gracilis,* which has its FO at the base of the *M. gracilis* Zone (base of upper Albian), whereas *P. pseudomacrocephala* has its FO in the next, younger zone, the *P. pseudomacrocephala* Zone. Furthermore, the faunas are dominated by large, long-ranging Spumellarids, *Patellula* ssp., and *Orbiculiforma* ssp. Both the genera *Patellula* and *Orbiculiforma* are represented in Hole 641C by different species that are undescribed but are known to characterize the Albian.

The second interval ranges from Samples 103-641C-3R-5, 8–12 cm, to 103-641C-9R-1, 75–78 cm, and represents the lower Albian to middle Aptian, based on planktonic foraminifers. Lithologies include greenish gray and black, homogeneous and laminated claystones in the upper part and greenish gray marlstones, microturbidites, and limestone conglomerate in the lower part. Radiolarians are common in the upper part of the interval and less common in the lower part. Again, a pronounced dissolution of the silica-preserved radiolarian tests obscures the taxa-characteristic pore frame structure, and zeolite casts inhibit studies in transmitted light. More SEM studies are required to precisely establish the radiolarian biostratigraphy of this interval. Age-diagnostic species are rare, but the common occurrence of *M. gracilis* and the lack of *P. pseudomacrocephala* indicate a middle Albian age. In Sample 103-641C-6R-2, 81–82 cm, *M. gracilis* is absent, but *H. barbui* is a common faunal element. This assemblage might be indicative of the *H. barbui* Zone, which suggests a late early Albian age. Below this sample down to Section 103-641C-9R, CC, no age-diagnostic species have been found, but the faunal compositions still suggest an Albian age.

Samples 103-641C-9R, CC (11–14 cm), and 103-641C-10R-5, 5–9 cm, contain a pyrite-replaced radiolarian association that is diverse but largely fragmented. *A. diaphorogona*, *A. umbilicata*, *Alievium helenae*, *Conocaryomma* sp. A, *Conosphaera tuberosa*, *Cyclastrum infundibuliforme*, *Godia*(?) ssp., *Hagiastrids* (*Angulobracchia*(?) *portmanni*), *P. lanceola*, *Paronaella* cf. *P. bandy*, *Orbiculiforma railensis*, *Patellula*(?) sp. A, *Pseudocrucella*(?) sp. B and other forms with a central depression, *T. hybum*, *A. metacryst*, *Archaeodictyomitra apiara* (rare), *Archaeodictyomitra lacrimula*, *Archaeodictyomitra vulgaris*, *Cryptamphorella* sp., *Cyrtocapsa grutterinki*, *D. tytthopora*, *Eucyrtis* sp., *Holocryptocanium* sp. B (pyrite replacement is never observed), *Podobursa triacantha*, *Siphocampium*(?) *davidi*, *Thanarla conica*, *Thanarla pulchra*, *Sethocapsa orca*, *Sethocapsa trachyostraca*, *Williriedellum gilkeyi*, and *Xitus spicularius*.

This association is similar to those of Sample 103-638B-21R-5, 52–54 cm, and is the characteristic association of the Barremian/lowermost Aptian (*C. pythiae* Zone, respectively the base of the *S. euganea* Zone).

In the underlying interval, which corresponds to lithologic Unit VI, radiolarians are rare and the preservation is poor. Between Samples 103-641C-12R-3, 35–37 cm, and 103-641C-15R-2, 99–102 cm, the diversity of radiolarian faunas decreases (re-

working?), and they are less fragile and commonly not age diagnostic. Included in this assemblage are *A. diaphorogona*, *A. umbilicata*, *C. tuberosa*, *P. lanceola*, *A. vulgaris*, *P. carpatica*, *T. conica*, and *X. spicularius*.

The common occurrence of *S. orca* restricts this interval from upper Hauterivian to lowermost Aptian. In Sample 103-641C-12R-5, 38–41 cm, the last occurrence (LO) of *Sethocapsa uterculus* marks the Barremian/Aptian boundary interval. Sample 103-641C-15R-2, 99–102 cm, in which the preservation is somewhat better than in the younger samples, contains a fauna that is quite similar to that in Section 103-640A-3R, CC, consisting of age-diagnostic species such as *S. orca*, *S. trachyostraca*, *W. gilkeyi*, and *Williriedellum peterschmittae*. These taxa indicate a Hauterivian/Barremian age for the last downhole occurrence of a radiolarian-rich sample.

The radiolarian associations from Section 103-641C-9R, CC, downhole are comparable with those from Sites 638 and 640 and are characteristic of the Blake-Bahama Formation. Therefore, the boundary between this formation and the overlying Hatteras Formation is tentatively placed within Core 103-641C-9R, CC.

## SITE 638

### Holes 638B and 638C

Rare to common radiolarians of varying preservation occur throughout the Cretaceous sequence at Hole 638B. Biostratigraphically useful radiolarians were found only in lithologic Unit II. This unit is characterized by bioturbated nannofossil marlstone, limestone, and calcareous mudstone. This unit is divided by the shipboard scientists into two subunits ("Site 638" chapter; Boillot, Winterer, et al., 1987). Radiolarian occurrences and mode of preservation permit two biostratigraphic intervals to be recognized within the Cretaceous sedimentary section of Hole 638B. These intervals coincide roughly with the shipboard-defined lithologic units.

Radiolarians from Subunit IIA, pelagic limestone alternating with laminated marlstone rich in terrigenous material, are preserved as silica and can be regarded as true *in-situ* associations. Radiolarians from the Subunit IIB bioturbated marlstone are replaced by pyrite. Several faunas may even be reworked. A compilation of the sediment-radiolarian relationships at this site is given in the "Site 638" chapter (Boillot, Winterer, et al., 1987). A description of the different diagenetic features is presented by Thurow (this volume).

Twenty-five samples, from all lithologies, were studied from Subunit IIA. Radiolarians are abundant but are generally altered to calcite, which obscures the skeletal meshwork. Commonly, calcite steinkerns are the remains of the original faunal component (Thurow, this volume). However, in rare cases, a part of the faunal assemblage remains preserved as quartz, which allows biostratigraphic evaluation.

*In-situ* radiolarians were etched from lightly bioturbated limestones in the interval between Samples 103-638B-21R-1, 4–6 cm, and 103-638B-22R-5, 138–140 cm. The radiolarians are fragile and show imprints of calcite crystals on the test surfaces.

A rich and diverse fauna was found in Sample 103-638B-21R-5, 52–54 cm. The most characteristic species are *Archaeodictyomitra puga*, *A. vulgaris*, *C. pythiae*, *Cryptamphorella* ssp. (*Cryptamphorella dumitricai*, *C.* cf. *conara*), *C. grutterinki*, *D. tytthopora*, *Godia*(?) ssp., *Mita* ssp., *Parvicingula boesii*, *Parvicingula*(?) sp., *P. triacantha*, *Podobursa tricola*, *Pseudodictyomitra lilyae*, *S. orca*, *S. trachyostraca*, *S. uterculus*, *Siphocampium*(?) *davidi*, *Stichocapsa cribata*, *T. conica*, *T. pulchra*, *X. alievi*, *X. spicularius*, *A. diaphorogona*, *A. umbilicata*, *A. trizonalis*, *A. helenae*, *Angulobracchia*(?) *portmanni*, *A. tehamaensis*, *C. tuberosa*, *Hexastylurus magnificus*, *O. railensis*, *C. infundibuliforme*, *P. lanceola*, and *T. echoides*.

A comparably well-preserved and diverse fauna was found in Sample 103-638B-21R-4, 38–40 cm, including *A. diaphorogona*, *A. umbilicata*, *A. helenae*, *A. lacrimula*, *Archaeodictyomitra pseudoscalaris*, *A. tehamaensis*, *C. infundibulum*, *Eucyrtis* cf. *elido*, *Eusyringium* sp., *Godia*(?) ssp., *Mirifusus chenodes*, *Orbiculiforma* ssp., *P. lanceola*, *Paronaella* sp., *Patulibracchium* sp., *Pseudocrucella* aff. *P. theokaftensis*(?), *P. carpatica*, *P. lilyae*, *T. hybum*, *T. conica*, *T. pulchra*, *Napora* sp., *W. peterschmittae*, *X. alievi*, *X. spicularius*, and an unknown spumellarian gen. et sp. indet. 20.

The occurrence of the short-ranging species *M. chenodes*, *C. pythiae*, and *D. tytthopora* is characteristic of the *C. pythiae* Zone and allows a precise age assignment of middle Barremian. The co-occurrence of *S. orca*, *S. uterculus*, and *A. helenae* in Sample 103-638B-21R-5, 52–54 cm, and the occurrence of *T. hybum* in Sample 103-638B-21R-4, 38–40 cm, support this age assignment, which is in good accordance with the ages provided by calcareous microfossils (nannoplankton: late Barremian/?early Aptian; foraminifers: late Barremian).

This resulting age assignment affects the ranges of several biostratigraphically important species, *S. trachyostraca* and *Siphocampium*(?) *davidi*, which have been said to become extinct at the end of the Hauterivian.

Fifty samples were studied from all of the Subunit IIB (Sections 103-638B-23R-3 to 103-638B-32R-2) lithologies. Enrichments of sufficiently preserved radiolarians are mainly in the dark gray clay-rich marlstone, which alternates with light gray nannofossil marlstone containing radiolarians replaced by coarse calcite. Radiolarians are common in the dark marlstone but pyrite-replaced and poorly preserved. Rather well-preserved faunas were in Section 103-638B-25R, CC, and Sample 103-638B-26R-1, 21–25 cm; both associations are identical. Important biostratigraphic markers include: *A. diaphorogona*, *A. umbilicata*, *A. helenae*, *A. tehamaensis*, *C. septemporatus*, *A. lacrimula*, *A. vulgaris/pseudoscalaris*, *P. boesii*, *Godia*(?) ssp., *P. triacantha*, *S. orca*, *S. trachyostraca*, *Siphocampium(?) davidi*, *Syringocapsa agolarium*, *T. conica*, *W. peterschmittae*, and *X. spicularius*.

This faunal association does not differ from that in Subunit IIA, but the presence of *C. septemporatus* indicates an age not younger than early Barremian. A hiatus in Section 103-638B-23R-3, which is likely based on the nannofossil results (Applegate and Bergen, this volume), is not confirmed by the radiolarian results. However, the potential biostratigraphic resolution of radiolarians is still quite coarse and does not allow the separation of different datum levels within a stage.

In Sample 103-638B-31R-2, 34–36 cm, the following were found: *A. diaphorogona*, *A. umbilicata*, *A. helenae*, *Angulobracchia*(?) *portmanni*, *"Cenosphaera"* sp., *C. tuberosa*, several species of *Hagiastrids*, *Homoeoparonaella* sp., *Orbiculiforma* ssp., *Pseudocrucella*(?) sp. A, *Pseudocrucella*(?) sp. B, *S. martini*, *T. hybum* gen. et sp. indet. 12, *A. vulgaris*, *D. tytthopora*, *Godia*(?) sp., *E. elido*, *P. boesii*, *P. triacantha*, *P. carpatica*, *Sethocapsa dorysphaeroides* (Schaaf, 1985, p. 155, Pls. 6a and 6b), *Sethocapsa leiostraca*, *S.* cf. *S. simplex*, *S. trachyostraca*, *S. uterculus* (1 specimen), *Siphocampium*(?) *davidi*, *S. cribata*, *Stichomitra* sp., *T. conica*, *W. peterschmittae* (rare), *X. spicularius*, and unknown spumellarian gen. et sp. indet. 17.

The co-occurrence of *D. tytthopora*, *S. leiostraca*, and *S. cribata* indicates the *D. tytthopora* Zone of middle Hauterivian age. According to the radiolarian data presented, Subunit IIB sediments are of middle Hauterivian to Barremian age. However, reworking is a common feature in this interval, and an age assignment to this subunit by means of radiolarians may be impaired.

Lithologic Unit III (Sections 103-638B-32R-2 to 103-638B-45R, CC, and 103-638C-1R-1 to 103-638C-14R, CC) is characterized by the occurrence of terrigenous turbidites. Sixty samples were studied from Unit III. Radiolarians are generally common, but confined to silty-sandy layers. All faunas are replaced by pyrite with strong crystal overgrowth. Except for a few specimens, the radiolarians are preserved as pyrite molds that are useless for biostratigraphic analysis (see Thurow, this volume).

## SITE 640

### Hole 640A

Radiolarians were found in only four samples at Site 640 (Samples 103-640A-3R-3, 138–142 cm, and 103-640A-3R-4, 11–13 cm, and Sections 103-640A-3R, CC, and 103-640A-5R, CC), all within lithologic Unit III (dark gray calcareous clays and marls, clayey limestones, silty calcareous clays, and sandstones—similar to the sequence at Holes 638B and 638C). All specimens are replaced by pyrite and only one sample, from Section 103-640A-3R, CC, contains radiolarians that are sufficiently preserved for a biostratigraphic evaluation. This fauna is selected as a reference for this time interval. The fauna is diverse, and several age-diagnostic species were distinguished, including *A. diaphorogona*, *A. umbilicata*, *Acanthocircus dicranacanthos*, *A. helenae*, *Angulobracchia*(?) cf. *portmanni*, *Conosphaera tuberosa*, *P. lanceola*, *Pseudocrucella*(?) sp., *Tritrabs* sp., *A. lacrimula*, *Archaeodictyomitra nuda*, *A. pseudoscalaris*, *A. puga*, *A. vulgaris*, *Cryptamphorella* ssp., *C. grutterinki*, *E. elido*, *P. boesii*, *P. triacantha*, *Pseudodictyomitra leptoconica*, *P. lilyae*, *S. trachyostraca*, *S. uterculus*, *Siphocampium*(?) *davidi*, *Theocorys renzae*, *Triactoma* cf. *hybum*, *T. conica*, *T. pulchra*, *W. gilkeyi*, *W. peterschmittae*, *X. alievi*, and *X. spicularius*.

The co-occurrence of *A. dicranacanthos*, *A. lacrimula*, *S. trachyostraca*, *S. uterculus*, and *T. pulchra* gives an age that coincides rather well with the Hauterivian/Barremian boundary but is considerably older than the age provided by the nannofossils (middle to late Barremian). The results from Hole 638B indicate that *S. trachyostraca* also occurs in the Barremian. The other problem is the presence of *A. dicranacanthos*, which would restrict the age of the sample to Hauterivian or older. However, the overall faunal composition compares well to that of Sample 103-638B-21R-5, 52–54 cm, the reference sample for Hole 638B. Therefore, a Barremian age for the sample from Section 103-640-3R, CC, seems possible.

The presence of completely pyritized radiolarians makes it rather difficult to discriminate between several Lower Cretaceous genera of Nassellarians; however, it is possible to ascribe morphotypes present in the studied material to several genera already erected or quoted in the past. Because it is impossible to study the specimens in transmitted light, I assign the morphotypes to those genera.

The overall faunal composition is somewhat strange; in fact, a large part of the age-diagnostic species is restricted to the 45–63 μm size fraction, whereas the coarser fraction is dominated by nondiverse, long-ranging spumellarids. In the western Tethys, radiolarian assemblages representing this time interval are characterized by the occurrence of large nassellarians that are almost absent in Section 103-640A-3R, CC. It is not clear if this absence is a result of sorting during transport or if such forms are missing in middle- to high-latitude areas. Taking into account the results from Hole 638B and the fact that below Section 103-640A-5R, CC, the sediments are mainly turbidites, the former explanation seems more likely.

## DISCUSSION

The Cretaceous North Atlantic Ocean is not known as a favorable site for radiolarian preservation. Cretaceous radiolarians are rare in the North Atlantic deep-sea sequences, and they are generally not as well preserved as those in the Pacific and Indian basins. Examination of the Mesozoic sequences at Sites 398, 638, 640, and 641 from the Northeast Atlantic continental margin and Site 603 from the Northwest Atlantic continental margin reconfirm this observation, but there are exceptions.

It is not the purpose of this paper to focus on this problem, but one explanation for the poor radiolarian preservation may be the relatively small amount of silica deposited in the Cretaceous Atlantic Basin. Unfavorable living conditions resulting from the great outflow of salt brine from the western Tethys, respective to the Atlantic borderlands, may be another explanation.

Within the Upper Cretaceous, from which radiolarians are only rarely documented, two short intervals of radiolarian-rich sedimentation are distinguished (Fig. 5). The younger bloom is restricted to the Campanian, but calibration with other planktonic groups is not yet well established to definitely restrict the Campanian radiolarian occurrences to a distinct global siliceous event. The older bloom coincides with the well-known CTBE (e.g., Thurow et al., this volume). Because radiolarian-rich occurrences now are widespread and can be traced into Atlantic marginal seas, radiolarians are commonly recorded in onshore outcrops.

The Campanian radiolarian spike at Site 603 coincides with a worldwide enrichment of radiolarian-rich or siliceous Campanian sediments in different tectonic settings, as recorded by several authors (compilation in Empson-Morin, 1984). Low-latitude sediments have similar radiolarian associations (Herm, 1962; Butt, 1981; Taketani, 1982; compilation of various occurrences in Empson-Morin, 1984; Iwata and Tajika, 1986). These biosiliceous sediments are predominantly detectable in pelagic or "flyschoid" sediments. Fine-grained calcilutitic layers of turbidite series within the Great Valley sequence (California; Pessagno, 1976), in Japan, in the Gibraltar Arch area, and in the Eastern Alps evidence the strong influence of this biosiliceous "event." However, it also coincides with some significant shallow-marine manganese deposits, sulfide/umber associations upon ophiolite suites (Robertson and Hudson, 1974; Tippit et al., 1981; Blome and Irwin, 1985; Schlanger, 1986), the end of Oceanic Anoxic Event 3 (Arthur et al., 1987), and probably with the end of the middle Cretaceous magnetic quiet zone.

In the Gosau Basin close to Bad Reichenhall (northern calcareous limestone Alps, Bavaria, Federal Republic of Germany), a short-lived spike of radiolarian-rich sediments is reported from the Campanian (Herm, 1962; Butt, 1981). Butt (1981) figured some of the radiolarians (pl. 20), and Empson-Morin (1984) described some of the fauna. The faunal composition is highly similar to that of samples from Core 603B-26. Similar faunal associations are widely reported. Most of the occurrences cannot be calibrated with planktonic foraminifers, but one exception is in the Gosau Basin. Sections in this area also contain planktonic foraminifers, which allows direct calibration with the radiolarians. Herm's (1962) sample 223, which marks the peak in radiolarian abundance, and Butt's (1981) sample 84 (nearly 100% radiolarians) are both from the upper part of the Röthelbach Section, which is the planktonic foraminifer *Globotruncana elevata* Zone of Butt (1981). Both authors report the FO of *Globotruncana calcarata* several meters above the radiolarian peak, which points to an early to middle Campanian age for this radiolarian bloom, thereby confirming the results of Moullade et al. (this volume) for the North Atlantic.

The older, Upper Cretaceous radiolarian event coincides with the well-recorded CTBE (Oceanic Anoxic Event 2 of Schlanger and Jenkyns, 1976; Brumsack and Thurow, 1986; Herbin et al., 1986; Kuhnt et al., 1986; Schlanger et al., 1987; Thurow and Kuhnt, 1986; Thurow et al., this volume), an almost global oce-

anic event that is recorded in the deep sea by a strongly condensed biosiliceous black shale sedimentation enriched in trace metals. The true black shale deposits of this event rarely have the well-preserved radiolarians commonly observed in DSDP black shale samples, in exclusion of Bralower and Thierstein's (1984) contention that rich radiolarian occurrences are preferentially found in black shales because of a better fossilization potential, thereby denying the idea that such radiolarian blooms may be a result of higher surface productivities.

The reason for the biosiliceous sedimentation and high preservation of radiolarian faunas at the CTBE is not fully understood, but currently a widely accepted explanation is that it results from a combined effect of sea-level highstand, low deep-sea sedimentation rates because of starved terrigenous material, overall enhanced surface productivity, and coastal upwelling leading to high surface productivity and high sedimentation rates in certain areas. Transportation of radiolarians from upwelling areas downslope may also contribute to radiolarian enrichments in deep-sea sediments (Thurow and Kuhnt, 1986).

The two Lower Cretaceous intervals are characterized by rich and comparably well-preserved radiolarian associations in the upper Albian and a longer-ranging interval from the upper Barremian to Albian. The younger "event" has not been intensively studied, but it is coincident with the first occurrence of red, oxic sediments at several sites in the North Atlantic, as well as in bordering areas (e.g., western Tethys; Thurow, 1987). Furthermore, there is strong paleontological evidence that the first deep-water connection between the South Atlantic and central North Atlantic was established at approximately this time (Moullade and Guérin, 1982; Wiedmann and Neugebauer, 1978).

The older sequence of radiolarian-rich sediments is coincident with the Oceanic Anoxic Event 1 of Schlanger et al. (1986) (approximately uppermost part of the Blake-Bahama Formation and lower part of the Hatteras Formation), a widespread and thick layer of sediments deposited in environments that were not as well oxygenated. The first rich and well-preserved radiolarian faunas occur at the end of the high-productivity nannofossil limestone sequences that are characteristic of the top of Blake-Bahama Formation. Age-equivalent radiolarian enrichments can be traced far into the Tethys (Majolica Limestone). The wide connection between the Tethys and the North Atlantic has narrowed since the Aptian, and circulation in the North Atlantic has decreased, causing the North Atlantic to become a restricted basin. Rather abruptly onshore and gradationally in the North Atlantic, the typical sediments change to less calcareous, mainly clayey sediments that are commonly a sink for organic carbon, chiefly of terrestrial origin, which could affect the climate in the borderlands. Radiolarians are common in the clayey layers, but preservation is poor. The first oxygenated sediments in the Albian mark the decline of radiolarian preservation in the Upper Cretaceous North Atlantic.

In summary, radiolarians are a common, but rarely well-preserved, part of the North Atlantic Cretaceous planktonics. Rich and well-preserved occurrences reflect major oceanic events (e.g., upwelling, change in the carbonate compensation depth, change in oceanic circulation pattern, or increase in volcanic activity), initiated by quite different phenomena that are mainly related to the formation of the Atlantic Basin but are not as yet completely understood.

## ACKNOWLEDGMENTS

I wish to thank the Ocean Drilling Program for the invitation to participate on Leg 103 aboard the *JOIDES Resolution* and to sample Sites 638, 640, and 641. The National Science Foundation provided the samples from DSDP Leg 47B/Site 398 and Leg 93/Site 603. The technical assistance of Horst Hüttemann (SEM, Tübingen) is appreciated.

I thank Dr. Casey for improving the manuscript through review and criticism and Drs. Hemleben, Blome, and Schaaf for their reviews and valuable advice.

This work was supported by the German National Science Foundation (D.F.G.) Grant Wi 112-25.

## REFERENCES

Aliev, K. S., 1961. Novye vidy radioliarii nizhnego melo severo-vostochnogo Azerbaidzhana. *Uch. Zap. Minist. Vyssh. Sredn. Spets. Obrax. Ax. SSR, Ser. Geol. Geogr. Nauk*, 2:25–38.

_____, 1965. Radiolyarii nizhnemelovykh otlozhenii Severo-Vostochnogo Azerbaidzhana i ikh stratigraficheskoe znachenie. *Izv. Akad. Nauk Az. SSR*, 1–124.

Arthur, M. A., Schlanger, S. O., and Jenkyns, H. C., 1987. The Cenomanian-Turonian Oceanic Anoxic Event, II. Paleoceanographic controls on organic matter production and preservation. *In* Brooks, J., and Fleet, A. (Eds.), *Marine Petroleum Source Rocks*: Geol. Soc. Spec. Publ. London, 26:401–420.

Basov, V. A., Lopatin, B. G., Gramberg, I. S., Danjushevskaya, A. I., Kaban'kov, V. Ya, Lazurkin, V. M., and Patrunov, D. K., 1979. Lower Cretaceous lithostratigraphy near Galicia Bank. *In* Sibuet, J.-C., Ryan, W.B.F., et al., *Init. Repts. DSDP*, 47, Pt. 2: Washington (U.S. Govt. Printing Office), 683–717.

Baumgartner, P. O., 1980. Late Jurassic *Hagiastridae* and *Patulibracchiidae* (Radiolaria) from the Argolis Peninsula (Peloponnesus, Greece). *Micropaleontology*, 26:274–322.

_____, 1984. A Middle Jurassic–Early Cretaceous low-latitude radiolarian zonation based on unitary associations and age of Tethyan radiolarites. *Eclogae Geol. Helv.*, 77:729–837.

Baumgartner, P. O., de Wever, P., and Kocher, R., 1980. Correlation of Tethyan Late Jurassic–Early Cretaceous radiolarian events. *Cah. Micropaleontol.*, 2:23–72.

Blome, C. D., and Irwin, W. P., 1985. Equivalent radiolarian ages from ophiolitic terranes of Cyprus and Oman. *Geology*, 13:401–404.

Boillot, G., Winterer, E. L., et al., 1987. *Proc. ODP, Init. Repts.*, 103: College Station, TX (Ocean Drilling Program).

Bralower, T. J., and Thierstein, H. R., 1984. Low productivity and slow deep-water circulation in mid-Cretaceous oceans. *Geology*, 12:614–618.

Brumsack, H.-J., and Thurow, J., 1986. The geochemical facies of black shales from the Cenomanian/Turonian Boundary Event (CTBE). *In* Degens, E. T., Meyers, P. A., and Brassell, S. C. (Eds.), *Biogeochemistry of Black Shales*: Mitt. Geol. Palaeontol. Inst. Univ. Hamburg, 60:247–265.

Butt, A., 1981. Depositional environments of the Upper Cretaceous rocks in the northern part of the Eastern Alps. *Spec. Publ. Cushman Found. Foraminiferal Res.*, 20:1–121.

Campell, A. S., and Clark, B. L., 1944. Radiolaria from Upper Cretaceous of middle California. *Spec. Pap. Geol. Soc. Am.*, 57:1–61.

Cita, M. B., 1964. Ricerche micropaleontologiche e stratigrafiche sui sedimenti pelagici del Giurassico superiore e del Cretaceo inferiore nella catena del Monte Baldo. *Mem. Riv. Ital. Paleontol. Stratigr.*, 10:1–182.

Cita, M. B., and Pasquare, G., 1959. Osservazioni micropaleontologiche sul Cretaceo delle Dolomiti. *Riv. Ital. Paleontol. Stratigr.*, 65: 385–442.

Davis, A. G., 1950. The Radiolaria of the Hawasina series of Oman. *Proc. Geol. Assoc.*, 61:206–217.

de Wever, P., 1981. Spyrids, artostrobiids, and Cretaceous radiolarians from the western Pacific, DSDP Leg 61. *In* Larson, R. L., Schlanger, S. O., et al., *Init. Repts. DSDP*, 61: Washington (U.S. Govt. Printing Office), 507–520.

de Wever, P., and Thiébault, F., 1981. Les radiolaires d'âge Jurassique supérieur à Crétacé supérieur dans les radiolarites du Pinde-Olonos (presqu'île de Koroni; Péleponnése méridional, Grèce). *Geobios*, 14: 577–609.

Dinkelmann, M. G., 1973. Radiolarian stratigraphy: Leg 16 DSDP. *In* van Andel, T. H., Heath, G. R., et al., *Init. Repts. DSDP*, 16: Washington (U.S. Govt. Printing Office), 747–813.

Dumitrica, P., 1970. Cryptocephalic and cryptothoracic Nassellaria in some Mesozoic deposits of Romania. *Rev. Roum. Geol. Geophys. Geogr.: Geol.*, 14:1–124.

_____, 1972. Cretaceous and Quaternary Radiolaria in deep sea sediments from the northeast Atlantic Ocean and Mediterranean Sea. *In* Ryan, W.B.F., Hsü, K. J., et al., *Init. Repts. DSDP*, 13, Pt. 2: Washington (U.S. Govt. Printing Office), 829–901.

_____, 1975. Cenomanian Radiolaria at Podul Dimbovitei. *In Micropaleontological Guide to the Mesozoic and Tertiary of the Romanian Carpathians*: 14th Eur. Micropaleontol. Colloq. Bucarest, 87–89.

Dundo, O. P., and Zhamoida, A. I., 1963. Stratigrafya mezozoiskikh otlozhenii basseina r. Velikoi i kharakternyi kompleks valanzhinskikh radiolyarii. *In* Egiazarova, E.B.Kh. (Ed.), *Geologiya Koryakskogo Nagorya*: Moscow (Gosudarstvennoe Nauchno-Tekhnicheskoe Izdatel'stvo Literatury po Gornomu Delu), 64–85.

Empson-Morin, K. M., 1981. Campanian Radiolaria from DSDP Site 313, Mid-Pacific Mountains. *Micropaleontology*, 27:249–292.

_____, 1982. Reexamination of the Late Cretaceous radiolarian genus *Amphipyndax* Foreman. *J. Paleontol.*, 56:507–519.

_____, 1984. Depth and latitude distribution of Radiolaria in Campanian (Late Cretaceous) tropical and subtropical oceans. *Micropaleontology*, 30:87–115.

Fischli, H., 1916. Beitrag zur kenntnis der fossilen Radiolarien in der Riginagelfluh. *Mitt. Naturwiss. Ges. Winterthur.*, 11:44–47.

Foreman, H. P., 1966. Two Cretaceous radiolarian genera. *Micropaleontology*, 12:355–359.

_____, 1968. Upper Maestrichtian Radiolaria of California. *Spec. Pap. Palaeontol.*, 3:1–82.

_____, 1971. Cretaceous Radiolaria, Leg 7, DSDP. *In* Winterer, E. L., Riedel, W. R., et al., *Init. Repts. DSDP*, 7: Washington (U.S. Govt. Printing Office), 1673–1693.

_____, 1973a. Radiolaria of Leg 10 with systematics and ranges for the families Amphipyndacidae, Artostrobiidae, and Theoperidae. *In* Worzel, J. L., Bryant, W., et al., *Init. Repts. DSDP*, 10: Washington (U.S. Govt. Printing Office), 407–474.

_____, 1973b. Radiolaria from DSDP Leg 20. *In* Heezen, B. C., MacGregor, I. D., et al., *Init. Repts. DSDP*, 20: Washington (U.S. Govt. Printing Office), 249–305.

_____, 1975. Radiolaria from the North Pacific, Deep Sea Drilling Project, Leg 32. *In* Larson, R. L., Moberly, R., et al., *Init. Repts. DSDP*, 32: Washington (U.S. Govt. Printing Office), 579–676.

_____, 1977. Mesozoic Radiolaria from the Atlantic Basin and its borderlands. *In* Swain, F. M. (Ed.), *Stratigraphic Micropaleontology of Atlantic Basin and Borderlands*: Amsterdam (Elsevier), 305–320.

_____, 1978a. Cretaceous Radiolaria in eastern South Atlantic, Deep Sea Drilling Project, Leg 40. *In* Bolli, H. M., Ryan, W.B.F., et al., *Init. Repts. DSDP*, 40: Washington (U.S. Govt. Printing Office), 839–843.

_____, 1978b. Mesozoic Radiolaria in the Atlantic Ocean off the northwest coast of Africa, Deep Sea Drilling Project, Leg 41. *In* Lancelot, Y., Seibold, E., et al., *Init. Repts. DSDP*, 41: Washington (U.S. Govt. Printing Office), 739–761.

Heitzer, I., 1930. Die radiolarien-fauna der mitteljurassischen Kieselmergel im Sonnwendgebirge. *Jahrb. Geol. Bundesanst. (Austria)*, 80:381–406.

Herbin, J.-P., Masure, E., and Roucaché, J., 1987. Cretaceous formations from the lower continental rise off Cape Hatteras: organic geochemistry, dinoflagellate cysts, and the Cenomanian/Turonian boundary at Sites 603 (Leg 93) and 105 (Leg 11). *In* van Hinte, J. E., Wise, S. W., Jr., et al., *Init. Repts. DSDP*, 93: Washington (U.S. Govt. Printing Office), 1139–1162.

Herbin, J.-P., Montadert, L., Müller, C., Gomez, R., Thurow, J., and Wiedmann, J., 1986. Organic-rich sedimentation at the Cenomanian-Turonian Boundary in oceanic and coastal basins in the North Atlantic and Tethys. *In* Summerhayes, C. P., and Shackleton, N. J. (Eds.), *North Atlantic Palaeooceanography*: Geol. Soc. Spec. Publ. London, 21:389–422.

Herm, D., 1962. Stratigraphische und mikropaläontologische Untersuchungen der Oberkreide im Lattengebirge und Nierental (Gosaubecken von Reichenhall und Salzburg). *Abh. Bayer. Akad. Wiss., Math. Naturwiss. Kl.*, 104:1–119.

Hinde, G. J., 1900. Description of fossil Radiolaria from the rocks of Central Borneo. *In* Molengraaf, G.A.F. (Ed.), *Borneo-Expeditie: Geologische Verkenningstochten in Central Borneo (1893–1894)*: Leiden (Brill), 1–51, 54–56.

Ishida, H., 1983. Stratigraphy and radiolarian assemblages of the Triassic and Jurassic siliceous sedimentary rocks in Konose Valley, Tokushima Prefecture, southwest Japan. *J. Sci. Coll. Gen. Edu., Univ. Tokushima*, 16:111–141.

Iwata, K., and Tajika, J., 1986: Late Cretaceous radiolarians of the Yubetsu Group, Tokoro Belt, northeast Hokkaido. *J. Fac. Sci. Hokkaido Univ. Ser. 4*, 21:619–644.

Jansa, L. F., Enos, P., Tucholke, B. E., Gradstein, F. M., and Sheridan, R. E., 1979. Mesozoic-Cenozoic sedimentary formations of the North American Basin; western North Atlantic. *In* Talwani, M., Hay, W., and Ryan, W.B.F. (Eds.), *Deep Drilling Results in the Atlantic Ocean: Continental Margins and Paleoenvironment*: Am. Geophys. Union, Maurice Ewing Ser., 3:1–57.

Kanie, Y., Taketani, Y., Sakai, A., and Miyata, Y., 1981. Lower Cretaceous deposits beneath the Yezo Group in the Urakawa area, Hokkaido. *Bull. Geol. Soc. Jpn.*, 87:527–533.

Kent, D. V., and Gradstein, F. M., 1985. A Cretaceous and Jurassic geochronology. *Geol. Soc. Am. Bull.*, 96:1419–1427.

Kling, S. A., 1971. Radiolaria: Leg 6 of the Deep Sea Drilling Project. *In* Fischer, A. G., Heezen, B. C., et al., *Init. Repts. DSDP*, 6: Washington (U.S. Govt. Printing Office), 1069–1117.

_____, 1982. Radiolarians from the Mariana Trough and Trench region: Deep Sea Drilling Project Leg 60. *In* Hussong, D. M., Uyeda, S., et al., *Init. Repts. DSDP*, 60: Washington (U.S. Govt. Printing Office), 537–555.

Kocher, R. N., 1981. Biochronostratigraphische untersuchungen oberjurassischer radiolarienführender Gesteine insbesondere der Südalpen. *Mitt. Geol. Inst. Edig. Tech. Hochsch. Univ. Zurich*, 234:1–184.

Kozlova, G. E., and Gorbovetz, A. N., 1966. Radiolyarii verkhnemelovykh i verkhneeotsenovykh otlozhenii Zapadno-Sibirskoi nizmennosti. *Tr. Vses. Neft. Naucho. Issled. Geologorazved. Inst.*, 248:1–159.

Kuhnt, W., Thurow, J., Wiedmann, J., and Herbin, J.-P., 1986. Oceanic anoxic conditions around the Cenomanian/Turonian Boundary and the response of the biota. *In* Degens, E. T., Meyers, P. A., and Brassell, S. C. (Eds.), *Biogeochemistry of Black Shales*: Mitt. Geol. Palaeontol. Inst. Univ. Hamburg, 60:205–246.

Lozyniak, P. Yu., 1969. Radioliarii nizhnemelovykh otlozhenii Ukrainskikh Karpat. *In* Vialov, O. C. (Ed.), *Iskopaemye i Sovremannye Radioliarii*: L'vov (Geol. O-vo., Lv'ov Univ.), 29–41.

_____, 1975. Nekotorye radiolyarii melovykh otlozhenii Skibovoi zony Ukrainskikh Karpat. "*Vischa Shkola*," *Sb. Geol. Ved. Paleontol.*, 12:48–53.

Mattson, P. H., and Pessagno, E. A., 1979. Jurassic and Early Cretaceous radiolarians in Puerto Rican ophiolite—tectonic implications. *Geology*, 7:440–444.

Moore, T. C., Jr., 1973. Radiolaria from Leg 17 of the Deep Sea Drilling Project. *In* Winterer, E. L., Ewing, J. I., et al., *Init. Repts. DSDP*, 17: Washington (U.S. Govt. Printing Office), 797–869.

Moullade, M., and Guérin, S., 1982. Le problème des rélations de l'Atlantique Sud et de l'Atlantique Central au Crétacé moyen: nouvelles données microfauniques d'après les forages D.S.D.P. *Bull. Soc. Geol. Fr.*, 24:511–517.

Müller, C., Schaaf, A., and Sigal, J., 1983. Biochronostratigraphie des formations d'âge Crétacé dans les forages du DSDP dans l'océan Atlantique Nord. *Rev. Inst. Fr. Pet.*, 38:683–708.

_____, 1984. Biochronostratigraphie des formations d'âge Crétacé dans les forages du DSDP dans l'océan Atlantique Nord. *Rev. Inst. Fr. Pet.*, 39:3–23.

Muzavor, S.N.X., 1977. Die oberjurassische Radiolarienfauna von Oberaudorf am Inn [Ph.D. dissert.]. Univ. München.

Nakaseko, K., and Nishimura, A., 1981. Upper Jurassic and Cretaceous Radiolaria from the Shimanto Group in southwest Japan. *Sci. Rep. Coll. Gen. Edu. Osaka Univ.*, 30:133–203.

Nakaseko, K., Nishimura, A., and Sugano, K., 1979. Cretaceous Radiolaria from the Shimanto Belt, Japan. *Spec. Vol. News Osaka Micropaleontol.*, 2:1–49.

Neviani, A., 1901. Novi generi e sottogeneri di radiolari e briozoi fossili italiani. *Boll. Soc. Geol. Ital.*, 19:645–671.

Parona, C. F., 1890. Radiolarie nei noduli selciosi del calcare giurese di Cittiglo presso Laveno. *Boll. Soc. Geol. Ital.*, 9:132–175.

Parona, C. F., and Rovereto, G., 1895. Diaspri Permiani a radiolarie di Montenotte (Liguria Occidentale): *Atti Accad. Sci. Torino, Cl. Sci. Fis., Mat. Nat.*, 31:167–181.

Pessagno, E. A., 1962. The Upper Cretaceous stratigraphy and micropaleontology of south central Puerto Rico. *Micropaleontology*, 8: 349–368.

_____, 1963. Upper Cretaceous Radiolaria from Puerto Rico. *Micropaleontology*, 9:197–214.

_____, 1969. The *Neosciadiocapsidae*, a new family of Upper Cretaceous Radiolaria. *Bull. Am. Paleontol.*, 58:377–439.

_____, 1971b. Jurassic and Cretaceous *Hagiastridae* from the Blake-Bahama Basin (Site 5A, JOIDES Leg 1) and the Great Valley Sequence, California Coast Ranges. *Bull. Am. Paleontol.*, 60:1-80.

_____, 1972. Cretaceous Radiolaria. Part I: The *Phaseliformidae*, new family, and other *Spongodiscacea* from the Upper Cretaceous portion of the Great Valley sequence. Part II: *Pseudoaulophacidae* Riedel from the Cretaceous of California and the Blake-Bahama Basin (JOIDES Leg 1). *Bull. Am. Paleontol.*, 61:267–328.

_____, 1973. Upper Cretaceous Spumellariina from the Great Valley Sequence, California Coast Ranges. *Bull. Am. Paleontol.*, 63:49–102.

_____, 1975. Upper Cretaceous Radiolaria from DSDP Site 275. *In* Kennett, J. P., Houtz, R. E., et al., *Init. Repts. DSDP*, 29: Washington (U.S. Govt. Printing Office), 1011–1029.

_____, 1976. Radiolarian zonation and stratigraphy of the Upper Cretaceous portion of the Great Valley Sequence, California Coast Ranges. *Micropaleontology Spec. Publ.*, 2:1–95.

_____, 1977a. Upper Jurassic Radiolaria and radiolarian biostratigraphy of the California Coast Ranges. *Micropaleontology*, 23:56–113.

_____, 1977b. Lower Cretaceous radiolarian biostratigraphy of the Great Valley Sequence and Franciscan Complex, California Coast Ranges. *Spec. Pap. Cushman Found. Foraminiferal Res.*, 15:1–87.

_____, 1977c. Radiolaria in Mesozoic stratigraphy. *In* Ramsay, A.T.S. (Ed.), *Oceanic Micropaleontology* (Vol. 2): London (Academic), 913–950.

Pessagno, E. A., and Longoria, T.J.F., 1973. Mesozoic foraminifera, Leg 15, DSDP. *In* Edgar, N. T., Saunders, J. B., et al., *Init. Repts. DSDP*, 15: Washington (U.S. Govt. Printing Office), 549–552.

Pessagno, E. A., and Michael, F. Y., 1974. Results of shore laboratory studies on Mesozoic planktonic foraminifera from Leg 26, Sites 255, 256, 257, and 258. *In* Barker, P., Dalziel, I.W.D., et al., *Init. Repts. DSDP*, 36: Washington (U.S. Govt. Printing Office), 969–972.

Petrushevskaya, M. G., and Kozlova, G. E., 1972. Radiolaria: Leg 14, DSDP. *In* Hayes, D. E., Pimm, A. C., et al., *Init. Repts. DSDP*, 14: Washington (U.S. Govt. Printing Office), 495–648.

Renz, G. W., 1974. Radiolaria from Leg 27 of the Deep Sea Drilling Project. *In* Veevers, J. J., Heirtzler, J. R., et al., *Init. Repts. DSDP*, 27: Washington (U.S. Govt. Printing Office), 769–841.

Riedel, W. R., and Sanfilippo, A., 1970. Radiolaria, Leg 4, Deep Sea Drilling Project. *In* Bader, R. G., Gerard, R. D., et al., *Init. Repts. DSDP*, 4: Washington (U.S. Govt. Printing Office), 503–575.

_____, 1973. Cenozoic Radiolaria from the Caribbean, DSDP Leg 15. *In* Edgar, N. T., Saunders, J. B., et al., *Init. Repts. DSDP*, 15: Washington (U.S. Govt. Printing Office), 705–751.

_____, 1974. Radiolaria from the southern Indian Ocean, DSDP Leg 26. *In* Davies, T. A., Luyendyk, B. P., et al., *Init. Repts. DSDP*, 26: Washington (U.S. Govt. Printing Office), 771–813.

Riedel, W. R., and Schloecker, J., 1956. Radiolaria from the Franciscan Group, Belmont, California. *Micropaleontology*, 2:357–360.

Robertson, A.H.F., and Hudson, J. D., 1974. Pelagic sediments in the Cretaceous and Tertiary history of the Troodos Massif, Cyprus. *In* Hsü, K. J., and Jenkyns, H. C. (Eds.), *Pelagic Sediments: On Land and under the Sea*: Spec. Publ. Int. Assoc. Sedimentol., 1:403–436.

Rüst, D., 1885. Beiträge zur Kenntnis der fossilen Radiolarien aus Gesteinen des Jura. *Palaeontographica Abt.*, 31:269–321.

_____, 1898. Neue Beiträge zur Kenntnis der fossilen Radiolarien aus Gesteinen des Jura und der Kreide. *Palaeontographica Abt.*, 45: 1–67.

Sanfilippo, A., and Riedel, W. R., 1976. Radiolarian occurrences in the Caribbean region. *Publ. VII Conf. Geol. Caraïbes*, 145–168.

_____, 1985. Cretaceous Radiolaria. *In* Bolli, H. M., Saunders, J. B., Perch-Nielson, K. (Eds.), *Plankton Stratigraphy*: Cambridge (Cambridge Univ. Press), 573–630.

Sarti, M., and von Rad, U., 1987. Early Cretaceous turbidite sedimentation at Deep Sea Drilling Project Site 603, off Cape Hatteras (Leg 93). *In* van Hinte, J. E., Wise, S. W., Jr., et al., *Init. Repts. DSDP*, 93: Washington (U.S. Govt. Printing Office), 891–940.

Sato, T., Nishizono, Y., and Murata, M., 1982. Paleozoic and Mesozoic radiolarian faunas from the Shakumasan Formation. *Spec. Vol. News Osaka Micropaleontol.*, 5:301–310.

Schaaf, A., 1981. Late Early Cretaceous Radiolaria from Deep Sea Drilling Project Leg 62. *In* Thiede, J., Vallier, T. L., et al., *Init. Repts. DSDP*, 62: Washington (U.S. Govt. Printing Office), 419–470.

_____, 1984. Les radiolaires du Crétacé inférieur et moyen: biologie et systematique. *Sci. Geol., Mem.*, 75:1–189.

_____, 1985. Un nouveau canevas biochronologique du Crétacé inférieur et moyen: les biozones à radiolaires. *Sci. Geol., Bull.*, 38: 227–269.

Schlanger, S. O., 1986. High frequency sea-level fluctuations in Cretaceous time: an emerging geophysical problem. *In* Hsü, K. J. (Ed.), *Mesozoic and Cenozoic Oceans*: Washington (Am. Geophys. Union), 61–74.

Schlanger, S. O., Arthur, M. A., Jenkyns, H. C., and Scholle, P. A., 1987. The Cenomanian-Turonian Oceanic Anoxic Event, I. Stratigraphy and distribution of organic carbon-rich beds and the marine δ13C excursion. *In* Brooks, J., and Fleet, A. (Eds.), *Marine Petroleum Source Rocks*: Geol. Soc. Spec. Publ. London, 26:371–399.

Schlanger, S. O., and Jenkyns, H. C., 1976. Cretaceous anoxic events: causes and consequences. *Geol. Mijnbouw*, 55:179–184.

Schmidt-Effing, R., 1980. Radiolarien der Mittel-Kreide aus dem Santa Elena Massiv von Costa Rica. *Neues Jahrb. Geol. Palaeontol. Abh.*, 160:241–257.

Shipboard Scientific Party, 1969. Site 4. *In* Ewing, M., Worzel, J. L., et al., *Init. Repts. DSDP*, 1: Washington (U. S. Govt. Printing Office), 10–83.

_____, 1979. Site 398. *In* Sibuet, J.-C., Ryan, W.B.F., et al., *Init. Repts. DSDP*, 47, Pt. 2: Washington (U.S. Govt. Printing Office), 23–233.

_____, 1987. Site 603. *In* van Hinte, J. E., Wise, S. W., Jr., et al., *Init. Repts. DSDP*, 93: Washington (U.S. Govt. Printing Office), 25–276.

Sigal, J., 1979. Chronostratigraphy and ecostratigraphy of Cretaceous formations recovered on DSDP Leg 47B, Site 398. *In* Sibuet, J.-C., Ryan, W.B.F., et al., *Init. Repts. DSDP*, 47, Pt. 2: Washington (U.S. Govt. Printing Office), 287–326.

Squinabol, S., 1903. Le Radiolarie dei noduli selciosi nella Scaglia degli Euganei: contribuzione I. *Riv. Ital. Paleontol.*, 9:105–150.

_____, 1904. Radiolarie cretacei degli Euganei. *Atti Mem. Accad. Patav. Sci., Lett. Arti.*, 20:171–244.

_____, 1914. Contributo alla conoscenza dei Radiolari fossili del Veneto. Appendice—Di un genere di Radiolari caratteristico del Secondario. *Mem. Ist. Geol. Mineral. Univ. Padova*, 2:249–306.

Taketani, Y., 1982. Cretaceous radiolarian biostratigraphy of the Urakawa and Obira areas, Hokkaido. *Sci. Rep. Tohoku Univ., Ser. 2*, 52:1–76.

Tan Sin Hok, 1927. Over de samenstelling en het onstaan van krijt-en mergelgesteenten van de Molukken. *Jaarb. Mijn. Nederlandsch Oost-Indie, Jaargang 1926*, 55:5–165.

Thurow, J., 1987. Die kretazischen Turbiditserien im Gibraltarbogen: Bindeglied zwischen atlantischer und tethyaler Entwicklung [Ph.D. dissert.]. Univ. Tübingen.

Thurow, J., and Anderson, O. R., 1986. An interpretation of skeletal growth patterns of some middle Cretaceous and modern radiolarians. *Micropaleontology*, 32:289–302.

Thurow, J., and Kuhnt, W., 1986. Mid-Cretaceous of the Gibraltar Arch area. *In* Summerhayes, C. P., and Shackleton, N. J. (Eds.), *North Atlantic Palaeooceanography*: Geol. Soc. Spec. Publ. London, 21: 423–445.

Thurow, J., Kuhnt, W., and Wiedmann, J., 1982. Zeitlicher und paläogeographischer Rahmen der Phthanit- und Black Shale-Sedimentation in Marokko. *Neues Jahrb. Geol. Palaeontol., Abh.*, 165:147–176.

Tippit, P. R., Pessagno, E. A., and Smewing, J. D., 1981. The biostratigraphy of sediments in the volcanic unit of the Samail Ophiolite. *J. Geophys. Res.*, 86(B4):2756–2762.

Turner, J., 1965. Upper Jurassic and Lower Cretaceous microfossils from the Hautes-Alpes. *Paleontology*, 8:391–396.

von Rad, U., and Sarti, M., 1986. Early Cretaceous "events" in the evolution of the eastern and western North Atlantic continental margins. *Geol. Rdsch.*, 75:139–158.

White, M. P., 1928. Some index Foraminifera of the Tampica Embayment area of Mexico (Part II). *J. Paleontol.*, 2:280–317.

Wiedmann, J., and Neugebauer, J., 1978. Lower Cretaceous ammonites from the South Atlantic Leg 40 (DSDP), their stratigraphic value and sedimentologic properties. *In* Bolli, H. M., Ryan, W.B.F., et

al., *Init. Repts. DSDP*, Suppl. 38, 39, 40, 41: Washington (U.S. Govt. Printing Office), 709–721.
Wolfart, R., 1982. Cretaceous radiolaria from the northwest African continental margin. *In* von Rad, U., Hinz, K., Sarnthein, M., and Seibol, E. (Eds.), *The Geology of the Northwest African Continental Margin*: New York (Springer-Verlag), 345–365.
Wu Hao-Ruo, 1986. Some new genera and species of Cenomanian Radiolaria from southern Xizang (Tibet). *Weishengwu Xuebao*, 3:347–363.
Zhamoida, A. I., 1969. Pervye rezu'taty izuchenia mezozoiskikh radioliarii Sakhalina. *In* Vialov, O. C. (Ed.), *Iskopaemye i Sovremennye Radioliarii*: L'vov (Geol. O-vo., L'vov Univ.), 17–28.
_____, 1972. Biostratigrafiya mezozoiskikh kremnistykh tolshch vostoka SSSR na osnove izucheniya radioliarii. *Tr. Vses. Neft. Naucho. Issled. Geologorazved. Inst.*, 183:1–243.

**Date of initial receipt: 6 May 1987**
**Date of acceptance: 17 February 1988**
**Ms 103B-148**

## APPENDIX
### Taxonomic Notes

*Acaeniotyle diaphorogona* Foreman
(Pl. 9, Fig. 8)

*Acaeniotyle diaphorogona* Foreman, 1973b, p. 258, pl. 2, figs. 2–5; Foreman, 1975, p. 607, pl. 2F, figs. 1–5, and pl. 3, figs. 1 and 2; Schaaf, 1981, p. 431, pl. 15, fig. 2; Baumgartner, 1984, p. 753, pl. 1, figs. 1 and 2; Schaaf, 1984, p. 104–105, text figs. 1–5, H; Sanfilippo and Riedel, 1985, p. 586–587, text fig. 4 (1a and 1b).
*Acaeniotyle tribulosa* Foreman, 1973b, p. 258, pl. 2, fig. 8.
*Acaeniotyle* sp. aff. *A. diaphorogona* Foreman, 1973b, pl. 2, figs. 6 and 7, and pl. 16, fig. 16; Empson-Morin, 1981, p. 261, pl. 3, figs. 8A–8D.
*Acaeniotyle gedrangta* Empson-Morin, 1981, pl. 3, figs. 6 and 7.

**Range and occurrences.** This form is recorded worldwide in strata of Tithonian to middle Albian age, and closely related forms are recorded up to the Upper Cretaceous.

*Acaeniotyle* sp. cf. *A. diaphorogona* Foreman
(Pl. 6, Fig. 4)

**Remarks.** This form is very similar in shape and size to *A. diaphorogona*, but it has slightly twisted spines.

*Acaeniotyle umbilicata* (Rüst)
(Pl. 9, Fig. 7)

*Xiphosphaera umbilicata* Rüst, 1898, p. 7, pl. 1, fig. 9; Dumitrica, 1972, p. 832, pl. 1, fig. 1; Renz, 1974, p. 799, pl. 2, figs. 9–12, and pl. 9, fig. 21.
*Xiphosphaera tuberosa* Tan Sin Hok, 1927, p. 35, pl. 5, fig. 8.
Spumellariinid Pessagno, 1969, p. 610, pl. 4, fig. N.
*Acaeniotyle umbilicata* (Rüst)—Foreman, 1973b, p. 258, pl. 1, figs. 13, 14, and 16; Foreman, 1975, p. 607, pl. 2E, figs. 14–17, and pl. 3, fig. 3; Kocher, 1981, p. 51, pl. 12, figs. 1 and 2; Schaaf, 1981, p. 431, pl. 6, fig. 11, and pl. 15, figs. 3a and 3b; Schaaf, 1984, p. 148–149, text figs. 1–3b, H; Sanfilippo and Riedel, 1985, p. 587, text fig. 4 (2a–2d).

**Range.** Tithonian(?) to Albian.
**Occurrences.** Recorded worldwide.

*Acaeniotyle* sp. A
(Pl. 6, Fig. 2)

**Remarks.** This form differs from other species within this genus by its four large spines arranged in an angle of 90°.

*Acanthocircus dicranocanthos* (Squinabol)
(Pl. 10, Fig. 3)

*Saturnalis dicranacanthos* Squinabol, 1914, p. 289, fig. 1, pl. 22, figs. 4 and 6 (not figs. 5 and 7), and pl. 23, fig. 8.
*Saturnalis novalensis* Squinabol, 1914, p. 297, pl. 20, fig. 1, and pl. 23, fig. 7.
*Saturnulus* sp. Fischli, 1916, p. 46, fig. 53.
*Spongosaturnalis dicranacanthos* (Squinabol)—Pessagno, 1969, p. 610, pl. 4, figs. A and B; Moore, 1973, p. 824, pl. 3, figs. 1 and 3.
*Acanthocircus dizonius* (Rüst)—Foreman, 1973b, p. 260, pl. 4, figs. 4 and 5; Riedel and Sanfilippo, 1974, pl. 2, figs. 4 and 5 (not fig. 3).
*Acanthocircus dicranacanthos* (Squinabol)—Foreman, 1975, p. 610, pl. 2D, figs. 5 and 6; Pessagno, 1977a, p. 73, pl. 3, fig. 5; Pessagno, 1977b, p. 31, pl. 2, fig. 6; Kocher, 1981, p. 51–52, pl. 12, fig. 3; Schaaf, 1981, p. 431, pl. 7, fig. 1, and pl. 16, fig. 3; Baumgartner, 1984, p. 754, pl. 1, fig. 7; Schaaf, 1984, p. 106–107, text figs. 1–5; Sanfilippo and Riedel, 1985, p. 591–592, text fig. 5 (2a–2c).

**Range.** Kimmeridgian (in Europe), Tithonian (in North America) to the base of Barremian.
**Occurrences.** Recorded worldwide.

*Acanthocircus* sp. cf. *A. dicranacanthos* (Squinabol)
(Pl. 10, Fig. 4)

**Remarks.** This form is very similar in shape and size to *A. dicranacanthos*, but the characteristic dovetail-like shape of the spine is not clear.

*Acanthocircus trizonalis* (Rüst)
(Pl. 10, Fig. 2)

*Saturnulus trizonalis* Rüst, 1898, p. 9, pl. 2, fig. 4; Fischli, 1916, p. 46, fig. 52.
*Saturnalis amissus* Squinabol, 1914, p. 296, pl. 23, figs. 2–5.
*Saturnalis*? aff. *amissus* Squinabol—Zhamoida, 1969, p. 19, fig. 9, p. 24.
*Spongosaturnalis amissus* (Squinabol)—Moore, 1973, p. 824, pl. 3, fig. 2.
*Acanthocircus trizonalis* (Rüst)(?)—Foreman, 1973b, p. 261, pl. 4, figs. 6–8; Schaaf, 1981, p. 431, pl. 16, fig. 1; Sanfilippo and Riedel, 1985, p. 592, text fig. 5 (1a–1d).
*Acanthocircus dizonius* (Rüst)—Riedel and Sanfilippo, 1974, pl. 2, fig. 3 (not figs. 4 and 5).

**Range.** Valanginian to approximately Aptian.
**Occurrences:** Worldwide.

*Acanthocircus* sp.
(Pl. 10, Fig. 1)

*Acanthocircus* sp. Schaaf, 1981, p. 431, pl. 7, fig. 7.
*Afens liriodes* Riedel and Sanfilippo (Pl. 2, Fig. 1)
*Afens liriodes* Riedel and Sanfilippo, 1974, p. 775, pl. 11, fig. 11, and pl. 13, figs. 14–16; Foreman, 1978b, p. 750, pl. 5, fig. 24; Kling, 1982, p. 548, pl. 1, figs. 23 and 24, and pl. 3, figs. 5 and 6.
*Afens liriodes* Sanfilippo and Riedel, 1985, p. 624, text fig. 13 (3a–3c).
*Incertae sedis* sp. A Moore, 1973, pl. 13, figs. 1–3.

**Remarks.** Sanfilippo and Riedel (1985, p. 624) describe rare *A. liriodes* from the Cismon section, northern Italy. The co-occurrence of Turonian planktonic foraminifera (*Hedbergella lehmanni* and *Globotruncana helvetica*) suggests that *A. liriodes* occurred previously in the Turonian part of the *O. somphedia* Zone.

**Range.** *A. pseudoconulus* Zone to the *A. tylotus* Zone of Sanfilippo and Riedel (1985); approximately Campanian.
**Occurrences.** North Atlantic, Japan, central Pacific, the Caribbean region, and North Italy.

*Alievium antiquum* Pessagno

*Alievium antiquum* Pessagno, 1972, p. 298, pl. 24, figs. 1–4; Pessagno, 1977b, p. 29, pl. 3, figs. 14, 17, 21, and 22; Schaaf, 1981, p. 431, pl. 8, fig. 2, not pl. 7, fig. 10.

**Range.** Barremian(?) to Cenomanian, *A. antiquum* s.s. ranges from upper Albian to Cenomanian.
**Occurrences.** Central Pacific, California, and North Atlantic.

*Alievium gallowayi* (White)
(Pl. 2, Fig. 3)

*Baculogypsina*(?) *gallowayi* White, 1928, p. 305, pl. 4, figs. 9 and 10.
*Aulophacus gallowayi* (White)—Pessagno, 1962, p. 364, pl. 3, figs. 5 and 6.
*Pseudoaulophacus gallowayi* (White)—Pessagno, 1963, p. 202, pl. 2, figs. 1, 3, and 6, pl. 4, figs. 2, 5, and 7, and pl. 7, figs. 2 and 4; Ship-

board Scientific Party, 1969, pp. 206, 209; (?)Riedel and Sanfilippo, 1970, p. 505, pl. 2, fig. 5; (non) Petrushevskaya and Kozlova, 1972, pl. 6, fig. 1.

*Alievium gallowayi* (White)—Pessagno, 1972, p. 299, pl. 25, figs. 4–6, pl. 26, fig. 5, and pl. 31, figs. 2 and 3; Pessagno, 1976, p. 27, pl. 8, figs. 13 and 14, and pl. 9, fig. 1; 1977c, pl. 6, figs. 5 and 6; Pessagno and Longoria, 1973, p. 550; Pessagno and Michael, 1974, p. 969; Foreman, 1975, p. 613, pl. 1D, figs. 2 and 3, and pl. 5, fig. 11; Foreman, 1977, p. 315; 1978a, p. 840; Nakaseko and Nishimura, 1981, p. 142, pl. 2, fig. 3; de Wever, 1981, p. 516; Kling, 1982, p. 548, pl. 1, figs. 15 and 16(?); Taketani, 1982, p. 50, pl. 10, fig. 7; Sanfilippo and Riedel, 1985, p. 594, text fig. 6(1).

*Pseudoaulophacus superbus* (Squinabol)—Riedel and Sanfilippo, 1974, p. 780, pl. 3, figs. 1–3 (in part).

**Range.** *A. pseudoconulus* Zone through the *A. tylotus* Zone of Sanfilippo and Riedel (1985), Campanian through Maestrichtian.

**Occurrences.** North Atlantic, East Indian Ocean, Japan, west and central Pacific, California, the Caribbean region, Bavaria, and Cyprus.

*Alievium helenae* Schaaf
(Pl. 9, Fig. 9)

*Alievium helenae* Schaaf, 1981, p. 431, pl. 7, fig. 9, and pl. 10, figs. 2a and 2b; Kocher, 1981, p. 53, pl. 12, fig. 6; Baumgartner, 1984, p. 755, pl. 1, figs. 8–10; Schaaf, 1984, p. 112–113, text figs. 1–3b, H.

*Alievium* sp. Foreman, 1973b, p. 262, pl. 9, figs. 1 and 2; Foreman, 1975, p. 613, pl. 2D, figs. 7 and 8, and pl. 5, fig. 14.

**Range.** Upper Berriasian to the base of the Aptian.

**Occurrences.** Recorded worldwide.

*Alievium superbum* (Squinabol)
(Pl. 2, Fig. 2)

*Theodiscus superbus* Squinabol, 1914, p. 271, pl. 20, fig. 4.

*Pseudoaulophacus superbus* (Squinabol)—(?)Kling, 1971, pl. 6, figs. 13 and 14; (?)Petrushevskaya and Kozlova, 1972, p. 527, pl. 3, figs. 1–3; (?)Dinkelman, 1973, p. 790, pl. 1, fig. 9; (?)Moore, 1973, p. 825, pl. 12, figs. 4 and 5; (in part) Riedel and Sanfilippo, 1974, p. 780, pl. 3, figs 1–3.

*Alievium superbus* (Squinabol)—Pessagno, 1972, p. 302, pl. 24, figs. 5 and 6, and pl. 25, fig. 1.

*Alievium superbum* (Squinabol)—Dumitrica, 1975, fig. 2; Pessagno, 1976, p. 27, pl. 3, fig. 12; Pessagno, 1977c, pl. 6, fig. 3; Foreman, 1977, p. 315; Schmidt-Effing, 1980, p. 245, fig. 14; Nakaseko and Nishimura, 1981, p. 142, pl. 2, fig. 2; Taketani, 1982, p. 51, pl. 10, fig. 8; Thurow and Kuhnt, 1986, text fig. 9 (7).

(?)*Alievium* sp. cf. *A. superbum* (Squinabol)—Nakaseko et al., 1979, p. 21, pl. 5, fig. 3.

**Range.** *C. cachensis* Zone to the (?) *A. pseudoconulus* Zone (approximately Turonian to Campanian).

**Occurrences.** North Atlantic, eastern Indian Ocean, Japan, central Pacific, California, the Caribbean region, southern Europe, and northwestern Africa.

*Alievium superbum* (Squinabol)—"Cenomanian" form
(Pl. 5, Fig. 11)

**Remarks.** This species, already present in the upper Albian, and described by Schaaf (1984) as *A. superbum*, differs from *A. antiquum* Pessagno by its pillow-shaped outline and the already clearly visible octagonal growth pattern of the meshwork of the skeleton. This species seems to be a transitional form between *A. antiquum* Pessagno and *A. superbum* Pessagno.

*Alievium* sp. A
(Pl. 5, Fig. 12)

**Remarks.** This form differs from other species within this genus by the knobby surface of the test.

*Alievium* sp. B
(Pl. 5, Fig. 16)

*Alievium antiquum* Schaaf, 1981 p. 431, pl. 7, fig. 10.

*Amphipyndax mediocris* (Tan Sin Hok)
(Pl. 1, Fig. 7, and Pl. 4, Fig. 5)

*Dictyomitra mediocris* Tan Sin Hok, 1927, p. 55, pl. 10, fig. 82.

*Stichocapsa stocki* Campbell and Clark, 1944, p. 44, pl. 8, figs. 31–33.

*Stichocapsa megalocephalia* Campbell and Clark, 1944, p. 44, pl. 8, figs. 26 and 34.

*Dictyomitra uralica* Kozlova and Gorbovets, 1966, p. 116, pl. 6, figs. 6 and 7.

*Amphipyndax stocki* (Campbell and Clark)—Foreman, 1968, p. 78, pl. 81, figs. 12a–12c; Foreman, 1973a, p. 430, pl. 13, fig. 5; Petrushevskaya and Kozlova, 1972, p. 545, pl. 8, figs. 16 and 17; Moore, 1973, p. 827, pl. 11, fig. 6; Riedel and Sanfilippo, 1974, p. 775, pl. 11, figs. 1–3, and pl. 15, fig. 11; Pessagno, 1975, p. 1016, pl. 3, figs. 4–8.

*Amphipyndax mediocris* (Tan Sin Hok)—Renz, 1974, p. 788, pl. 5, figs. 7–9, and pl. 12, fig. 3; Schaaf, 1981, p. 431, pl. 3, fig. 11, and pl. 22, figs. 7a and 7b.

**Range.** Not well established in Cretaceous.

**Occurrences.** Recorded worldwide.

*Amphipyndax pseudoconulus* Pessagno
(Pl. 1, Fig. 8)

*Lithostrobus pseudoconulus* Pessagno, 1963, p. 210, pl. 1, fig. 8, and pl. 5, figs. 6 and 8.

*Lithostrobus punctulatus* Pessagno, 1963, pl. 5, figs. 4 and 5 (not holotype, pl. 1, fig. 1).

*Amphipyndax enesseffi* Foreman, 1966, p. 356, text figs. 10 and 11; 1973b, pl. 15, fig. 19; Foreman, 1977, p. 313, pl. 1, fig. 2; Foreman, 1978b, p. 745, pl. 4, fig. 3; Dinkelman, 1973, p. 790, pl. 1, fig. 10; Moore, 1973, p. 827, pl. 11, fig. 5; Riedel and Sanfilippo, 1974, p. 775, pl. 10, figs. 12 and 13; Nakaseko and Nishimura, 1981, pl. 17, fig. 14; Kling, 1982, p. 548, pl. 2, fig. 12, and pl. 4, figs. 2 and 3.

*Amphipyndax* sp. A Petrushevskaya and Kozlova, 1972, p. 545, pl. 8, fig. 18.

*Amphipyndax pseudoconulus* (Pessagno)—Empson-Morin, 1982, p. 510, pl. 1, fig. 5, and pl. 2, figs. 1–5, 9, 10, and 12; Sanfilippo and Riedel, 1985, p. 598, text fig. 7 (1a–1c).

**Range.** Restricted to *A. pseudoconulus* Zone (Campanian).

**Occurrences.** North Atlantic, western Australia, Indonesia, Japan, central Pacific, Alaska, California, the western interior of North America, the Caribbean region, and southern Europe.

*Amphipyndax*(?) sp.
(Pl. 4, Fig. 6)

**Remarks.** This form is tentatively assigned to the *Amphipyndacidae*, but it differs from other species within the genus *Amphipyndax* by its spindle-shaped outline and the decrease in width of the last segments, which are terminally closed.

*Angulobracchia*(?) *portmanni* Baumgartner
(Pl. 10, Figs. 13 and 15)

*Angulobracchia*(?) *portmanni* Baumgartner, 1984, p. 757, pl. 2, figs. 1–3.

*Hagiastrids* gen. et sp. indet. Foreman, 1973b, pl. 7, figs. 1, 3, and 5 (not 2, 4, 6, and 7).

*Paronaella* sp. Schaaf, 1981, p. 436, pl. 8, fig. 7.

**Range and occurrences.** This form is recorded from Berriasian to Barremian in the Pacific, North Atlantic, southern Spain, and the Southern Alps.

*Archaeodictyonitra lacrimula* (Foreman)
(Pl. 3, Fig. 8)

*Archaeodictyomitra lacrimula* (Foreman)—Schaaf, 1981, p. 432, pl. 22, figs. 3a and 3b; Sanfilippo and Riedel, 1985, p. 598–599, text fig. 7 (3a–3c).

*Dictyomitra*(?) *lacrimula* Foreman, 1973b, p. 263, pl. 10, fig. 11; Foreman, 1975, p. 614, pl. 2G, figs. 5 and 6, and pl. 6, fig. 1; Nakaseko et al., 1979, p. 22, pl. 4, fig. 1.

*Cornutana conica* Aliev—Moore, 1973, p. 830, pl. 14, figs. 1 and 2 (not Aliev, 1965, pl. 6, fig. 1).

**Range.** Middle Valanginian to middle Aptian (base of the *S. septemporatus* Zone to the base of the *A. umbilicata* Zone).
**Occurrences.** Recorded worldwide.

*Archaeodictyomitra* sp. cf. *A. lamellicostata* (Foreman)
(Pl. 1, Fig. 14)

**Remarks.** The specimen figured is tentatively assigned to *A. lamellicostata* (Foreman) because of the poor preservation of the specimens observed.

*Archaeodictyomitra pseudoscalaris* (Tan Sin Hok)
(Pl. 7, Fig. 14)

*Archaeodictyomitra pseudoscalaris* (Tan Sin Hok)—Schaaf, 1981, p. 432, pl. 4, fig. 5, and pl. 21, figs. 13a and 13b.
*Stichomitra pseudoscalaris* Tan Sin Hok, 1927, p. 56, pl. 11, fig. 84; (not Renz, 1974, pl. 8, figs. 5 and 6, and pl. 11, fig. 34).

**Range.** Not well established; Lower Cretaceous.
**Occurrences.** North Atlantic, Pacific, and Indonesia.

*Archaeodictyomitra puga* Schaaf
(Pl. 6, Fig. 15)

*Archaeodictyomitra puga* Schaaf, 1981, p. 432, pl. 3, fig. 7, and pl. 21, figs. 11a and 11b.
*Dictyomitra*(?) sp. Dumitrica, 1972, pl. 4, fig. 7.

**Range and occurrences.** Recorded from Barremian in the North Atlantic and Pacific.

*Archaeodictyomitra* sp. cf. *A. puga* Schaaf
(Pl. 6, Fig. 18, and Pl. 7, Fig. 15)

**Remarks.** This form differs from *A. puga* Schaaf by its pronounced costae and the different diameter of the pores in the upper and lower rows.

*Archaeodictyomitra simplex* Pessagno
(Pl. 3, Fig. 9)

*Archaeodictyomitra simplex* Pessagno, 1977b, p. 43, pl. 6, figs. 1, 24, and 28, and pl. 12, fig. 12.

**Range and occurrences.** Recorded from Albian to Cenomanian in California, North Atlantic, and southern Europe.

*Archaeodictyomitra squinaboli* Pessagno

*Archaeodictyomitra squinaboli* Pessagno, 1976, p. 50, pl. 5, figs. 2–8; Blome and Irwin, 1985, text fig. 4 (9).

**Range and occurrences.** Recorded from Albian to Campanian strata of California, approximately Albian of the North Atlantic, and Turonian of Cyprus.

*Archaeodictyomitra vulgaris* Pessagno
(Pl. 6, Fig. 19)

*Dictyomitra* sp. Foreman, 1973b, pl. 10, fig. 8.
*Archaeodictyomitra vulgaris* Pessagno, 1977b, p. 44, pl. 6, fig. 15; Schaaf, 1981, p. 432, pl. 4, fig. 2.

**Range and occurrences.** Recorded from Barremian to Aptian strata of the central Pacific, California, and the North Atlantic.

*Archaeodictyomitra* sp. cf. *A. vulgaris* Pessagno
(Pl. 7, Fig. 13)

**Remarks.** This form differs from *A. vulgaris* by the two rows of pores of each segment, respectively, by the more conical test.

*Archaeodictyomitra* sp. A
(Pl. 3, Fig. 10)

**Remarks.** This form differs from other species within this genus by the inflated second last segment and the tubelike shape of the last segment, which exhibits large rounded pores between the costae.

*Archaeodictyomitra*(?) sp. B
(Pl. 7, Fig. 10)

**Remarks.** This form is tentatively assigned to *Archaeodictyomitra* Pessagno because of its similarities in shape and size.

*Archaeospongoprunum cortinaensis* Pessagno
(Pl. 9, Fig. 19)

*Archaeospongoprunum cortinaensis* Pessagno, 1973, p. 60–61, pl. 9, figs. 4–6; Riedel and Sanfilippo, 1974, p. 775, pl. 1, fig. 9; Pessagno, 1976, p. 33, pl. 1, fig. 3; Pessagno, 1977b, p. 29, pl. 1, fig. 8; Schmidt-Effing, 1980, p. 246, fig. 15; Schaaf, 1981, pl. 7, fig. 11; Taketani, 1982, p. 48–49, pl. 2, fig. 2.

**Range and occurrences.** Recorded worldwide from middle Aptian to lower Campanian.

*Archaeospongoprunum* sp. cf. *A. tehamaensis* Pessagno
(Pl. 6, Fig. 1)

**Remarks.** This form differs from *A. tehamaensis* Pessagno by its large test and the triradiate outline of the polar spines.

*Cavaspongia californiaensis* Pessagno
(Pl. 2, Fig. 21)

*Cavaspongia californiaensis* Pessagno, 1973, p. 77, pl. 19, figs. 2–4; 1976, p. 37, pl. 4, figs. 2 and 3; Kuhnt et al., 1986, pl. 8L.

**Range and occurrences.** Lower Turonian of southern Europe and North Atlantic; lower to middle Turonian of California.

*Cecrops septemporatus* (Parona)
(Pl. 9, Fig. 18)

*Staurosphaera septemporata* Parona, 1890, p. 151, pl. 2, figs. 4 and 5; Cita and Pasquare, 1959, p. 398, fig. 3, no. 7; Moore, 1973, p. 824, pl. 2, fig. 2; Foreman, 1973b, p. 259, pl. 3, fig. 4; Riedel and Sanfilippo, 1974, p. 780, pl. 1, figs. 6–8; Foreman, 1975, p. 609, pl. 2E, fig. 7, and pl. 3, fig. 6; Schaaf, 1981, p. 439, pl. 7, figs. 8a and 8b, and pl. 16, figs. 10a and 10b.
*Cecrops septemporatus* (Parona)—Pessagno, 1977b, p. 33, pl. 3, fig. 11; Kocher, 1981, p. 60, pl. 12, fig. 25; Baumgartner, 1984, p. 761, pl. 2, figs. 17 and 18; Schaaf, 1984, p. 136, p. 137, figs. 1–3b, H.

**Range and occurrences.** Valanginian to Barremian, recorded worldwide.

*Clathropyrgus titthium* Riedel and Sanfilippo
(Pl. 2, Fig. 24)

*Theoperid* gen. et sp. indet. Kling, 1971, pl. 8, figs. 7 and 8; Foreman, 1971, p. 1676, pl. 3, fig. 3; Foreman, 1973a, p. 430, pl. 13, fig. 1; Riedel and Sanfilippo, 1973, pl. 4, fig. 15.
*Artopilium* sp. A Moore, 1973, p. 830, pl. 11, fig. 7.
*Clathropyrgus titthium* Riedel and Sanfilippo, 1974, p. 775, pl. 3, fig. 12, and pl. 12, figs. 9–12; Foreman, 1975, p. 613, pl. 6, fig. 10; Foreman, 1977, p. 315; Foreman, 1978b, p. 746, pl. 5, fig. 19; Kling, 1982, p. 548, pl. 1, fig. 21, and pl. 3, fig. 7; Sanfilippo and Riedel, 1985, p. 616, text fig. 13 (2a–2e).

**Range.** *A. pseudoconulus* Zone into the *A. tylotus* Zone of Sanfilippo and Riedel (1985) (restricted to Campanian).
**Occurrences.** West and East Atlantic, central and North Pacific, and the Caribbean region.

*Conocaryomma lipmanae* (Pessagno)
(Pl. 5, Fig. 9)

*Praeconocaryomma lipmanae* Pessagno, 1976, p. 41, pl. 4, figs. 12 and 13; Taketani, 1982, p. 47, pl. 9, fig. 3.

**Range and occurrences.** Middle Cenomanian to Turonian of Japan, upper Cenomanian to lower Turonian of California, and upper Albian of the North Atlantic.

*Conocaryomma* sp. aff. *C. lipmanae* (Pessagno)
(Pl. 5, Fig. 10)

**Remarks.** This form is very similar in shape and size to *C. lipmanae* but is lacking the spines circular in axial section.

*Conocaryomma universa* (Pessagno)
(Pl. 2, Fig. 18)

*Praeconocaryomma universa* Pessagno, 1976, p. 42, pl. 6, figs. 14–16; Taketani, 1982, p. 47, pl. 1, figs. 3a, 3b, and 4, and pl. 9, fig. 4; Thurow and Kuhnt, 1986, text fig. 9 (22).

*Conocaryomma universa* (Pessagno)—Empson-Morin, 1981, pl. 3, fig. 5.

**Remarks.** Pessagno's (1976) holotype shows remains of radial spines that are triradiate in axial section. Campanian forms do not show such spines clearly, or they are lacking (Empson-Morin, 1981, pl. 3, fig. 5).

**Range.** *C. cachensis* Zone to the *A. pseudoconulus* Zone (Turonian to middle Campanian).

**Occurrences.** North Atlantic, Japan, central Pacific, the Caribbean region, Cyprus, and Bavaria.

*Conocaryomma* sp. cf. *C. universa* Pessagno
(Pl. 2, Figs. 17a and 17b)

*Conocaryomma* sp. A—Empson-Morin, 1984, pl. 1, fig. 9.

**Remarks.** This form differs from *C. universa* in having strongly conical shaped tubercles or mammae.

**Range and occurrences.** Recorded from the Campanian of the North Atlantic, Caribbean region, Bavaria, Cyprus, and central Pacific.

*Conocaryomma* sp. A
(Pl. 9, Fig. 5)

*Praeconocaryomma* sp. A Pessagno, 1977b, p. 34, pl. 3, fig. 23.
*Conocaryomma*(?) sp. (Pl. 9, Fig. 6)

**Remarks.** This form is tentatively assigned to *Conocaryomma* (Pessagno) because of its similarities in shape and size.

*Conosphaera tuberosa* Tan Sin Hok
(Pl. 9, Fig. 3)

*Conosphaera tuberosa* Tan Sin Hok, 1927, p. 36, pl. 6, fig. 10; Schaaf, 1981, p. 432, pl. 12, figs. 5a and 5b.
?*Conosphaera tuberosa* Tan Sin Hok—Renz, 1974, p. 789, pl. 2, figs. 6–8, and pl. 17, fig. 17.

**Remarks.** This form is similar to *Conocaryomma* Pessagno in many respects, but lacks spines.

**Range and occurrences.** Recorded from Barremian (approximately) sediments in the North Atlantic, Indian Ocean, Pacific, and Indonesia.

*Crolanium pythiae* Schaaf
(Pl. 6, Fig. 23)

*Dictyomitra*(?) sp. Foreman, 1975, p. 615, pl. 2H, fig. 4.
*Crolanium pythiae* Schaaf, 1981, p. 432, pl. 20, figs. 5a–5c.

**Range.** *C. pythiae* ranges from the base of the *C. pythiae* Zone into the *S. euganea* Zone (Barremian to lower Aptian).

**Occurrences.** North Atlantic and Pacific.

*Crolanium* sp. cf. *C. triquetrum* Pessagno
(Pl. 3, Fig. 14)

**Remarks.** This species differs from *C. triquetrum* Pessagno and from *C. cunetus* (Aliev and Smirnova) by its pronounced triangular outline and its prominent tubercles.

*Crucella cachensis* Pessagno
(Pl. 2, Fig. 13)

*Crucella cachensis* Pessagno, 1971b, p. 53–54, pl. 9, figs. 1–3; Pessagno, 1976, p. 31–32, pl. 3, figs. 14–15; Kuhnt et al., 1986, pl. 7J; Thurow and Kuhnt, 1986, text fig. 9 (5 and 6).
(probably *C. cachensis* Taketani, p. 50, pl. 9, fig. 16; non *Crucella* sp. cf. *C. cachensis*, Schaaf, p. 433, pl. 8, fig. 3).

**Range.** *C. cachensis* Zone, uppermost Cenomanian/base of Turonian to middle Turonian in Europe/North Atlantic and Turonian in California.

**Occurrences.** North Atlantic, southern Europe, California, and Japan.

*Crucella espartoensis* Pessagno
(Pl. 2, Fig. 14)

*Crucella espartoensis* Pessagno, 1971b, p. 54–55, pl. 18, figs. 1–4; Pessagno, 1976, p. 32, pl. 8, fig. 16; Taketani, 1982, p. 50, pl. 9, fig. 15.

**Range.** Santonian/Campanian of California, upper Coniacian to Campanian of Japan.

**Occurrences.** North Atlantic, the Caribbean region, California, and Japan.

*Crucella messinae* Pessagno
(Pl. 5, Fig. 22)

*Crucella messinae* Pessagno, 1971b, p. 56, pl. 6, figs. 1–3; Pessagno, 1976, p. 32, pl. 1, fig. 4; Pessagno, 1977b, p. 27, pl. 1, figs. 3, 4, and 13; Foreman, 1975, p. 612, pl. 5, fig. 2, and pl. 10, figs. 8 and 9; Taketani, 1982, p. 50, pl. 9, fig. 17.

**Range.** Approximately Aptian to Cenomanian.

**Occurrences.** North Atlantic, North Africa, southern Europe, the Carribbean region, California, North Pacific, and Japan.

*Crucella*(?) sp. A
(Pl. 2, Figs. 12 and 16)

*Crucella*? sp. A—Empson-Morin, 1984, pl. 1, figs. 4 and 5.

**Remarks.** This form differs from *Crucella* sp. by having short robust rays with low length-to-width ratio and a skeleton strongly biconvex in peripheral view.

**Range and occurrences.** Recorded from Campanian sediments: North Atlantic, the Caribbean region, Bavaria, Cyprus, and the central Pacific.

*Crucella* sp. B
(Pl. 2, Fig. 15)

**Remarks.** This form is quite similar to *C. espartoensis* but is lacking the central lacuna.

*Crucella*(?) sp. C
(Pl. 5, Fig. 21)

**Remarks.** This form is tentatively assigned to *Crucella* because of its four rays and the meshwork of its skeleton; it differs by the thickened terminal parts of the rays.

*Crucella*(?) sp. D
(Pl. 5, Fig. 23)

**Remarks.** This form is tentatively assigned to *Crucella* because of its four rays with terminal spines; it differs by the meshwork pattern of the central part of the skeleton.

*Cryptamphorella conara* (Foreman)
(Pl. 1, Fig. 2, and Pl. 5, Fig. 1)

*Hemicryptocapsa conara* Foreman, 1968, p. 35, pl. 4, figs. 11a and 11b.
*Cryptamphorella conara* (Foreman)—Dumitrica, 1970, p. 80, pl. 11, figs. 66a and 66c; Dumitrica, 1972, p. 842, pl. 1, figs. 2–5; Dumitrica, 1975, fig. 2, no. 28; Moore, 1973, p. 827, pl. 7, figs. 4 and 5(?); Nakaseko et al., 1979, p. 21, pl. 6, fig. 1; (non) Schaaf, 1981, p. 433, pl. 1, figs. 6a and 6b, and pl. 9, figs. 15a and 15b; Nakaseko and Nishimura, 1981, p. 148, pl. 5, figs. 11a and 11b; Kling, 1982, p. 549, pl. 5, figs. 10 and 11; Taketani, 1982, p. 67, pl. 7, figs. 6a, 6b, 7a, and 7b; Sanfilippo and Riedel, 1985, p. 613, text fig. 12 (1a–1c).
(non) *Cryptamphorella* sp. aff. *C. conara* (Foreman)—Petrushevskaya and Kozolova, 1972, p. 541, pl. 2, fig. 17.
(non) *Cryptamphorella* cf. *conara* (Foreman)—Dumitrica, 1972, p. 842, pl. 1, figs. 2–5.

**Range.** *A. umbilicata* through the *A. tylotus* Zone of Sanfilippo and Riedel (1985) (approximately Albian through Maestrichtian), *C. conara* (Pl. 8, Fig. 20) is from a sample dated as Barremian by nannofossils and benthic foraminifers.

**Occurrences.** North Atlantic, Japan, central Pacific, California, Romania, southern Europe, and northwestern Europe.

*Cryptamphorella* sp. cf. *C. conara*
(Pl. 8, Fig. 20)

**Remarks.** This form is similar in shape and size to *C. conara*, but the outer shape of the cephalic-thoracic part (no partly sunken thorax, no

central depression) and the development of the prominent sutural pore are different.

*Cryptamphorella dumitricai* Schaaf
(Pl. 8, Fig. 23, and Pl. 10, Fig. 19)

*Cryptamphorella dumitricai* Schaaf, 1981, p. 433, pl. 1, figs. 5a–5c, and pl. 9, figs. 5a, 5b, 13a, and 13b.

**Range and occurrences.** Recorded from Barremian strata of the central Pacific and the North Atlantic.

*Cryptamphorella macropora* Dumitrica
(Pl. 1, Fig. 3)

*Cryptamphorella macropora* Dumitrica, 1970, p. 37, pl. X, figs. 64a–64c and 65 (non pl. XI, figs. 67, 69–72a, and 72b).

**Range and occurrences.** This form is recorded from the lower Campanian of Romania and the North Atlantic.

*Cryptamphorella* sp. A
(Pl. 9, Fig. 2)

**Remarks.** This form is similar in shape and size to *C. conara*, but the outer shape of the cephalic-thoracic part and the development of the prominent sutural pore are different.

*Cryptamphorella* sp. B
(Pl. 8, Fig. 22)

**Remarks.** This form is similar in shape and size to *C. conara*, but differs in the outer shape of the cephalic-thoracic part and the development of a ring of large pores around it.

*Cyclastrum infundibuliforme* Rüst
(Pl. 9, Fig. 21)

*Cyclastrum infundibuliforme* Rüst, 1898, p. 28, pl. 9, fig. 5; Schaaf, 1981, p. 433, pl. 14, fig. 8.

**Range and occurrences.** Recorded from upper Barremian of the central Pacific and the North Atlantic.

*Cyrtocapsa* sp. cf. *C. grutterinki* Tan Sin Hok
(Pl. 8, Figs. 2 and 3)

*Cyrtocapsa grutterinki* Tan Sin Hok, 1927, p. 64, pl. 13, fig. 110; Schaaf, 1981, p. 433, pl. 6, figs. 6a and 6b.

*Dibolachras tytthopora* Foreman
(Pl. 7, Fig. 20)

*Dibolachras tytthopora* Foreman, 1973b, p. 265, pl. 11, fig. 4, and pl. 16, fig. 15; Foreman, 1975, p. 617, pl. 2L, figs. 2 and 3, and pl. 6, fig. 16; Schaaf, 1981, p. 433, pl. 5, figs. 3a and 3b, and pl. 26, figs. 1a, 1b, and 4; Schaaf, 1984, p. 146–147, text figs. 1–3b, H.

**Range.** *D. tytthopora* Zone into the *S. euganea* Zone (Hauterivian into lower Aptian).

**Occurrences.** Pacific, Indian Ocean, and North Atlantic.

*Dictyomitra formosa* Squinabol
(Pl. 1, Fig. 25)

*Dictyomitra formosa* Squinabol, 1904, p. 232, pl. X, fig. 4; Moore, 1973, p. 829, pl. 1, figs. 1 and 3 (non 2 and 4); Pessagno, 1976, p. 51, pl. 8, figs. 10–12; Taketani, 1982, p. 58, pl. 4, figs. 6a and 6b, and pl. 11, fig. 13; Kawabata, 1984, pl. 2, fig. 3.
*Dictyomitra torquata* Foreman—Butt, 1981, pl. 20, fig. 2 and ?3.
*Dictyomitra multicostata* Zittel—Pessagno, 1963, p. 206–208, pl. 1, fig. 10, pl. 4, figs. 1 and 3, and pl. 5, fig. 7.

**Remarks.** *D. formosa* Squinabol differs from *D. multicostata* Zittel s.s. by having deep strictures between the postabdominal chambers, more massive costae, a more markedly lobate test, and only weakly developed costae on the cephalis and thorax.

**Range.** *T. urna* Zone into the *A. pseudoconulus* Zone of Sanfilippo and Riedel (1985) (lower Coniacian to lower Campanian in California, lower Campanian of Bavaria, and Turonian to Campanian in the North Atlantic).

**Occurrences.** North Atlantic, Japan, Bavaria, central Pacific, and northern Italy.

*Dictyomitra* cf. *D. formosa*
(Pl. 1, Fig. 23)

**Remarks.** The length/width ratio and the number of coastae of the figured specimen are not in accordance with a strict definition of *D. formosa*. *Dictyomitra* cf. *D. formosa* might be an ancestor of *D. formosa*/*D. koslovae*.

*Dictyomitra koslovae* s.l.
(Pl. 1, Fig. 29)

(?)*Dictyomitra* sp. C Riedel and Schloecker, 1956, p. 360, text fig. 7.
*Dictyomitra* sp. Kling, 1971, p. 1090, pl. 8, fig. 2; Foreman, 1971, p. 1677, pl. 3, fig. 5; Foreman, 1973b, pl. 15, figs. 13–15.
(?)*Dictyomitra torquata* Foreman—Foreman, 1971, p. 1676, pl. 3; de Wever, 1981, p. 516.
*Dictyomitra duodecimcostata* (Squinabol) group—Petrushevskaya and Kozlova, 1972, p. 550, pl. 2, fig. 11 (not 10).
*Dictyomitra* cf. *D. torquata* Foreman—Moore, 1973, p. 829, pl. 9, figs. 1–4.
*Dictyomitra torquata* Foreman—Riedel and Sanfilippo, 1974, p. 778, pl. 5, figs. 1–4, and pl. 14, fig. 2.
*Dictyomitra koslovae* Foreman, 1975, p. 614, pl. 7, fig. 4; (non) Foreman, 1978b, p. 746, pl. 4, fig. 10; Nakaseko and Nishimura, 1981, p. 151, pl. 8, figs. 2–5, and pl. 16, figs. 2 and 3; de Wever, 1981, p. 516; Kling, 1982, p. 548, pl. 2, fig. 10 (not pl. 3, fig. 4); Taketani, 1982, p. 58, pl. 4, figs. 9 and 10, and pl. 11, figs. 14 and 15.
*Dictyomitra duodecimcostata duodecimcostata* (Squinabol)—Foreman, 1978b, pl. 4, fig. 9 (not 8); Kling, 1982, p. 549, pl. 4, fig. 6.
*Dictyomitra* cf. *duodecimcostata* (Squinabol)—Nakaseko et al., 1978, p. 22, pl. 7, fig. 2, and questionably pl. 8, figs. 15 and 16.
*Dictyomitra koslovae* s.l., Sanfilippo and Riedel, 1985, p. 599, text fig. 7 (4a–4e).
*Dictyomitra* cf. *D. multicostata* Zittel—Butt, 1981, pl. 20, fig. 1.

**Remarks.** Included here in this species are all specimens with a prominent fourth segment.

**Range.** *A. pseudoconulus* Zone into the *A. tylotus* Zone of Sanfilippo and Riedel (1985); approximately Campanian.

**Occurrences.** West and East Atlantic, Japan, central and northwest Pacific, California, the Caribbean region, Bavaria, and eastern Indian Ocean.

*Dumitricaia maxwellensis* Pessagno
(Pl. 2, Fig. 22)

*Dumitricaia maxwellensis* Pessagno, 1976, p. 38–39, pl. 4, figs. 10–11; Thurow and Anderson, 1986, pl. 5, fig. 3; Thurow and Kuhnt, 1986, text fig. 9 (23).

**Range and occurrences.** This form is recorded from lower Turonian strata in California, the North Atlantic, southern Europe, and northwest Africa.

*Eastonerius* sp. A
(Pl. 1, Fig. 16)

**Remarks.** This species is quite similar to *Eastonerius acuminatus* (Dumitrica), but the overall shape is more spindlelike and it posesses a long spine.

**Range.** Recorded from Campanian strata by Dumitrica (1970) and Empson-Morin (1981).

*Eucyrtidium*(?) sp. div. (*Eucyrtidium*(?) sp. A–J)
(Pl. 1, Figs. 9–12)

**Remarks.** Included are all forms that show close relationships to *Eucyrtidium* Ehrenberg. This genus contains various forms and has a long stratigraphic range. In view of phylogeny, one has to divide this genus into several genera; the species from Hole 603B herein are only tentatively assigned to *Eucyrtidium*.

*Eucyrtis* sp. A
(Pl. 4, Fig. 7)

**Remarks.** This form is similar in shape and size to *Eucyrtis* Haeckel but is lacking the apical spine.

*Eusyringium spinosum* Squinabol
(Pl. 4, Fig. 18)

*Eusyringium spinosum* Squinabol, 1903, p. 141, pl. 8, fig. 42; Taketani, 1982, p. 64, pl. 6, figs. 2a–2c, 3a, 3b, 4a, and 4b, and pl. 13, figs. 4 and 5.
*Eucyrtis bulbosus* Renz—Riedel and Sanfilippo, 1974, p. 778, pl. 5, fig. 8; Foreman, 1975, p. 615, pl. 2K, fig. 3, not figs. 4 and 5.
*Eucyrtis spinosus* (Squinabol)—Dumitrica, 1975, p. 87–89, text fig. 2, fig. 25.

**Range.** Not well established in the mid-Cretaceous. Recorded from Japan, Indian Ocean, Romania, northern Italy, and the North Atlantic.

*Eusyringium* sp. cf. *E. spinosum* Squinabol
(Pl. 4, Fig. 20)

**Remarks.** This form is similar in shape and size to *E. spinosum*, but each node terminates in a circular spine, and the postabdominal tube is missing (broken?).

*Eusyringium*(?) *formanae* Taketani
(Pl. 4, Fig. 19)

*Eusyringium*(?) *formanae* Taketani, 1982, p. 64, pl. 6, figs. 1a and 1b, and pl. 13, fig. 2.

**Range and occurrences.** Albian of the North Atlantic and Japan.

*Godia*(?) sp. A
(Pl. 5, Fig. 20)

*Godia*(?) sp. B
(Pl. 5, Fig. 17)

*Godia*(?) sp. C
(Pl. 5, Fig. 15)

*Godia*(?) sp. D
(Pl. 9, Fig. 15)

*Godia*(?) sp. E
(Pl. 9, Fig. 22)

*Godia*(?) sp. F
(Pl. 9, Fig. 23)

Gen. et sp. indet., Schaaf 1981, pl. 10, figs. 8a and 8b.

**Remarks.** All species are quite common in the interval at Site 398. They are tentatively assigned to the genera *Godia* Wu Hao-Ruo because of their morphologic similarities and coeval occurrence.

**Range and occurrences.** Uppermost Albian/Cenomanian of Tibet and Site 398.

*Halesium quadratum* Pessagno
(Pl. 2, Fig. 10)

*Halesium quadratum* Pessagno, 1971b, p. 23–25, pl. 3, figs. 1–6, and pl. 4, figs. 1 and 2; Pessagno, 1976, p. 29, pl. 1, fig. 5; Thurow and Kuhnt, 1986, text fig. 9 (16).

**Range and occurrences.** This form is recorded from Cenomanian/lower Turonian strata in California, the North Atlantic, southern Europe, northwest Africa, and the Middle East.

*Halesium sexangulum* Pessagno
(Pl. 6, Fig. 3)

*Halesium sexangulum* Pessagno, 1971b, p. 25–26, pl. 1, figs. 5 and 6, and pl. 2, figs. 1–6; Pessagno, 1976, p. 29, pl. 1, fig. 6; Tippit et al., 1981, text fig. 3 (9), Thurow and Kuhnt, 1986, text fig. 9 (15).
*Halesium* cf. *sexangulum*—Kuhnt et al., 1986, pl. 7E.

**Range and occurrences.** *Halesium sexangulum* s.s. is recorded from Cenomanian/lower Turonian strata in California, the North Atlantic, southern Europe, northwest Africa, and the Middle East. The form figured is common in Aptian/Albian samples at Sites 398D/641C, and it differs from Pessagno's holotype by lacking the pronounced alternations of the pores.

*Heliocryptocapsa* sp. A
(Pl. 1, Fig. 4)

*Heliocryptocapsa* sp. A—Empson-Morin, 1984, pl. 2, figs. 1 and 2.

**Remarks.** This species shows relationships to some extent with *H. neagui* Dumitrica (1970) from the lower Campanian of Romania. *H.* sp. A is recorded from the Campanian of the Caribbean region, the North Atlantic, Bavaria, and Cyprus.

*Hemicryptocapsa polyhedra* Dumitrica
(Pl. 1, Fig. 1)

*Hemicryptocapsa polyhedra* Dumitrica, 1970, p. 28, pl. 14, figs. 85a–85c; Tippit et al., 1981, text fig. 3 (6); Taketani, 1982, p. 66, pl. 7, figs. 5a and 5b.

**Range and occurrences.** This form is common in lower Turonian strata from the North Atlantic, southern Europe, Romania, and the Middle East.

*Hemicryptocapsa prepolyhedra* Dumitrica

*Hemicryptocapsa prepolyhedra* Dumitrica, 1970, p. 71, pl. 13, figs. 80a–80c and 81–83b, and pl. 20, fig. 131; probably Moore, 1973, p. 827, pl. 8, figs. 1 and 2.

**Range and occurrences.** Recorded from Cenomanian strata in Romania and from lower Turonian in the North Atlantic.

*Hemicryptocapsa* sp. cf. *H. polyhedra* Dumitrica
(Pl. 5, Fig. 2)

**Remarks.** This species is closely related to *H. polyhedra*, but it is distinguished by its less pronounced polygonal areas and smaller pores.

*Hemicryptocapsa*(?) sp. A
(Pl. 8, Fig. 18)

**Remarks.** This specimen, quite common in the interval, is tentatively assigned to the genus *Hemicryptocapsa* Dumitrica because of its internal skeletal elements.

*Hexapyramis pantanelli* Squinabol
(Pl. 6, Fig. 5)

*Hexapyramis pantanelli* Squinabol, 1903, p. 114, pl. 10, fig. 5.
*Histiastrum aster* Lipman—Schaaf, 1981, p. 435, pl. 8, fig. 1, and pl. 11, fig. 5.

**Remarks.** The form, figured by Schaaf (1981), is the common fragmentation product of *Hexapyramis pantanelli*, with two rays missing (compare with Pl. 9, Fig. 13).

**Range and occurrences.** Aptian to Cenomanian of northern Italy and Hole 398D.

*Hexastylurus magnificus* (Squinabol)
(Pl. 9, Fig. 16)

*Staurosphaera magnifica* Squinabol, 1904, p. 191, pl. 3, fig. 1.
*Hexastylurus magnificus* (Squinabol)—Schaaf, 1981, p. 435, pl. 7, fig. 2, and pl. 14, figs. 1a and 1b.

**Range and occurrences.** Not well established: Lower Cretaceous of Italy, the North Atlantic, and Pacific.

*Holocryptocanium barbui* Dumitrica
(Pl. 5, Figs. 5–8)

*Holocryptocanium barbui* Dumitrica, 1970, p. 76, pl. 17, figs. 105–108b, and pl. 21, fig. 136; Foreman, 1975, p. 618, pl. 1F, and pl. 6, fig. 13; Schaaf, 1981, p. 435, pl. 2, figs. 1a and 1b, and pl. 10, figs. 6a and 6b; Taketani, 1982, p. 67, pl. 7, figs. 1a and 1b, and pl. 13, figs. 18 and 19; Sanfilippo and Riedel, 1985, p. 614, text fig. 12 (2a–2c).
*Holocryptocanium japonicum* Nakaseko et al., 1979, p. 23, pl. 5, figs. 8 and 10; Taketani, 1982, p. 67, pl. 7, figs. 2a, 2b, and 3, and pl. 13, fig. 21.
*Holocryptocanium barbui japonicum* Dumitrica—Nakaseko and Nishimura, 1981, p. 154, pl. 3, figs. 5–7, and pl. 14, fig. 10.

**Remarks.** In the material observed there is a progressive trend in skeletal evolution from forms with a smooth surface and small pores to forms with hexagonal pore frames.

**Range and occurrences.** This form ranges from the *A. umbilicata* Zone into the *O. somphedia* Zone of Sanfilippo and Riedel (1985) (approximately middle Aptian to Cenomanian) and has been recorded from the North Atlantic, Romania, Japan, and northwest Pacific.

*Holocryptocanium* sp. A
(Pl. 4, Fig. 25)

**Remarks.** This species differs from all other species of this genus by having small tubercles alternating with large pores.

*Holocryptocanium* sp. B
(Pl. 9, Fig. 1)

*Cryptocephalic* Nasselaria gen. et sp. indet.—Schaaf, 1981, pl. 2, fig. 2.

**Remarks.** This form is always preserved as silica, even when all other specimens are replaced by pyrite.

*Holocryptocanium* sp. C
(Pl. 8, Fig. 21)

*Holocryptocanium* sp. Schaaf, 1981, pl. 2, fig. 8.

**Remarks.** This species differs from *H.* sp. B by having regularly arranged polygonal pores and replacement by pyrite.

*Homoeoparonaella* sp. A
(Pl. 10, Fig. 10)

**Remarks.** This species, quite common in the interval, differs from all other species of this genus by its spongy meshwork between the arms.

*Mita gracilis* (Squinabol)
(Pl. 3, Fig. 2)

*Sethoconus gracilis* Squinabol, 1903, p. 131, pl. 10, fig. 13.
*Mita magnifica* Pessagno—Schaaf, 1981, p. 435, pl. 6, fig. 10, and pl. 24, figs. 13a and 13b.
*Mita gracilis* (Squinabol)—Taketani, 1982, p. 60, pl. 5, figs. 2a and 2b, and pl. 12, fig. 3; Schaaf, 1984, p. 110–111, text figs. 5a–5c.

**Remarks.** The specimen figured shows a rounded cephalo-thoracic part, which is characteristic of *Mita gracilis*. Morphotypes that are similar but are lacking the slight inflation of the cephalo-thoracic part have their first appearance in the middle Albian (and would be named *M. magnifica* Pessagno), whereas *M. gracilis* already occurs in the lowermost Albian at Hole 398D.

*Mita* sp. A
(Pl. 3, Fig. 1)

**Remarks.** This species differs from all other species of this genus by its rounded apical area without horn and its oval outline in lateral view. It is probably synonymous to Pessagno's *Mita* sp. B (1977b, p. 45, pl. 7, fig. 6).

*Mita* sp. B
(Pl. 3, Fig. 3)

**Remarks.** This species differs from *M. gracilis* by its large inflated terminal segment. It was found only in samples from Core 398D-63. Figure 2 (p. 11) of Schaaf (1985) is probably a flattened fragment of *Mita* sp. B.

*Mita* sp. C
(Pl. 3, Fig. 4)

**Remarks.** This form similar to *Mita* sp. B is probably an ancestral form of the latter species.

*Mita*(?) sp. D
(Pl. 6, Fig. 21)

*Mita*(?) sp. E
(Pl. 6, Fig. 22)

**Remarks.** This species is tentatively assigned to the genus *Mita* because of its morphotypic similarities.

*Napora durhami* (Pessagno)
(Pl. 5, Fig. 4)

*Ultranapora durhami* Pessagno, 1977b, p. 39, pl. 5, figs. 1–3, 13, 14, and 19, and pl. 12, fig. 4.

**Range and occurrences.** Albian of California and northeastern Atlantic.

*Napora praespinifera* (Pessagno)
(Pl. 5, Fig. 3)

*Ultranapora praespinifera* Pessagno, 1977b, p. 39, pl. 5, figs. 4 and 8–10.

**Remarks.** The preservation of *Napora* ssp. in the samples studied (the apical horn missing) excludes, with a few exceptions, determination to a species level.

**Range and occurrences.** Upper Albian of California and northeastern Atlantic.

*Neosciadiocapsa diabloensis* Pessagno
(Pl. 2, Fig. 25)

*Neosciadiocapsa diabloensis* Pessagno, 1969, p. 410–411, pl. 35, figs. 3–10, and pl. 36, fig. 1; Pessagno, 1976, p. 47, pl. 13, fig. 5.

**Range.** Upper Campanian of California and lower to middle Campanian of Hole 603B.

**Occurrences.** North Atlantic and California.

*Novixitus mclaughlini* Pessagno
(Pl. 3, Fig. 21)

*Novixitus mclaughlini* Pessagno, 1977b, p. 54, pl. 9, fig. 17.

**Range and occurrences.** This species is recorded from uppermost Albian/lower Cenomanian of California, Hole 398D, and southern Spain.

*Novixitus weyli* Schmidt-Effing
(Pl. 4, Fig. 1)

*Novixitus weyli* Schmidt-Effing, 1980, p. 252–253, fig. 33; Taketani, 1982, p. 62, pl. 5, figs. 9a and 9b, and pl. 12, fig. 11.
(?)*Stichomitra elegans* (Squinabol)—Dumitrica, 1975, p. 87–89, text fig. 2, fig. 11.

**Range and occurrences.** This species is recorded from uppermost Albian/lower Cenomanian of southern Europe, North Atlantic, the Caribbean area, California, and Japan.

*Novixitus* sp. A Pessagno, 1977b, p. 54, pl. 9, fig. 6.

**Range and occurrences.** Upper Albian to Cenomanian of southern Europe, the North Atlantic, the Caribbean area, California, and Japan.

*Novixitus* sp. A
(Pl. 1, Fig. 28)

**Remarks.** This species differs from *Novixitus mclaughlini* by having only one circumferentially arranged row of large tubercles.

*Novixitus* sp. B
(Pl. 1, Fig. 30)

**Remarks.** This species differs from *Novixitus mclaughlini* by having only one circumferentially arranged row of large tubercles and small tubercles on the other rows.

*Novixitus* sp. C
(Pl. 3, Figs. 18 and 18A)

**Remarks.** This species differs from all other species of *Novixitus* by the "pseudomacrocephalic" appearance of its first segments. Common in the uppermost Albian at Hole 398D.

*Novixitus*(?) sp. D
(Pl. 1, Fig. 20)

*Novixitus*? sp. C—Empson-Morin, 1984, pl. 2, fig. 13.
*Theocampe* sp.—Butt, 1981, p. 20, fig. E.

**Range and occurrences.** Campanian of the North Atlantic and Bavaria.

*Obesacapsula*(?) sp. A
(Pl. 1, Fig. 19)

*Novixitus*? sp. B—Empson-Morin, 1984, pl. 2, fig. 12.

**Remarks.** The species is tentatively assigned to *Obesacapsula* Pessagno because of its morphotypic similarities with *O. somphedia*.

*Orbiculiforma railensis* Pessagno
(Pl. 5, Fig. 18, and Pl. 9, Fig. 20)

*Orbiculiforma railensis* Pessagno, 1977b, p. 28, pl. 1, figs. 14 and 21, and pl. 12, fig. 5.

**Range and occurrences.** Recorded from Albian strata in California and Hole 398D.

*Pantanellium lanceola* (Parona)
(Pl. 9, Fig. 14)

(?)*Stylosphaera lanceola* Parona, 1890, p. 150, pl. 1, fig. 19.
*Stylosphaera* sp. Parona, 1890, p. 150, pl. 1, fig. 18; Zhamoida in Dundo and Zhamoida, 1963, pl. 1, fig. 9; Kling, 1971, p. 1089, pl. 10, fig. 3.
*Tithatractus* sp. Parona and Rovereto, 1895, p. 175, fig. 27 (not fig. 28).
*Xiphostylus felsinae* Neviani, 1901, p. 649, pl. 9, fig. 7.
*Stylatractus ovatus* Hinde, 1900, p. 19, pl. 4, figs. 29, 31–33, and 36; Moore, 1973, p. 823, pl. 2, fig. 1.
*Stylatractus paronae* Hinde, 1900, p. 18, pl. 4, fig. 34.
*Stylosphaera squinaboli* Tan Sin Hok, 1927, p. 35, pl. 6, figs. 9a–9d.
Radiolarian (?)*Meyenella hensoni* Davis, 1950, p. 210, pl. 7, figs. 11 and 12. (gen. and sp. indet.) Turner, 1965, p. 394, pl. 52, figs. 14 and 15.
*Spumellariinid* Pessagno, 1969, p. 610, pl. 4, fig. D.
*Sphaerostylus lanceola* (Parona) group—Foreman, 1973b, p. 258, pl. 1, figs. 7–11; Foreman, 1975, p. 609, pl. 2E, figs. 3–6; Schaaf, 1981, p. 438, pl. 7, fig. 6; pl. 16, figs. 5a and 5b.
*Sphaerostylus lanceola* (Parona)—Riedel and Sanfilippo, 1974, pl. 1, figs. 1–3.
*Pantanellium corriganensis* Pessagno, 1977b, p. 33, pl. 3, figs. 5 and 6.
*Pantanellium riedeli* Pessagno, 1977b, p. 33, pl. 3, figs. 1.
*Pantanellium lanceola* (Parona)—de Wever and Thiebault, 1981, p. 589, pl. 2, fig. 9.
*Paronaella* sp. cf. *P. bandyi* Pessagno (Pl. 10, Fig. 12).
*Paronaella bandyi* Pessagno, 1977a, p. 69, pl. 1, figs. 4 and 5; Baumgartner, 1980, p. 300, pl. 9, fig. 4; Kocher, 1981, p. 79; Baumgartner, 1984, p. 777, pl. 6, fig. 16.
(?)*Paronaella mulleri* Pessagno—Ishida, 1983, pl. 10, fig. 4.

**Remarks.** The species figured differs from *P. bandyi* by lacking the terminal dovetail-like spines.

*Paronaella* sp. A
(Pl. 6, Fig. 7)

**Range and occurrences.** Common in Albian strata at Hole 398D.

*Paronaella* sp. B
(Pl. 6, Fig. 8)

**Remarks.** Numerous, but always fragmented. The lack of a complete specimen excludes determination to a species level.

*Paronaella* sp. C
(Pl. 10, Fig. 19)

*Parvicingula boesii* (Parona)
(Pl. 6, Fig. 9)

*Dictyomitra boesii* Parona, 1890, p. 170, pl. 6, fig. 9; Riedel and Sanfilippo, 1974, p. 778, pl. 4, figs. 5 and 6; Foreman, 1975, p. 613, pl. 2H, figs. 10 and 11, and pl. 7, fig. 9.
*Lithocampe ananassa* Rüst, 1885, p. 315, pl. 40, fig. 3; Moore, 1973, p. 828, pl. 4, figs. 7–9.
*Amphipyndax*(?) sp. Foreman, 1973b, p. 263, pl. 9, figs. 3 and 4.
*Parvicingula boesii* (Parona)—Pessagno, 1977b, p. 48, pl. 8, fig. 5; Schaaf, 1981, p. 436, pl. 3, figs. 13a and 13b, pl. 4, fig. 13, and pl. 18, figs. 6a and 6b.
*Mirifusus boesii* (Parona)—Foreman, 1978b, p. 746, pl. 2, fig. 6.
*Parvicingula boesii* (Parona) group—Kocher, 1981, p. 81–82, pl. 15, figs. 10 and 11.

**Range.** Upper Jurassic to Barremian (Albian/lower Cenomanian—Moore, 1973).
**Occurrences.** Recorded worldwide.

*Parvicingula malleola* (Aliev)

*Dictyomitra malleola* Aliev, 1961, p. 62, pl. 2, figs. 5–7; Aliev, 1965, p. 48, pl. 8, figs. 4–6; ?Renz, 1974, p. 790, pl. 8, fig. 20, and pl. 11, fig. 28.
*Parvicingula malleola* (Aliev) group—Schaaf, 1981, p. 436, pl. 21, figs. 2 and 12.
*Parvicingula malleola* (Aliev)—Schaaf, 1985, p. 159, fig. 11.

**Range.** Recorded as a common element of Aptian faunas by Schaaf (1984).

*Parvicingula*(?) sp.
(Pl. 6, Fig. 10)

**Remarks.** This species is tentatively assigned to *Parvicingula* Pessagno because of its morphotypic similarities with species of this genera.

*Patellula verteroensis* (Pessagno)
(Pl. 2, Figs. 19 and 20)

*Stylospongia verteroensis* Pessagno, 1963, p. 199.
*Patellula verteroensis* (Pessagno)—Empson-Morin, 1981, p. 257, pl. 2, figs. 1–5.

**Range and occurrences.** This form is recorded from Campanian sediments in the Caribbean region, North Atlantic, Bavaria, and Cyprus.

*Patellula*(?) sp. B
(Pl. 5, Fig. 19)

**Remarks.** Quite different forms of *Patellula* are included within these two species, but the insufficient preservation does not allow determination to the species level.

*Patulibracchium californensis* Pessagno
(Pl. 2, Fig. 9)

*Patulibracchium californensis* Pessagno, 1971b, p. 29, pl. 11, fig. 6, and pl. 12, figs. 1 and 2; Pessagno, 1976, p. 30, pl. 10, fig. 13; Empson-Morin, 1984, text fig. 9A–9C).

**Range.** Lower part of the *A. pseudoconulus* Zone (lower Campanian)
**Occurrences.** North Atlantic, the Caribbean region, Bavaria, Cyprus, and the Middle East.

*Patulibracchium* sp. cf. *P. davisi* Pessagno
(Pl. 6, Fig. 6)

*Patulibracchium davisi* Pessagno, 1976, p. 30, pl. 1, fig. 7.

**Remarks.** This form is always poorly preserved in the samples studied; therefore, assignment to *P. davisi* Pessagno is tentative.
**Range and occurrences.** *P. davisi* is recorded from the Cenomanian of California.

*Patulibracchium petroleumensis* Pessagno
(Pl. 2, Fig. 11)

*Patulibracchium petroleumensis* Pessagno, 1971b, p. 37–38, pl. 11, figs. 2–5; Pessagno, 1976, p. 30, pl. 10, fig. 15.

**Remarks.** *P. petroleumensis* occurs in lower Campanian strata of California.
**Occurrences.** North Atlantic and California.

*Podobursa triacantha* (Fischli)
(Pl. 7, Figs. 16 and 19)

*Theosyringium acanthophorum* Rüst var. *triacanthus* Fischli, 1916, p. 47, fig. 38.
*Theosyringium acanthophorum* Rüst var. *tetracanthus* Fischli, 1916, p. 47, fig. 39.
*Theosyringium acanthophorum* Rüst var. *polyacanthus* Fischli, 1916, p. 47, fig. 41.
*Podobursa triacantha* (Fischli)—Foreman, 1973b, p. 266, pl. 13, figs. 1–3; Foreman, 1975, p. 617, pl. 2L, figs. 4–6; Pessagno, 1977a, p. 92, pl. 12, fig. 6; Pessagno, 1977b, p. 57, pl. 11, fig. 6; Schaaf, 1981, p. 436, pl. 5, fig. 11, and pl. 25, figs. 1a and 1b.
*Podobursa* sp. Riedel and Sanfilippo, 1974, pl. 13, fig. 7.

**Range.** Upper Jurassic to lower Aptian.
**Occurrences.** Recorded worldwide.

*Podobursa tricola* Foreman
(Pl. 7, Fig. 17)

*Podobursa tricola* Foreman, 1973b, p. 267, pl. 13, fig. 9, and pl. 16, fig. 12; Foreman, 1975, p. 617, pl. 2L, figs. 7 and 8; Schaaf, 1981, p. 436, pl. 6, figs. 1a and 1b, and pl. 25, figs. 2a and 2b.

**Range.** Recorded from lower Hauterivian to upper Aptian.
**Occurrences.** North Atlantic and Pacific.

*Podobursa* sp. A
(Pl. 7, Fig. 18)

**Remarks.** This species differs from *P. tricola* by having two long terminal spines.

*Pseudoaulophacus floresensis* Pessagno
(Pl. 2, Fig. 5)

*Pseudoaulophacus floresensis* Pessagno, 1963, p. 200, pl. figs. 2 and 5, pl. 4, fig. 6, and pl. 7, figs. 1 and 5; Pessagno, 1972, p. 304, pl. 26, fig. 6, pl. 28, figs. 4–6, pl. 29, figs. 1 and 2, and pl. 31, fig. 1; Pessagno, 1976, p. 28, and pl. 9, fig. 6; Pessagno, 1977c, pl. 10, fig. 3; Foreman, 1971, p. 1675, pl. 2, fig. 6; Foreman, 1973a, p. 429, pl. 13, fig. 8; Pessagno and Longoria, 1973, p. 550; Moore, 1973, p. 824, pl. 12, figs. 2 and 3; Pessagno and Michael, 1974, p. 969; Nakaseko and Nishimura, 1981, p. 158, pl. 2, fig. 4; Kling, 1982, p. 548, pl. 1, fig. 11.
*Pseudoaulophacus* cf. *P. floresensis* Pessagno—Taketani, 1982.

**Remarks.** The three spines are always broken.
**Range.** *A. pseudoconulus* Zone to the *A. tylotus* Zone of Sanfilippo and Riedel (1985); Campanian through Maestrichtian.
**Occurrences.** North Atlantic, Japan, central Pacific, California, the Caribbean region, Cyprus, and the Middle East (Oman).

*Pseudoaulophacus lenticulatus* (White)
(Pl. 2, Fig. 6)

*Baculogypsina*(?) *lenticulata* White, 1928, p. 306, pl. 41, figs. 9 and 11.
*Aulophacus lenticulatus* (White)—Pessagno, 1962, p. 364, pl. 6, figs. 1 and 2.
*Pseudoaulophacus lenticulatus* (White)—Pessagno, 1963, p. 202, pl. 2, figs. 8 and 9; Pessagno, 1972, p. 306, pl. 2, figs. 5 and 6, and pl. 3, figs. 1–3; Pessagno, 1976, p. 28, pl. 9, figs. 11 and 12; Shipboard Scientific Party, 1969, p. 206; Pessagno and Longoria, 1973, p. 550; Dinkelmann, 1973, p. 790, pl. 1, fig. 12; (as *P. lenticularis*) Moore, 1973, pl. 12, fig. 1; Pessagno and Michael, 1974, p. 969; Foreman, 1977, p. 315; Butt, 1981, pl. 20, figs. Q and R; Nakaseko and Nishimura, 1981, p. 158, pl. 2, figs. 7a and 7b; Kling, 1982, p. 548, pl. 1, fig. 12; Taketani, 1982, p. 51, pl. 10, fig. 11; Sanfilippo and Riedel, 1985, p. 596, text fig. 6 (4a and 4b).

**Range.** *A. pseudoconulus* Zone (Campanian).
**Occurrences.** North Atlantic, Japan, central Pacific, California, Cyprus, Oman, the Caribbean region, and Bavaria.

*Pseudoaulophacus pargueraensis* Pessagno
(Pl. 2, Fig. 7)

*Pseudoaulophacus pargueraensis* Pessagno, 1963, p. 204, pl. 2, figs. 4 and 7, and pl. 6, figs. 4 and 5; Pessagno, 1972, p. 309, pl. 30, fig. 4; Shipboard Scientific Party, 1969, p. 206; Foreman, 1971, p. 1675, pl. 2, fig. 7; Foreman, 1973a, p. 429; Foreman, 1973b, pl. 15, fig. 18; Foreman, 1975, p. 613, pl. 5, fig. 8; Foreman, 1977, p. 315; Foreman, 1978b, p. 744, pl. 3, fig. 9; Moore, 1973, p. 824, pl. 12, figs. 6 and 7; Riedel and Sanfilippo, 1974, p. 780, pl. 2, figs. 12–14; Nakaseko and Nishimura, 1981, p. 158, pl. 2, fig. 5; Kling, 1982, p. 548, pl. 1, figs. 13(?) and 14; Sanfilippo and Riedel, 1985, p. 596, text fig. 6 (5a–5d).

**Range.** *A. pseudoconulus* Zone into the *A. tylotus* Zone of Sanfilippo and Riedel (1985); approximately Santonian to Campanian.
**Occurrences.** North Atlantic, Japan, north central Pacific, the Caribbean region, Austria, and Bavaria.

*Pseudoaulophacus putahensis* Pessagno
(Pl. 2, Fig. 4)

*Pseudoaulophacus putahensis* Pessagno, 1972, p. 310–311, pl. 27, fig. 1; Pessagno, 1976, p. 28, pl. 3, fig. 13; Thurow and Anderson, 1986, pl. 5, fig. 5; Thurow and Kuhnt, 1986, text fig. 9 (8).

**Range.** *C. cachensis* Zone (lower to middle Turonian).
**Occurrences.** North Atlantic, southern Europe, northwestern Africa, and California.

*Pseudoaulophacus* sp. A
(Pl. 2, Fig. 8)

**Remarks.** This species differs from all other *Pseudoaulophacidae* Pessagno by its triangular outline.

*Pseudoaulophacus* sp. B
(Pl. 5, Fig. 13)

**Remarks.** This species differs from *P. putahensis* by having large prominent secondary spines between the three major spines.

*Pseudoaulophacus*(?) sp. C
(Pl. 9, Fig. 17)

**Remarks.** This species is tentatively assigned to *Pseudoaulophacus* Pessagno because of its morphotypic similarities.

*Pseudoaulophacus*(?) sp. D
(Pl. 5, Fig. 14)

**Remarks.** This species is tentatively assigned to *Pseudoaulophacus* Pessagno because of its morphotypic similarities (especially to *P. lenticulatus*).

*Pseudocrucella* sp. A
(Pl. 10, Fig. 9)

*Pseudocrucella*(?) sp. B
(Pl. 10, Fig. 7)

**Remarks.** This species is tentatively assigned to *Pseudocrucella* Baumgartner because of its morphotypic similarities. Common in Hauterivian/Barremian strata in the northeast Atlantic.

*Pseudocrucella*(?) sp. C
(Pl. 10, Fig. 6)

**Remarks.** This species is tentatively assigned to *Pseudocrucella* Baumgartner because of its morphotypic similarities.

*Pseudodictyomitra carpatica* (Lozyniak)
(Pl. 6, Fig. 12)

*Dictyomitra carpatica* Lozyniak, 1969, p. 38, pl. 2, figs. 11–13.
*Dictyomitra carpatica* Lozyniak(?)—Foreman, 1973b, p. 263, pl. 10, figs. 1–3, and pl. 16, fig. 5; Foreman, 1975, p. 614, pl. 2G, figs. 11–14, and pl. 7, fig. 7 (not fig. 6).
*Pseudodictyomitra carpatica* (Lozyniak)—Schaaf, 1981, p. 436, pl. 3, figs. 1a–1c and 2, and pl. 20, figs. 4a and 4b; de Wever and Thiebault, 1981, p. 590–591, pl. 2, fig. 2; Schaaf, 1984, p. 94, figs. 1–3.

**Range.** Not well established, Valanginian to Turonian (Schaaf, 1984).
**Occurrences.** Recorded worldwide.

*Pseudodictyomitra leptoconica* (Foreman) Group
(Pl. 6, Fig. 11)

*Dictyomitra leptoconica* Foreman, 1973b, p. 264, pl. 10, fig. 4, and pl. 16, fig. 6.
*Pseudodictyomitra leptoconica* (Foreman)—Schaaf, 1981, p. 437, pl. 3, fig. 3, and pl. 18, figs. 3a and 3b; Schaaf, 1984, p. 117–118, figs. 1–7.

**Range.** Recorded from Berriasian–lower Aptian.

*Pseudodictyomitra lilyae* (Tan Sin Hok)
(Pl. 6, Figs. 13, 14, and 17)

*Dictyomitra lilyae* Tan Sin Hok, 1927, p. 55, pl. 10, fig. 83; Riedel and Sanfilippo, 1974, pl. 4, figs. 7–9, and pl. 12, fig. 13; Renz, 1974, p. 791, pl. 8, figs. 1–4, and pl. 11, fig. 33.
*Pseudodictyomitra lilyae* (Tan Sin Hok)—Schaaf, 1981, p. 437, pl. 3, fig. 8, and pl. 18, figs. 5a and 5b; Schaaf, 1984, p. 118–119, figs. 1–7.

**Range.** Upper Valanginian–Barremian (Schaaf, 1984).
**Occurrences.** Pacific, Indian Ocean, Indonesia, and the North Atlantic.

*Pseudodictyomitra lodogaensis* Pessagno
(Pl. 3, Fig. 12)

*Pseudodictyomitra lodogaensis* Pessagno, 1977b, p. 50, pl. 8, figs. 4, 21, and 28; Schaaf, 1981, p. 437, pl. 3, fig. 5.

**Range.** Upper Albian to Cenomanian.
**Occurrences.** Central Pacific, California, and the North Atlantic.

*Pseudodictyomitra nakasekoi* Taketani

*Pseudodictyomitra nakasekoi* Taketani, 1982, p. 60, pl. 12, figs. 4–6; Kuhnt et al., 1986, pl. 7S.
*Dictyomitra tiara* Holmes—Dumitrica, 1975, p. 87–89, text fig. 2, fig. 9.
*Dictyomitra*(?) sp. B—Nakaseko et al., 1979, p. 22, pl. 6, fig. 21.

**Range.** Cenomanian/Turonian.
**Occurrences.** Northwestern Africa, Japan, and the North Atlantic.

*Pseudodictyomitra pentacolaensis* Pessagno
(Pl. 3, Fig. 17)

*Pseudodictyomitra pentacolaensis* Pessagno, 1977b, p. 50, pl. 8, figs. 3, 17, and 23, and pl. 12, fig. 10.

**Range.** Upper Albian.
**Occurrences.** California and the North Atlantic.

*Pseudodictyomitra pseudomacrocephala* (Squinabol)
(Pl. 1, Fig. 13, and Pl. 3, Fig. 16)

*Dictyomitra pseudomacrocephala* Squinabol, 1903, p. 139, pl. 10, fig. 2; Cita, 1964, p. 143, pl. 12, figs. 8 and 9; Petrushevskaya and Kozlova, 1972, p. 550, pl. 2, fig. 5; Pessagno and Michael, 1974, p. 969; Foreman, 1975, p. 614, pl. 7, fig. 10; Foreman, 1977, p. 315; Dumitrica, 1975, fig. 2, no. 19; Pessagno, 1976, p. 53, pl. 3, figs. 2 and 3; Nakaseko et al., 1979, p. 22, pl. 6, figs. 12–15; Kozlova in Basov et al., 1979, fig. 4.
*Dictyomitra malleola* Aliev—Pessagno, 1969, p. 610, pl. 5, fig. A.
*Dictyomitra macrocephala* Squinabol—Moore, 1973, p. 829, pl. 9, figs. 8 and 9; Riedel and Sanfilippo, 1974, p. 778, pl. 4, figs. 10 and 11, and pl. 14, fig. 11.
*Dictyomitra dnistrensis* Lozyniak, 1975, p. 52, pl. 2, figs. 3–7.
*Dictyomitra* sp. Foreman, 1973, p. 264, pl. 14, fig. 16.
(?)*Dictyomitra sagitafera* Aliev, 1961, p. 25, pl. 1, figs. 1–3; Aliev, 1965, p. 55.
*Pseudodictyomitra pseudomacrocephala* (Squinabol)—Pessagno, 1977b, p. 51, pl. 8, figs. 10 and 11; Schmidt-Effing, 1980, p. 247, fig. 8; Schaaf, 1981, p. 437, pl. 24, figs. 1a and 1b; Nakaseko and Nishimura, 1981, p. 159, pl. 9, figs. 1–4, pl. 16, figs. 5 (not 6), 7, and 8; Taketani, 1982, p. 61, pl. 5, figs. 4a and 4b, and pl. 12, figs. 7 and 8; Sanfilippo and Riedel, 1985, p. 608, text fig. 10 (1a–1c); Kuhnt et al., 1986, pl. 7T; Thurow and Kuhnt, 1986, text fig. 9 (11).

**Range.** Base of the *P. pseudomacrocephala* Zone into the *C. cachensis* Zone (Albian to Turonian).

**Occurrences.** North Atlantic, Japan, central and northwest Pacific, California, Costa Rica, southern Europe, northwestern Africa, and Oman.

*Pseudodictyomitra* sp. cf. *P. pseudomacrocephala* (Squinabol)
(Pl. 3, Fig. 11)

**Remarks.** This species differs from *P. pseudomacrocephala* (Squinabol) by its less inflated cephalo/thorax.

*Pseudodyctiomitra vestalensis* Pessagno
(Pl. 3, Fig. 15)

*Pseudodyctiomitra vestalensis* Pessagno, 1977b, p. 51, pl. 8, figs. 4, 21, and 28; Schaaf, 1981, p. 437, pl. 3, fig. 10; Schaaf, 1985, p. 161, figs. 4a and 4b.

**Remarks.** This species is only tentatively assigned to *P. vestalensis* Pessagno because the preservation of this species is generally poor and it is always lacking the characteristic final chamber.
**Range and occurrences.** *P. vestalensis* Pessagno is common in Albian strata of the central Pacific, California, and at Hole 398D.

*Pyramispongia glascockensis* Pessagno
(Pl. 2, Fig. 23)

*Pyramispongia glascockensis* Pessagno, 1973, p. 79–80, pl. 21, figs. 2–5; Pessagno, 1976, p. 37, pl. 1, fig. 9; Taketani, 1982, p. 51, pl. 10, fig. 12; Thurow and Kuhnt, 1986, text fig. 9 (4).

**Range and occurrences.** *P. glascockensis* is reported from upper Cenomanian to middle Turonian (CTBE) strata in southern Europe and northwest Africa, from the Cenomanian/Turonian of California, and from the upper Cenomanian to lower Santonian of Japan.

*Rhopalosyringium majuroensis* Schaaf
(Pl. 4, Fig. 15)

*Rhopalosyringium majuroensis* Schaaf, 1981, p. 437, pl. 6, figs. 2 and 3, and pl. 23, fig. 5; Schaaf, 1985, p. 120–121, figs. 1–7b.
*Rhopalosyringium* sp. Foreman, 1971, p. 1682, pl. 3, fig. 9.
(?)*Rhopalosyringium* sp. A. Moore, 1973, p. 826, pl. 7, fig. 1.
*Artostrobium urna* Foreman—Schmidt-Effing, 1980, p. 254, fig. 4.

**Range.** Upper Cenomanian to (?)Turonian.
**Occurrences.** Recorded from Atlantic and Pacific sites.

*Rhopalosyringium* sp. A
(Pl. 1, Fig. 5)

**Remarks.** The poor preservation of the specimens does not allow determination to the species level, but they appear to be related to *Rhopalosyringium magnificum* Campell and Clark.

*Rhopalosyringium* sp. B
(Pl. 4, Fig. 16)

**Remarks.** This species differs from *R. majuroensis* by its much shorter and unradiated spine and by having additional spines on the thorax.

*Rhopalosyringium* sp. C
(Pl. 4, Fig. 17)

**Remarks.** This species differs from *R. majuroensis* by its long tube-like abdomen and by having additional spines on the thorax.

*Sethocapsa orca* Foreman
(Pl. 8, Fig. 4)

*Sethocapsa*(?) *orca* Foreman, 1975, p. 617, pl. 2J, figs. 1–2, and pl. 6, fig. 12.
*Sethocapsa orca* Foreman—Schaaf, 1981, p. 437, pl. 26, figs. 3a and 3b; Schaaf, 1985, p. 155, figs. 8a and 8b.

**Range.** Recorded from upper Valanginian to lowermost Aptian.

*Sethocapsa* sp. A cf. *S. simplex*
(Pl. 4, Fig. 23)

**Remarks.** This species shows close relationships to *S. simplex* Taketani, but its proximal part is slightly different.

*Sethocapsa trachyostraca* Foreman
(Pl. 8, Fig. 5)

*Sethocapsa trachyostraca* Foreman, 1973b, p. 268, pl. 12, fig. 4; Riedel and Sanfilippo, 1974, p. 780, pl. 9, figs. 5–7; Foreman, 1975, p. 617, pl. 2J, figs. 3 and 4; Muzavor, 1977, p. 119, pl. 6, fig. 5; Foreman, 1978b, p. 749, pl. 1, fig. 18; Schaaf, 1981, p. 437, pl. 23, figs. 1a and 1b; Sanfilippo and Riedel, 1985, p. 613, text fig. 10 (3a and 3b).
*Stichocapsa conosphaeroides* Rüst, 1898, p. 66, pl. 19, fig. 3; Moore, 1973, p. 827, pl. 4, figs. 5–6.

**Range.** Approximately Berriasian to Hauterivian.
**Occurrences.** Southern Europe, the North Atlantic, and Pacific.

*Sethocapsa uterculus* (Parona)
(Pl. 7, Fig. 21)

*Theocapsa uterculus* Parona, 1890, p. 168, pl. 5, fig. 17.
*Sethocapsa* sp. cf. *Theocapsa uterculus* Parona—Foreman, 1975, p. 617, pl. 21, figs. 21 and 22.
*Sethocapsa uterculus* (Parona)—Schaaf, 1981, p. 437, pl. 5, figs. 8a and 8b; pl. 26, figs. 5a and 5b; Schaaf, 1984, p. 150, fig. 1–4; Sanfilippo and Riedel, 1985, p. 613, text fig. 10 (6a–6e).

**Range.** Approximately Hauterivian to Barremian (from the *Dibolachras tytthopora* Zone to the *Crolanium pythiae* Zone).
**Occurrences.** Southern Europe, North Atlantic, and Pacific.

*Sethocapsa* sp. cf. *S. uterculus* (Parona)
(Pl. 7, Fig. 22)

**Remarks.** This species differs from *S. uterculus* by its irregular surface and the less pronounced first postabdominal chamber.

*Sethocapsa*(?) sp. A
(Pl. 7, Fig. 24)

**Remarks.** This species is tentatively assigned to *Sethocapsa* Haeckel by its morphologic similarities.

*Siphocampium*(?) *davidi* Schaaf
(Pl. 7, Fig. 25)

*Siphocampium*(?) *davidi* Schaaf, 1981, p. 437–438, pl. 5, fig. 7, and pl. 27, figs. 10a and 10b; Schaaf, 1985, p. 102–103, figs. 1–6b.

**Range.** Middle Hauterivian to lower Barremian (*Dibolachras tytthopora* Zone into the *Crolanium pythiae* Zone).
**Occurrences.** Recorded from the North Atlantic and Pacific.

*Squinabollum fossilis* (Squinabol)
(Pl. 4, Fig. 21)

*Clistosphaena fossilis* Squinabol, 1903, p. 130, pl. 10, fig. 11.
*Micromelissa ventricosa* Squinabol, 1903, p. 130, pl. 10, fig. 22.
*Xiphostylus communis* Squinabol, 1903, p. 111, pl. 10, fig. 20.
*Squinabollum fossilis* (Squinabol)—Dumitrica, 1970, p. 83, pl. 19, figs. 118a–118c, 119a–119c, 120, 121a–121c, and 122; Dumitrica, 1975, p. 87–89, text fig. 2, fig. 29; Nakaseko et al., 1979, p. 23, pl. 5, fig. 12; Taketani, 1982, p. 70, pl. 6, figs. 10a, 10b, 11a, and 11b, and pl. 13, figs. 10 and 11.

**Range.** Mid-Cretaceous.
**Occurrences.** Southern Europe, the North Atlantic, Japan, and the Pacific.

*Staurocyclia martini* (Rüst)
(Pl. 10, Fig. 8)

*Staurocycla martini* Rüst, 1898, p. 21, pl. 6, fig. 11; Schaaf, 1981, p. 439, pl. 11, figs. 2a and 2b.

**Range.** Recorded from Barremian to lower Aptian strata.

*Stichocapsa euganea* Squinabol
(Pl. 3, Figs. 6 and 7)

*Stichocapsa euganea*—Squinabol, 1903, pl. 8, fig. 30; Schaaf, 1981, p. 432, pl. 22, figs. 4 and 5, and pl. 23, fig. 7; Schaaf, 1985, p. 158–159, fig. 8.
(?)*Archicapsa similis* Parona, 1890, p. 163, pl. 5, fig. 4; Hinde, 1900, p. 28, pl. 3, fig. 22; Moore, 1973, p. 825, pl. 16, figs. 3 and 4.
*Cyrtocapsa perspicua* Squinabol, 1903, p. 142, pl. 10, fig. 16; Schaaf, 1985, p. 163, fig. 10.
*Mita* sp. A—Kuhnt et al., 1986, pl. 7P.

**Remarks.** Specimens from samples of the type section as well as from Hole 398D show no differences between *Stichocapsa euganea* and *Cyrtocapsa perspicua*, with all transitional forms occurring between these end-members. However, Squinabol's (1903) holotype of *Stichocapsa euganea* shows, according to his drawing, transverse pore rows, and his drawing of *Cyrtocapsa perspicua* shows vertical pore rows. The studied specimens have vertical pore rows (seen in lateral view).

**Range.** Lower Aptian to Cenomanian; *Stichocapsa euganea* Zone to *O. somphedia* Zone of Schaaf (1985).
**Occurrences.** Southern Europe, the North Atlantic, and Pacific.

*Stichomitra communis* Squinabol
(Pl. 4, Fig. 10)

*Stichomitra communis* Squinabol, 1903, p. 141, pl. 8, fig. 40; Taketani, 1982, p. 54–55, pl. 3, fig. 9, and pl. 11, fig. 5; Schaaf, 1984, p. 162, figs. 8a and 8b; Kuhnt et al., 1986, pl. 7W.
(?)*Stichomitra* sp. Dumitrica, 1975, p. 87–89, text fig. 2, fig. 21.
*Parvicingula*(?) *tekschaensis* (Aliev)—Schaaf, 1981, pl. 3, fig. 12, and pl. 20, figs. 3a and 3b.

**Remarks.** This species is recorded from upper Cenomanian to lowermost Coniacian strata of Japan, from Cenomanian to Turonian strata of southern Europe and northwest Africa, and from Albian to Turonian strata at Hole 398D and Oman.

*Stichomitra* sp. cf. *S. communis* Squinabol
(Pl. 4, Fig. 9)

**Remarks.** This species differs from *S. communis* by the tubelike segment on the final postabdominal chamber and by the less pronounced polygonal meshwork on the test.

*Stichomitra*(?) sp. A
(Pl. 1, Fig. 17)

**Remarks.** This species is tentatively assigned to *Stichomitra* Cayeux because of its morphotypic similarities.

*Stichomitra*(?) sp. B
(Pl. 1, Fig. 17)

**Remarks.** This species is tentatively assigned to *Stichomitra* because of its morphotypic similarities; however, it differs by having three circular spines extending from the final postabdominal chamber.

*Thanarla conica* (Aliev)
(Pl. 6, Fig. 20, and Pl. 7, Figs. 5 and 11)

*Cornutanna conica* Aliev, 1965, p. 34–35, pl. 6, fig. 1; Moore, 1973, p. 830, pl. 14, figs. 1 and 2.
*Dictyomitra*(?) *lacrimula* Foreman, 1973b, p. 263, pl. 10, fig. 11; Foreman, 1975, p. 614, pl. 2G, figs. 5 and 6, and pl. 6, fig. 1.
*Thanarla conica* (Aliev)—Pessagno, 1977b, p. 45, pl. 7, figs. 1, 13, and 15; Mattson and Pessagno, 1979, figs. 2A, 2D, and 2E; Taketani, 1982, p. 59, pl. 4, figs. 11a–11c.

**Range.** Valanginian to lower Aptian.
**Occurrences.** California, the Caribbean region, North Atlantic, Russia, Japan, and the Pacific.

*Thanarla*(?) sp. A aff. *T. conica* (Aliev)
(Pl. 7, Figs. 7 and 8)

**Remarks.** This species differs from *T. conica* by its clearly visible segmentation.

*Thanarla* sp. B aff. *T. conica* (Aliev)
(Pl. 7, Fig. 12)

*Thanarla* sp. aff. *T. conica* (Aliev)—Pessagno, 1977b, p. 46, pl. 7, figs. 8 and 14.

**Remarks.** This species differs from *T. conica* by having more widely spaced costae.

*Thanarla elegantissima* (Cita)
(Pl. 4, Fig. 11)

*Thanarla elegantissima* (Cita)—Pessagno, 1977b, p. 46, pl. 7, fig. 10; Schmidt-Effing, 1980, p. 246, figs. 2 and 21 (not 22); de Wever, 1981, p. 516; Taketani, 1982, p. 59, pl. 4, fig. 12, and pl. 11, figs. 17 and 18; Sanfilippo and Riedel, 1985, p. 600, text fig. 8 (1a–1e).

*Lithocampe elegantissima* Cita, 1964, p. 148, pl. 12, figs. 2 and 3; Riedel and Sanfilippo, 1974, p. 779, pl. 6, figs. 8–10, and pl. 13, figs. 2–4; Pessagno, 1976, p. 55, pl. 3, fig. 6.

*Sethamphora pulchra* Squinabol—Moore, 1973, p. 826, pl. 3, fig. 4 (only).

*Thanarla pulchra* (Squinabol)—Nakaseko and Nishimura, 1981, p. 163, pl. 7, figs. 4 and 7, and pl. 15, fig. 12.

**Range.** Hauterivian to Cenomanian (*Dibolachras tytthopora* Zone to *Obesacapsula somphedia* Zone of Schaaf, 1985).

**Occurrences.** Worldwide.

*Thanarla pulchra* (Squinabol)
(Pl. 7, Fig. 9)

*Sethamphora pulchra* Squinabol 1904, p. 213, pl. 5, fig. 8; Moore, 1973, p. 825, pl. 3, figs. 5 and 6 (not fig. 4); Riedel and Sanfilippo, 1974, pl. 13, fig. 5.

*Cryptocephalus*(?) sp.—Riedel and Schloecker, 1956, p. 358, fig. 2.

*Dictyomitra pulchra* (Squinabol)—Dumitrica, 1975, p. 87, text fig. 2, fig. 7.

*Lithocampe elegantissima* Cita—Foreman, 1975, p. 616, pl. 2G, figs. 3 and 4; Muzavor, 1977, p. 100, pl. 8, fig. 1; Nakaseko et al., 1979, p. 23, pl. 4, fig. 2.

*Thanarla pulchra* (Squinabol)—Pessagno, 1977b, p. 46, pl. 7, figs. 7, 21, and 26; Nakaseko and Nishimura, 1981, p. 163, only pl. 15, fig. 11; Schaaf, 1981, p. 439, pl. 4, fig. 10, and pl. 19, figs. 7a and 7b; Taketani, 1982, p. 59, pl. 11, fig. 19; Schaaf, 1984, p. 132, figs. 1–7.

*Thanarla elegantissima* (Cita)—Schmidt-Effing, 1980, p. 246, fig. 22.

**Remarks.** Sanfilippo and Riedel (1985) distinguish between *T. elegantissima* and *T. pulchra* on the base of the distension of the last segment, and the latter form is said to range only from approximately Berriasian to Barremian, but their text figure 8 (2d) shows Pessagno's (1977b) type specimen, which is from the lower Cenomanian of the Great Valley sequence.

*Thanarla veneta* (Squinabol)
(Pl. 4, Figs. 13 and 14)

*Phormicyrtis veneta* Squinabol, 1903, p. 134, pl. 9, fig. 30.

*Phormicyrtis*(?) *veneta* Squinabol—Pessagno, 1976, p. 35, pl. 3, fig. 10.

*Dictyomitra veneta* (Squinabol)—Petrushevskaya and Kozlova, 1972, p. 550, pl. 2, fig. 2; Foreman, 1973b, p. 264, pl. 14, fig. 11; Riedel and Sanfilippo, 1974, p. 778, pl. 5, figs. 5 and 6; Foreman, 1975, p. 614, pl. 1G, fig. 4; Dumitrica, 1975, p. 87–89, text fig. 2, fig. 17.

*Thanarla veneta* (Squinabol)—Pessagno, 1977b, p. 46, pl. 7, figs. 5, 12, 17, 19, and 25, and pl. 12, fig. 8; Schmidt-Effing, 1980, p. 247, figs. 3 and 23; Nakaseko and Nishimura, 1981, p. 164, pl. 6, figs. 13 and 15, and pl. 15, fig. 15; Taketani, 1982, p. 60, pl. 5, figs. 1a–1c, and pl. 11, fig. 20 (not 21); Sanfilippo and Riedel, 1985, p. 602, text figs. 8a–8f.

**Range.** *Pseudodictyomitra pseudomacrocephala* Zone into the *O. somphedia* Zone of Schaaf (1985); upper Albian to Cenomanian.

**Occurrences.** Recorded worldwide.

*Thanarla*(?) sp. aff. *T. veneta* (Squinabol)
(Pl. 1, Figs. 15 and 27)

*Thanarla*(?) aff. *T. veneta* (Squinabol)—Empson-Morin, 1984, pl. 2, fig. 8.

**Range and occurrences.** Recorded from Campanian strata in the Caribbean region, the central Pacific, and Romania.

*Thanarla* sp. C
(Pl. 4, Fig. 12, and Pl. 7, Fig. 6)

**Remarks.** This species differs from *T. veneta* by possessing an upper conical and a lower barrel-like part.

*Theocampe tina* (Foreman)
(Pl. 1, Fig. 6)

*Artostrobium tina* Foreman, 1971, p. 1678, pl. 4, fig. 3; Foreman, 1973a, p. 430; 1975, p. 613, pl. 1F, figs. 3–5, and pl. 6, fig. 5; (non) Moore, 1973, p. 826, pl. 8, fig. 6; Taketani, 1982, p. 53, pl. 2, figs. 11a and 11b.

*Artostrobium urna* Foreman—Nakaseko et al., 1979, p. 21, pl. 8, fig. 13; Taketani, 1982, pl. 10, fig. 17.

*Theocampe tina* (Foreman)—Sanfilippo and Riedel, 1985, p. 605, text fig. 9 (5a–5c).

**Range.** Upper part of *C. cachensis* Zone to the *A. pseudoconulus* Zone (approximately Turonian to Campanian).

**Occurrences.** Western Atlantic, Japan, central and North Pacific, the Caribbean region, and northern Italy.

*Theocapsomma ancus* Foreman
(Pl. 4, Fig. 8)

*Theocapsomma ancus* Foreman, 1968, p. 32, pl. 4, fig. 3; Schaaf, 1981, p. 440, pl. 24, figs. 4, 9a, and 9b.

*Diacanthocapsa* cf. *ancus* (Foreman)—Dumitrica, 1970, p. 64, pl. 6, figs. 35a and 35b, pl. 7, fig. 40, and pl. 20, fig. 125.

*Theoconus coronatus* Squinabol Group
(Pl. 4, Fig. 2)

*Theoconus coronatus* Squinabol, 1904, p. 220, pl. 8, fig. 3.

*Stichomitra*(?) *zamoraensis* Pessagno, 1976, p. 54, pl. 3, figs. 7–9.

*Spongocapsula zamoraensis* (Pessagno)—Pessagno, 1977b, p. 53, pl. 9, figs. 5 and 16.

*Spongocapsula*? *zamoraensis* Pessagno—Schaaf, 1981, p. 438, pl. 24, figs. 2a and 2b; Taketani, 1982, p. 62, pl. 5, figs. 6a and 6b, and pl. 12, figs. 12 and 13.

*Theoconus coronatus* Squinabol—Kuhnt et al., 1986, pl. 7Q.

**Remarks.** This form is recorded from Albian to ?Campanian strata in the central Pacific, Japan, California, North Atlantic, and northern Italy, but it is never found within CTBE intervals. *T. coronatus* s.s. became extinct with the onset of the CTBE, but it is probably an ancestral form of the Late Cretaceous age *Novixitus*(?) sp. D (Pl. 1, Fig. 20).

*Theoconus* sp. A cf. *T. coronatus* Squinabol
(Pl. 4, Figs. 3 and 4)

**Remarks.** This species differs from *T. coronatus* by its pronounced segmentation and the lack of a spongy meshwork on the final postabdominal chambers.

*Theocorys renzae* Schaaf
(Pl. 8, Fig. 1)

*Theocorys renzae* Schaaf, 1981, p. 440, pl. 5, figs. 13a–13c, and pl. 27, figs. 1a and 1b; Schaaf, 1985, p. 134–135, figs. 1–6b.

**Range.** Hauterivian to Barremian (*D. tytthopora* Zone into *Crolanium pythiae* Zone).

**Occurrences.** North Atlantic and Pacific.

*Triactoma echoides* Foreman
(Pl. 9, Fig. 12)

*Triactoma echoides* Foreman, 1973b, p. 260, pl. 3, fig. 1, and pl. 16, fig. 21; Foreman, 1975, p. 609, pl. 2F, figs. 9 and 10, and pl. 3, fig. 10; Baumgartner et al., 1980, p. 64, pl. 2, fig. 10; Kocher, 1981, p. 101, pl. 17, figs. 8 and 9; Kanie et al., 1981, pl. 1, fig. 7; Baumgartner, 1984, p. 789, pl. 10, fig. 2; Thurow and Kuhnt, 1986, text fig. 9 (19).

**Range.** Upper Jurassic to upper Aptian.

**Occurrences.** North Atlantic, southern Europe, and Pacific.

*Triactoma hybum* Foreman
(Pl. 9, Fig. 11)

*Triactoma hybum* Foreman, 1975, p. 609, pl. 2F, figs. 6 and 7, and pl. 3, figs. 7 and 9; Schaaf, 1981, p. 440, pl. 12, fig. 7.

*Triactoma* sp. cf. *T. echoides* Foreman, 1973b, pl. 3, fig. 2 (not 3).

**Range.** Uppermost Hauterivian to Aptian (base of the *Acaeniotyle umbilicata* Zone of Schaaf, 1985).

*Tritrabs* sp. cf. *T. rhododactylus* Baumgartner
(Pl. 10, Fig. 14)

*Tritrabs rhododactylus* Baumgartner, 1980, p. 294, pl. 4, figs. 12–15, and pl. 11, fig. 15.
*Tritrabs rhododactyla* Baumgartner—Kocher, 1981, p. 106, pl. 17, fig. 2.
*Tritrabs* sp. cf. *T. casmaliaensis* (Pessagno)—Sato et al., 1982, pl. 3, fig. 5.

**Remarks.** The species figured differs from *T. rhododactylus* by having numerous short spines at the end of each arm.

*Tritrabs* sp.
(Pl. 10, Fig. 17)

**Remarks.** Fragments of *Tritrabs* ssp. are common in the samples studied.

*Vitorfus campbelli* Pessagno
(Pl. 10, Fig. 5)

*Vitorfus campbelli* Pessagno, 1977b, p. 35, pl. 3, figs. 1, 2, and 7.

*Vitorfus* ssp.

**Remarks.** Numerous in Lower Cretaceous strata at Hole 398D. The discrimination between the different species of this genus is based mainly on the number and arrangement of spines on the elliptical ring. The preservation of *Vitorfus* ssp. in the samples studied excludes, with a few exceptions, determination to a species level.

*Williriedellum* sp. aff. *W. carpathicum* Dumitrica
(Pl. 8, Fig. 11)

*Williriedellum carpathicum* Dumitrica, 1970, p. 70, pl. 9, figs. 56a, 56b, and 57–59, and pl. 10, fig. 61; Schaaf, 1981, p. 440, pl. 1, figs. 2a and 2b.

**Remarks.** The species figured differs from *W. carpathicum* by its more pronounced pores and by the tiny rounded spines.

*Williriedellum gilkeyi* Dumitrica
(Pl. 8, Figs. 10, 13, and 14)

*Williriedellum*(?) *gilkeyi* Dumitrica, 1972, p. 841, pl. 3, figs. 4 and 6, and pl. 4, figs. 1 and 2.
*Williriedellum gilkeyi* Dumitrica—Schaaf, 1981, p. 440, pl. 2, figs. 6a–6c.

**Range and occurrences.** Recorded from approximately Hauterivian to Albian in the North Atlantic and Pacific.

*Williriedellum peterschmittae* Schaaf
(Pl. 8, Fig. 8)

*Williriedellum peterschmittae* Schaaf, 1981, p. 440, pl. 1, figs. 3a and 3b, and pl. 9, figs. 3a and 3b.
*Hemicryptocapsa*(?) *nodosa* (Tan Sin Hok)—Dumitrica, 1972, p. 841, pl. 1, fig. 6, and pl. 2, figs. 1 and 2.

**Range and occurrences.** Recorded from Hauterivian/Barremian strata in the Pacific and North Atlantic.

*Williriedellum* sp. aff. *W. peterschmittae* Schaaf
(Pl. 8, Fig. 9)

**Remarks.** This species differs from *W. peterschmittae* by the lack of a central pore on each node.

*Williriedellum* sp. A
(Pl. 8, Fig. 12)

**Remarks.** This species differs from *W. peterschmittae* by the lack of a central pore on each node and the large sutural pore, which is closed by bridge growth.

*Xitus alievi* (Foreman)
(Pl. 7, Fig. 2)

*Xitus alievi* (Foreman)—Schaaf, 1981, p. 440, pl. 5, figs. 4a and 4b, and pl. 19, figs. 1a, 1b, 8a, and 8b.
*Dictyomitra alievi* Foreman, 1973b, p. 263, pl. 9, fig. 10, and pl. 16, fig. 4; Foreman, 1975, p. 613, pl. 2H, figs. 8 and 9, and pl. 7, fig. 2.

**Range.** Uppermost Valanginian to middle Aptian (upper Albian if *X. plenus* is a junior synonym of *X. alievi*).
**Occurrences.** Pacific, California, North Atlantic, and southern Europe.

*Xitus* sp. cf. *Xitus alievi* (Foreman)
(Pl. 7, Fig. 3)

**Remarks.** This species differs from *X. alievi* by the decreased width of the distal segments.

*Xitus plenus* Pessagno
(Pl. 3, Fig. 22)

*Xitus plenus* Pessagno, 1977b, p. 55, pl. 9, figs. 15, 21, 22, and 26, and pl. 12, fig. 15.

**Remarks.** The form figured complies with the definition given by Pessagno (1977b) to discriminate *X. plenus* Pessagno from other *Xitidae*; however, Sanfillippo and Riedel (1985) describe *X. plenus* as a younger synonym of *X. alievi*, which implies that the latter form ranges into the upper Albian.
**Range and occurrences.** Upper Albian of California and northeast Atlantic.

*Xitus spicularius* (Aliev)
(Pl. 3, Fig. 19, and Pl. 7, Fig. 1)

*Xitus spicularius* (Aliev)—Pessagno, 1977b, p. 56, pl. 9, fig. 7, and pl. 10, fig. 5; Schaaf, 1981, p. 440–441, pl. 4, fig. 11, pl. 5, figs. 12a and 12b, and pl. 19, figs. 2a and 2b.
?*Dictyomitra spicularia* Aliev, 1961, p. 34, pl. 2, figs. 1 and 2; Aliev, 1965, p. 39, pl. 6, fig. 9.
*Dictyomitra* sp. cf. *D. spicularia* Aliev—Foreman, 1973b, p. 264, pl. 9, figs. 8 and 9; Nakaseko et al., 1979, pl. 3, fig. 5.

**Range.** Berriasian to Cenomanian.
**Occurrences.** Recorded worldwide.

*Xitus*(?) sp.
(Pl. 3, Figs. 20 and 20A)

**Remarks.** This species, which is numerous in the interval, is tentatively assigned to *Xitus* Pessagno because of its morphological similarities, although the double layer structure is not obvious.

*Zhamoidellum ornatum*(?) (Zhamoida)
(Pl. 8, Fig. 15)

*Zhamoidellum ornatum* (Zhamoida)—Foreman, 1975, p. 618, pl. 21, figs. 15 and 16.
*Tricolocapsa ornata* Zhamoida, 1972, p. 117, pl. 4, fig. 2, and pl. 5, fig. 5.
*Conosphaera sphaeraconus* Rüst—Heitzer, 1930, p. 386, pl. 27, fig. 4.

**Remarks.** The type specimen is recorded from Jurassic strata only.

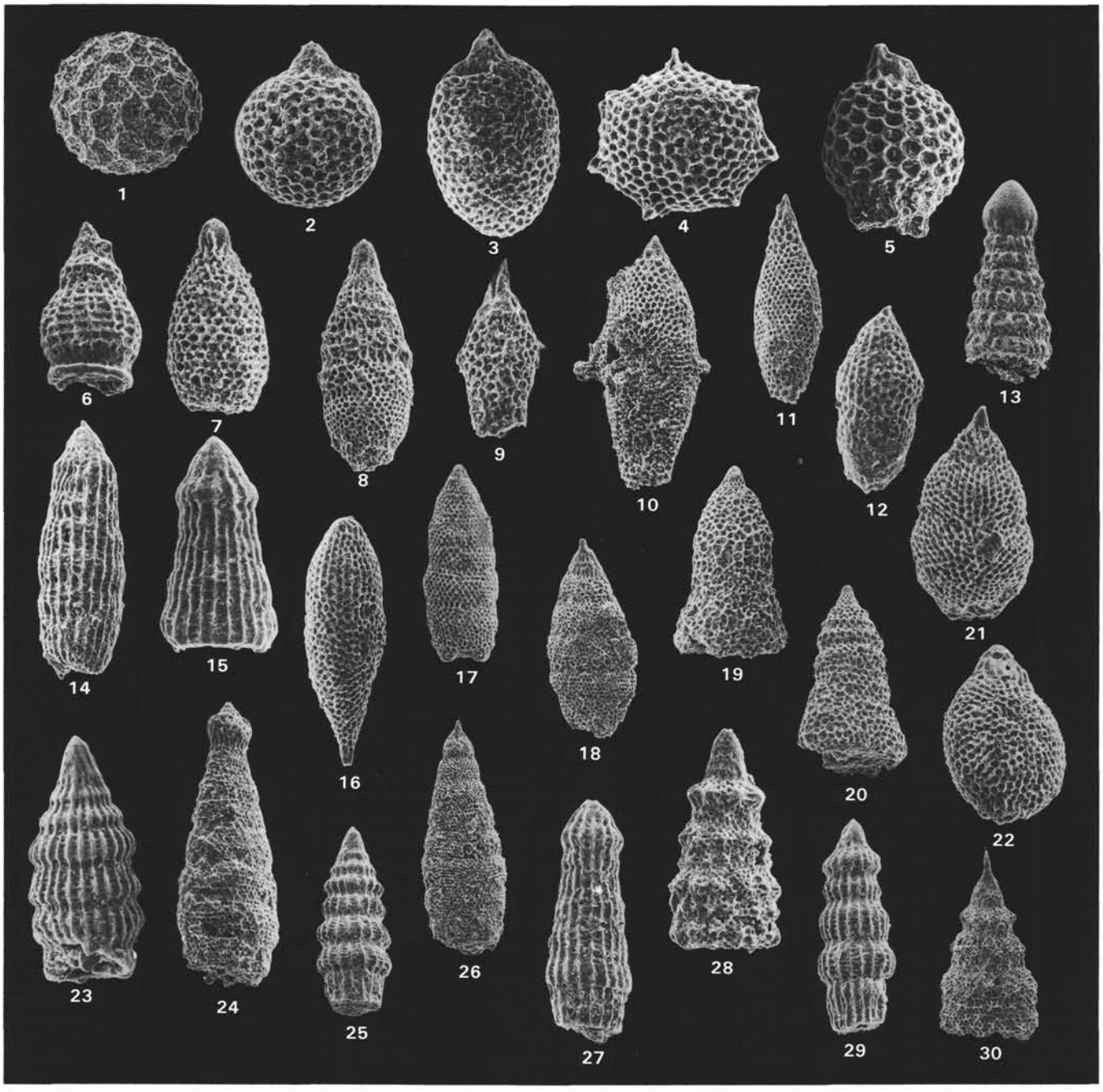


Plate 1. SEM micrographs. Specimens figured are characteristic of the Cenomanian/Turonian Boundary Event and the Campanian biosiliceous interval. All specimens are replaced by clinoptilolite and/or opal-CT. **1.** *Hemicryptocapsa polyhedra* Dumitrica. Sample 603B-33-3, 90–93 cm. **2.** *Cryptamphorella conara* Foreman. Sample 603B-26-3, 90–93 cm. **3.** *Cryptamphorella macropora* Dumitrica. Sample 603B-26-1, 90–93 cm. **4.** *Heliocryptocapsa* sp. A. Sample 603B-26-2, 90–93 cm. **5.** *Rhopalosyringium* sp. A. Sample 603B-26-2, 90–93 cm. **6.** *Theocampe tina* (Foreman). Sample 603B-26-1, 90–93 cm. **7.** *Amphipyndax metacryst* (Tan Sin Hok). Sample 603B-26-1, 90–93 cm. **8.** *Amphipyndax pseudoconulus*. Sample 603B-26-3, 90–93 cm. **9.** *Eucyrtidium*(?) sp. A. Sample 603B-26-1, 90–93 cm. **10.** *Eucyrtidium*(?) sp. B. Sample 603B-26-3, 90–93 cm. **11.** *Eucyrtidium*(?) sp. C. Sample 603B-26-3, 90–93 cm. **12.** *Eucyrtidium*(?) sp. D. Section 603B-25, CC. **13.** *Pseudodictyomitra pseudomacrocephala* (Squinabol). Sample 603B-33-3, 90–93 cm. **14.** *Archaeodictyomitra* sp. cf. *A. lamellicostata* (Foreman). Sample 603B-26-3, 90–93 cm. **15.** *Thanarla*(?) sp. A aff. *T. veneta*. Sample 603B-26-2, 90–93 cm. **16.** *Eastonerius* sp. A. Sample 603B-26-2, 90–93 cm. **17.** *Stichomitra* sp. Sample 603B-26-3, 90–93 cm. **18.** Gen. et sp. indet. 1. Sample 603B-26-3, 90–93 cm. **19.** *Obesacapsula*(?) sp. A. Sample 603B-26-1, 90–93 cm. **20.** *Novixitus*(?) sp. D. Sample 603B-26-3, 90–93 cm. **21.** Gen. et sp. indet. 2. Sample 603B-26-3, 90–93 cm. **22.** Gen. et sp. indet. 3. Sample 603B-26-1, 90–93 cm. **23.** *Dictyomitra* cf. *D. formosa* Squinabol. Sample 603B-33-3, 90–93 cm. **24.** Gen. et sp. indet. 4. Sample 603B-26-3, 90–93 cm. **25.** *Dictyomitra formosa* Squinabol. Sample 603B-26-3, 90–93 cm. **26.** Gen. et sp. indet. 5. Sample 603B-26-3, 90–93 cm. **27.** *Thanarla*(?) sp. aff. *T. veneta*. Sample 603B-25, CC. **28.** *Novixitus* sp. A. Sample 603B-26-3, 90–93 cm. **29.** *Dictyomitra koslovae* Foreman. Sample 603B-26-3, 90–93 cm. **30.** *Novixitus* sp. B. Sample 603B-26-3, 90–93 cm.

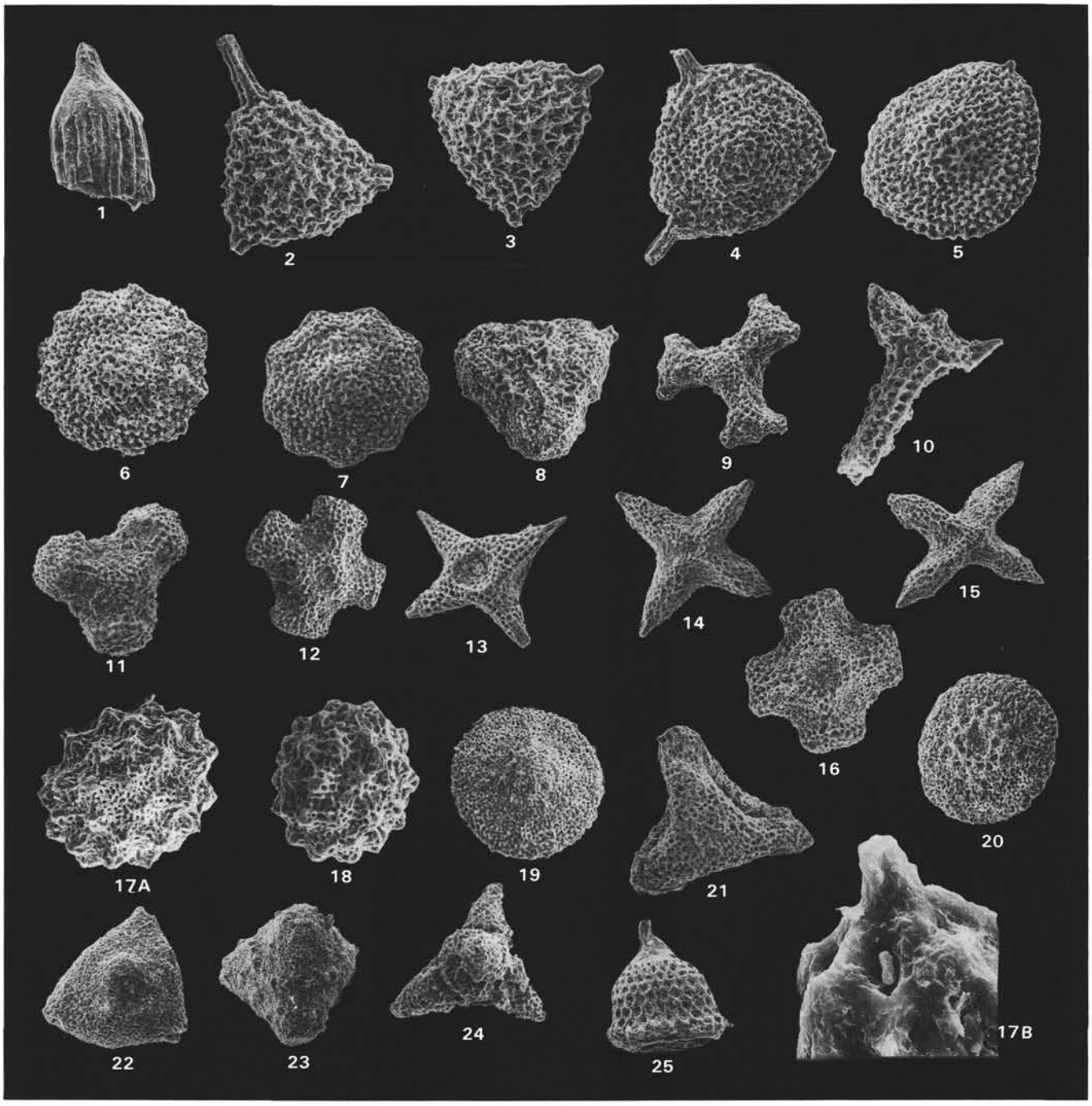


Plate 2. SEM micrographs. Specimens figured are characteristic of the Cenomanian/Turonian Boundary Event and the Campanian biosiliceous interval. **1.** *Afens liriodes* Riedel and Sanfilippo. Sample 603B-26-1, 90–93 cm. **2.** *Alievium superbum* (Squinabol). Sample 603B-33-3, 90–93 cm. **3.** *Alievium gallowayi* (White). Sample 603B-26-3, 90–93 cm. **4.** *Pseudoaulophacus putahensis* Pessagno. Sample 603B-33-3, 90–93 cm. **5.** *Pseudoaulophacus floresensis* Pessagno. Sample 603B-26-3, 90–93 cm. **6.** *Pseudoaulophacus lenticulatus* (White). Sample 603B-26-3, 90–93 cm. **7.** *Pseudoaulophacus parguerensis* Pessagno. Sample 603B-26-1, 90–93 cm. **8.** *Pseudoaulophacus* sp. A. Sample 603B-26-3, 90–93 cm. **9.** *Patulibracchium californiaensis* Pessagno. Sample 603B-26-3, 90–93 cm. **10.** *Halesium quadratum* Pessagno (fragment with a single ray is preserved), Sample 603B-33-3, 90–93 cm. **11.** *Patulibracchium petroleumensis* Pessagno. Sample 603B-26-3, 90–93 cm. **12.** *Crucella*(?) sp. A. Sample 603B-26-2, 90–93 cm. **13.** *Crucella cachensis* Pessagno. Sample 603B-33-3, 90–93 cm. **14.** *Crucella espartoensis* Pessagno. Sample 603B-26-3, 90–93 cm. **15.** *Crucella* sp. B. Sample 603B-26-2, 90–93 cm. **16.** *Crucella*(?) sp. A. Sample 603B-26-3, 90–93 cm. **17.** *Conocaryomma* sp. cf. *C. universa* (Pessagno). Sample 603B-26-3, 90–93 cm. Note (?)triradiate spine in Figure 17B. **18.** *Conocaryomma universa* (Pessagno). Sample 603B-26-2, 90–93 cm. **19 and 20.** *Patellula verteroensis* (Pessagno), (convex side and plane side, respectively). Sample 603B-26-3, 90–93 cm. **21.** *Cavaspongia californiaensis* Pessagno. Sample 603B-33-3, 90–93 cm. **22.** *Dumitricaia maxwellensis* Pessagno. Sample 603B-33-3, 90–93 cm. **23.** *Pyramispongia glascockensis* Pessagno. Sample 603B-33-3, 90–93 cm. **24.** *Clathropyrgus titthium* Riedel and Sanfilippo. Sample 603B-25, CC. **25.** *Neosciadiocapsa diabloensis* Pessagno. Sample 603B-26-3, 90–93 cm.

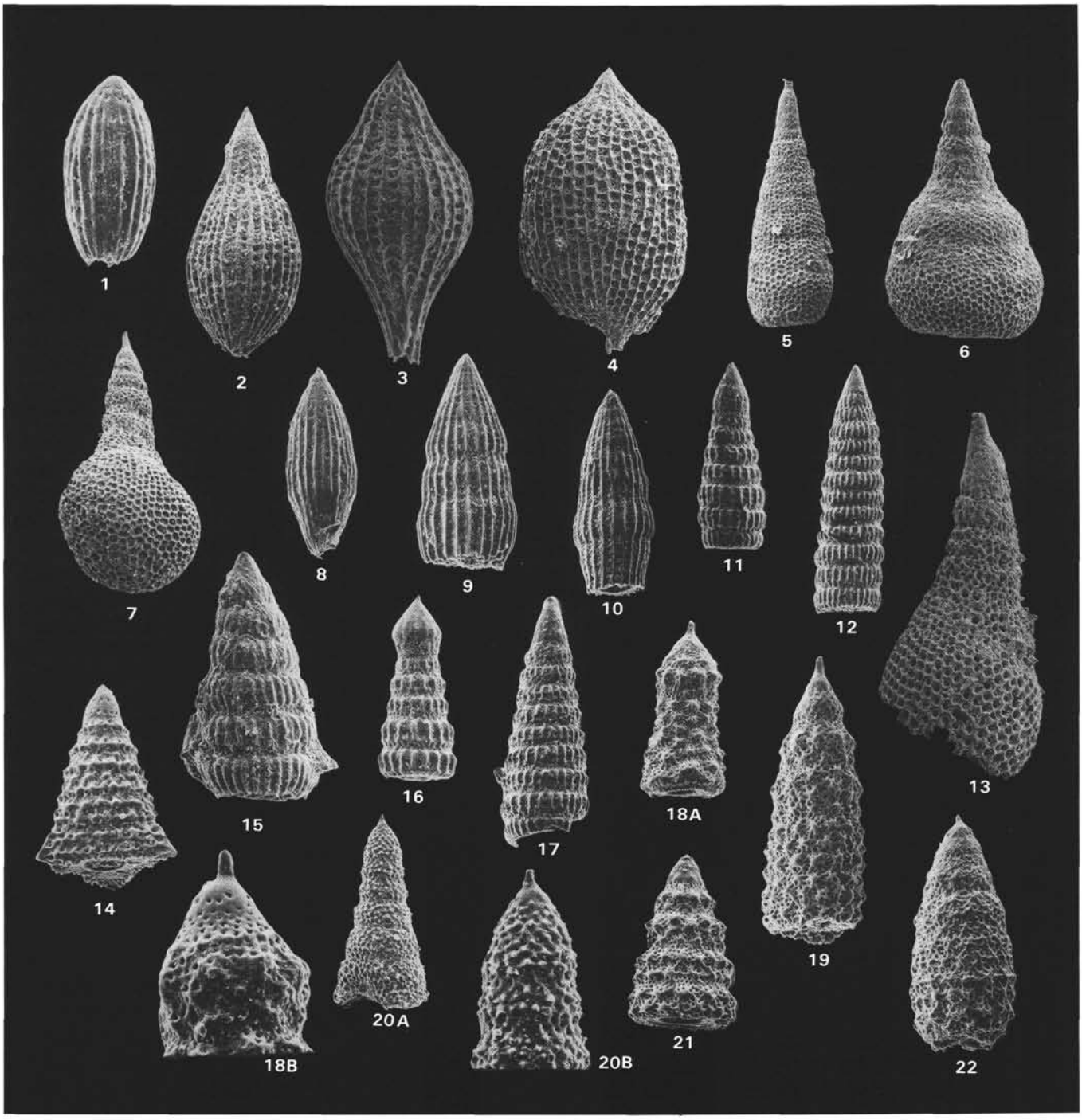


Plate 3. SEM micrographs. Specimens are characteristic of the Albian. If not otherwise indicated, specimens are from Sample 398D-63-4, 135–139 cm, and are replaced by opal-CT. **1.** *Mita* sp. A. **2.** *Mita gracilis* (Squinabol). **3.** *Mita* sp. B. **4.** *Mita* sp. C. From bulk sample from Core 398D-82. **5.** *Cyrtocapsa* (?*Sethocapsa*) *perspicua* Squinabol (note parallel pore rows). Pyrite replacement. Sample 398D-100-3, 148–150 cm. **6 and 7.** *Stichocapsa* (?*Sethocapsa*) *euganea* Squinabol. Figure 6 from Sample 398D-99-6, 120–124 cm; Figure 7, replaced by opal-CT, from Core 398D-82 bulk sample. **8.** *Archaeodictyomitra lacrimula* (Foreman). **9.** *Archaeodictyomitra simplex* Pessagno. **10.** *Archaeodictyomitra* sp. A. **11.** *Pseudodictyomitra* sp. cf. *P. pseudomacrocephala* (Squinabol) (?*P. sagitafera* Aliev). **12.** *Pseudodictyomitra lodogaensis* Pessagno (*P.* sp. B, Taketani 1982). **13.** *Cyrtocapsa* (?*Sethocapsa*) *perspicua* Squinabol (note parallel pore rows). Opal-CT replacement. Sample 103-641C-13R-5, 92–95 cm. **14.** *Crolanium* sp. cf. *C. triquetrum* Pessagno. **15.** *Pseudodictyomitra vestalensis* Pessagno. Sample 398D-97-4, 61–65 cm. **16.** *Pseudodictyomitra pseudomacrocephala* (Squinabol). **17.** *Pseudodictyomitra pentacolaensis* Pessagno. **18A.** *Novixitus* sp. C. **18B.** Detail of Figure 18A with proximal segments. Note the morphological similarity with *P. pseudomacrocephala*. **19.** *Xitus spicularius* Pessagno, Sample 398D-97-4, 45–50 cm. **20A.** *Xitus*(?) sp. A. **20B.** Detail of Figure 20A cephalis, thorax, abdomen, and proximal early postabdominal chambers. **21.** *Novixitus mclaughlini* Pessagno. **22.** *Xitus plenus* Pessagno.

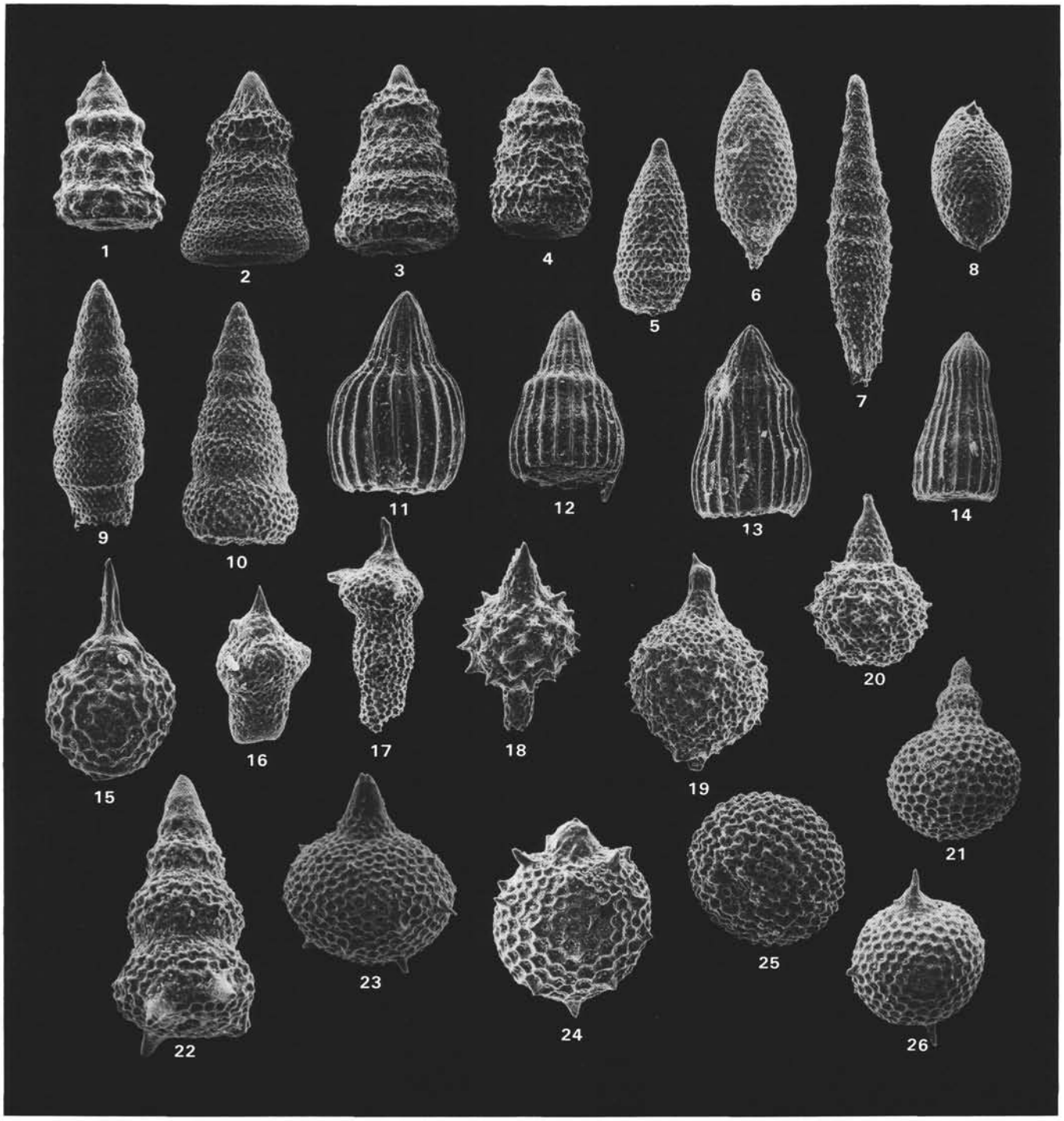


Plate 4. SEM micrographs. Specimens are characteristic of the Albian. If not otherwise indicated, specimens are from Sample 398D-63-4, 135–139 cm, and are replaced by opal-CT. **1.** *Novixitus weyli* Schmidt-Effing. **2.** *Theoconus coronatus* Squinabol. **3 and 4.** *Theoconus* sp. A aff. *T. coronatus* Squinabol. **5.** *Amphipyndax metacryst* (Tan Sin Hok). **6.** *Amphipyndax*(?) sp. **7.** *Eucyrtis* sp. A. **8.** *Theocapsomma ancus* (Foreman). **9.** *Stichomitra* sp. cf. *S. communis* Squinabol. **10.** *Stichomitra communis* Squinabol. **11.** *Thanarla elegantissima* (Cita). **12.** *Thanarla* sp. A. **13 and 14.** *Thanarla veneta* (Squinabol). **15.** *Rhopalosyringium majuroensis* Schaaf. **16.** *Rhopalosyringium* sp. B. **17.** *Rhopalosyringium* sp. C. **18.** *Eusyringium spinosum* Squinabol. **19.** *Eusyringium*(?) *formanae* Taketani. **20.** *Eusyringium* sp. cf. *E. spinosum* Squinabol. **21.** *Squinabollum fossilis* (Squinabol). **22.** *Stichomitra*(?) sp. B, note spines at the last chamber. **23.** *Sethocapsa* sp. cf. *S. simplex* Taketani, numerous in this interval. **24.** Gen. et sp. indet. 6, numerous in this interval. **25.** *Holocryptocanium* sp. A, numerous in this interval. **26.** Gen. et sp. indet. 7, numerous in this interval.

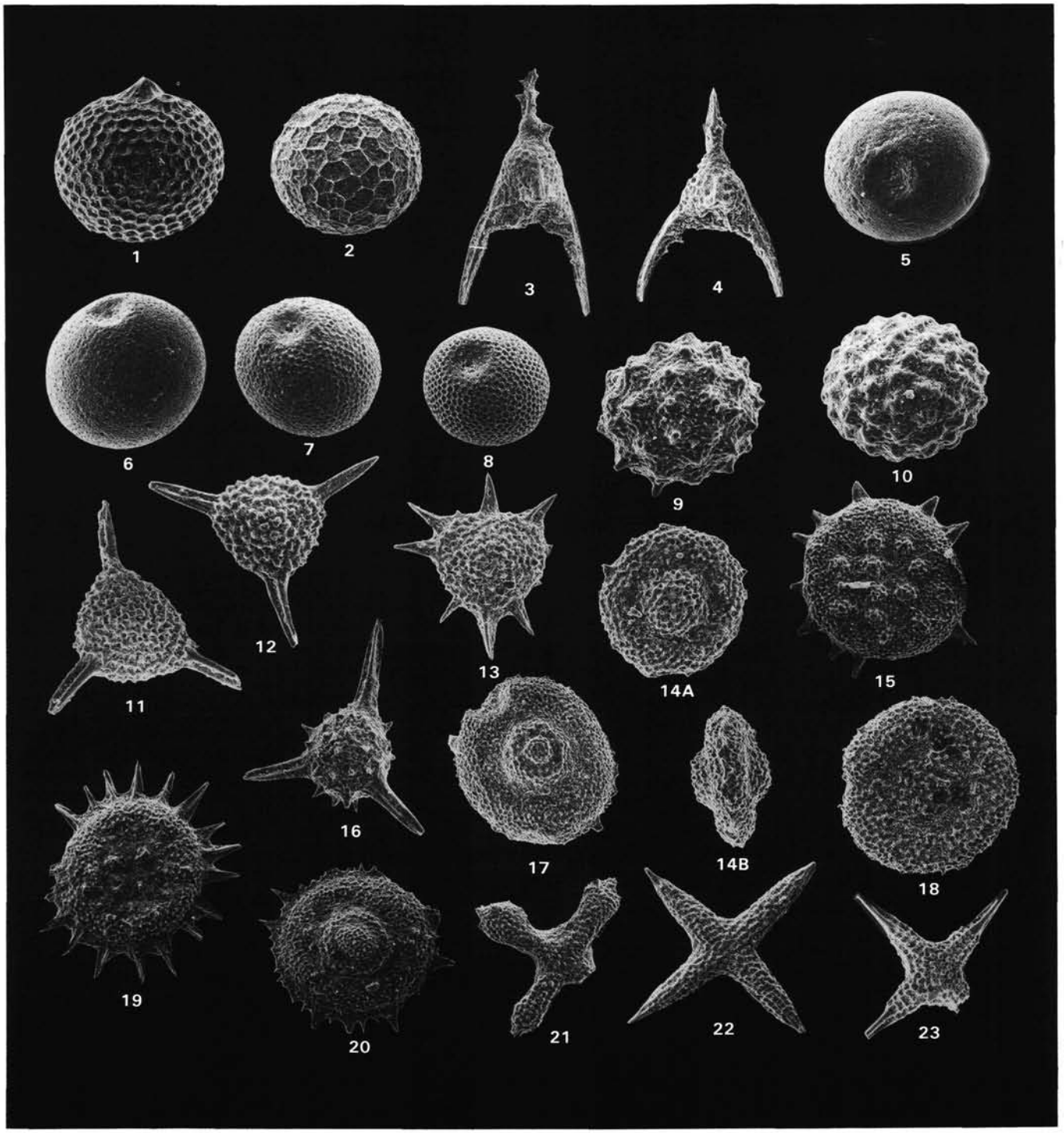


Plate 5. SEM micrographs. Specimens are characteristic of the Albian. If not otherwise indicated, specimens are from Sample 398D-63-4, 135–139 cm, and are replaced by opal-CT. **1.** *Cryptamphorella conara* (Foreman), note prominent sutural pore. **2.** *Hemicryptocapsa* sp. cf. *H. polyhedra* Dumitrica. **3.** *Napora praespinifera* Pessagno. Sample 398D-63-4, 42–46 cm. **4.** *Napora durhami* Pessagno, Sample 398D-84-1, 30–34 cm. **5–8.** *Holocryptocanium barbui* Dumitrica lineage. **9.** *Conocaryomma lipmanae* Pessagno. **10.** *Conocaryomma* sp. aff. *C. lipmanae* (Pessagno). **11.** *Alievium superbum* (Squinabol) "Cenomanian" form. Sample 398D-56-3, 57–61 cm. **12.** *Alievium* sp. A. **13.** *Pseudoaulophacus* sp. B, numerous in this interval. **14.** *Pseudoaulophacus*(?) sp. D. 14A. Lateral view. **15.** *Godia*(?) sp. C. **16.** *Alievium* sp. B. **17.** *Godia*(?) sp. B. **18.** *Orbiculiforma railensis* Pessagno. **19.** *Patellula*(?) sp. B. **20.** *Godia*(?) sp. A. **21.** *Crucella* sp. C. **22.** *Crucella messinae*. **23.** *Crucella* sp. D.

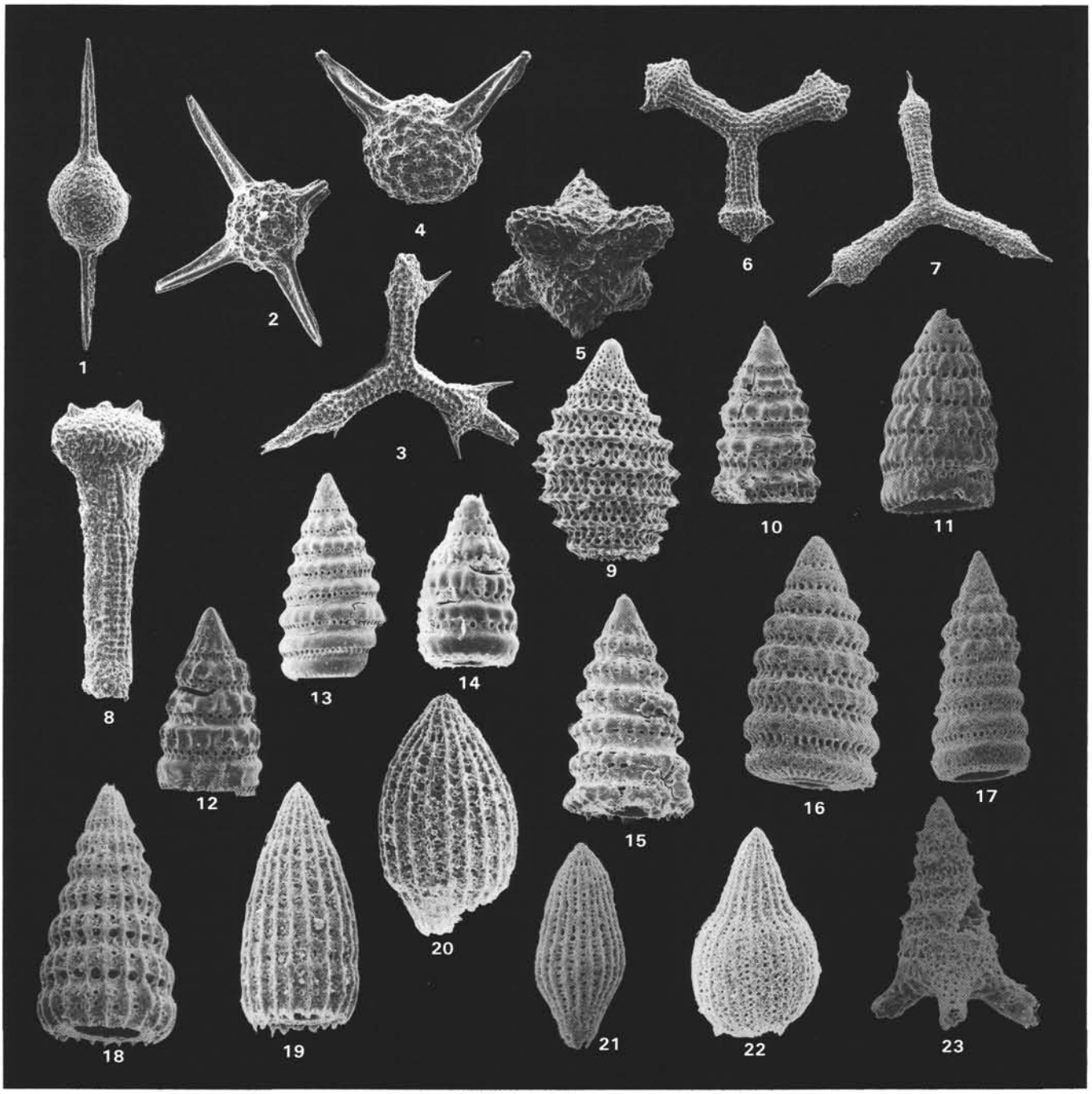


Plate 6. SEM micrographs. Specimens are characteristic of the Albian or upper Hauterivian to lower Aptian. If not otherwise indicated, specimens are from Sample 398D-63-4, 135–139 cm, and are replaced by opal-CT. **1.** *Archaeospongoprunum* sp. cf. *A. tehamaensis* Pessagno, Sample 398D-63-4, 42–46 cm. **2.** *Acaeniotyle* sp. A, note four spines. **3.** *Halesium sexangulum* Pessagno. **4.** *Acaeniotyle* sp. cf. *A. diaphorogona*, note twisted outline of spines. **5.** *Hexapyramis pantanellii* Squinabol. **6.** *Patulibracchium* sp. cf. *P. davisi* Pessagno. **7.** *Paronaella* sp. A, Sample 398D-84-1, 30–34 cm. **8.** *Paronaella* sp. B, numerous in this interval, always fragmented. **9.** *Parvicingula boesii* (Parona). Pyrite replacement. Sample 103-640A-3R-3, 138–142 cm. **10.** *Parvicingula*? sp. Pyrite replacement. Sample 103-640A-3R-3, 138–142 cm. **11.** *Pseudodictyomitra leptoconica* (Foreman). Pyrite replacement. Sample 103-640A-3R-3, 138–142 cm. **12.** *Pseudodictyomitra carpatica* (Lozyniak). Pyrite preservation. Sample 103-640A-3R-3, 138–142 cm. **13, 14, and 17.** *Pseudodictyomitra lilyae* (Tan Sin Hok). Pyrite replacement. Sample 103-640A-3R-3, 138–142 cm. **15.** *Archaeodictyomitra puga* Schaaf. Pyrite replacement. Sample 103-640A-3R-3, 138–142 cm. **16.** *Pseudodictyomitra* sp., transitional form between *P. leptoconica* (Lozyniak) and *P. lilyae* (Tan Sin Hok). **18.** *Archaeodictyomitra* sp. cf. *A. puga* Schaaf. Sample 103-638B-21R-5, 52–54 cm. **19.** *Archaeodictyomitra vulgaris* Pessagno. Sample 103-638B-21R-5, 52–54 cm. **20.** *Thanarla conica* (Aliev). Sample 103-638B-21R-5, 52–54 cm. **21.** *Mita* sp. C. Sample 103-638B-21R-5, 52–54 cm. **22.** *Mita*(?) sp. D. Sample 103-638B-21R-5, 52–54 cm. **23.** *Crolanium pythiae* Schaaf. Sample 103-638B-21R-5, 52–54 cm.

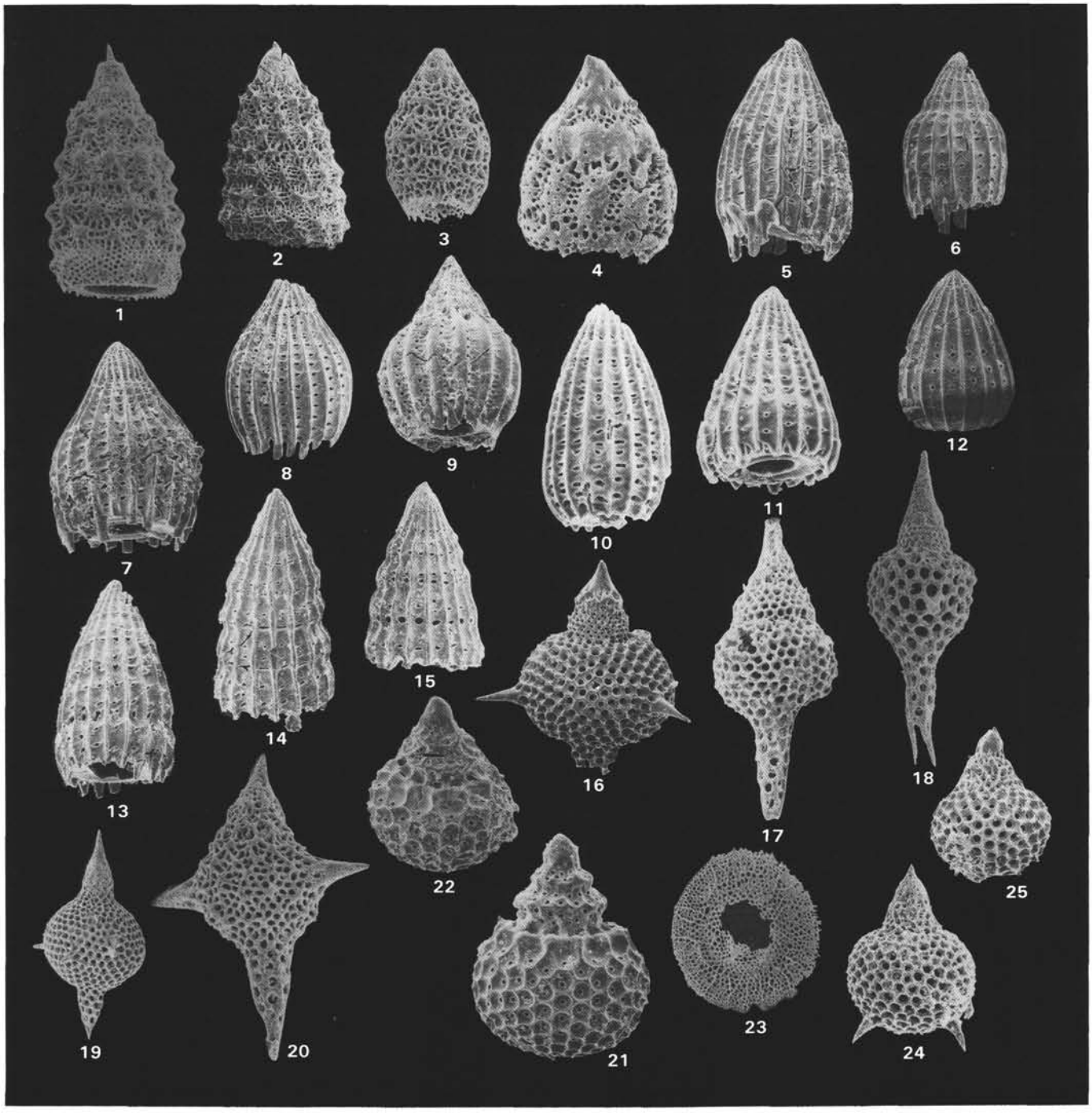


Plate 7. SEM micrographs. Specimens are characteristic of the upper Hauterivian to lower Aptian. If not otherwise indicated, specimens are from Sample 103-640A-3R-3, 138–142 cm, and are replaced by pyrite. **1.** *Xitus spicularius* (Aliev). **2.** *Xitus alievi* (Foreman). **3.** *Xitus* sp. A. cf. *Xitus alievi* (Foreman). **4.** Gen. et sp. indet. 8 (gen. et sp. indet. in Schaaf, 1981, pl. 6, figs. a and b). **5.** *Thanarla conica* (Aliev). **6.** *Thanarla* sp. C. **7 and 8.** *Thanarla*(?) sp. A aff. *T. conica* (Aliev). **9.** *Thanarla pulchra* (Squinabol). **10.** *Archaeodictyomitra*(?) sp. B. **11.** *Thanarla conica* (Aliev). **12.** *Thanarla*(?) sp. B aff. *T. conica* (Aliev). **13.** *Archaeodictyomitra* cf. *A. vulgaris* Pessagno. The bladelike feet are actually a terminal chamber fragment. The test differs from *A. vulgaris* by the two rows of pores on each segment. **14.** *Archaeodictyomitra pseudoscalaris* (Tan Sin Hok). **15.** *Archaeodictyomitra* sp. cf. *A. puga* Schaaf. **16.** *Podobursa triacantha* (Fischli). **17.** *Podobursa tricola* Foreman. Replaced by opal-CT. Sample 103-638-21R-5, 52–54 cm. **18.** *Podobursa* sp. A. Replaced by opal-CT. Sample 103-638-21R-5, 52–54 cm. **19.** *Podobursa triacantha* (Fischli). Replaced by opal-CT. Sample 103-638-21R-5, 52–54 cm. **20.** *Dibolachras tytthopora* Foreman. Replaced by opal-CT. Sample 103-638-21R-5, 52–54 cm. **21.** *Sethocapsa uterculus* (Parona). **22.** *Sethocapsa* cf. *S. uterculus* (Parona). **23.** *Neosciadiocapsidae* gen. et sp. indet. Replaced by opal-CT. Sample 103-638-21R-5, 52–54 cm. **24.** *Sethocapsa*(?) sp. A. Replaced by opal-CT. Sample 103-638-21R-5, 52–54 cm. **25.** *Siphocampium*(?) *davidi* Tan Sin Hok. Replaced by opal-CT. Sample 103-638-21R-5, 52–54 cm.

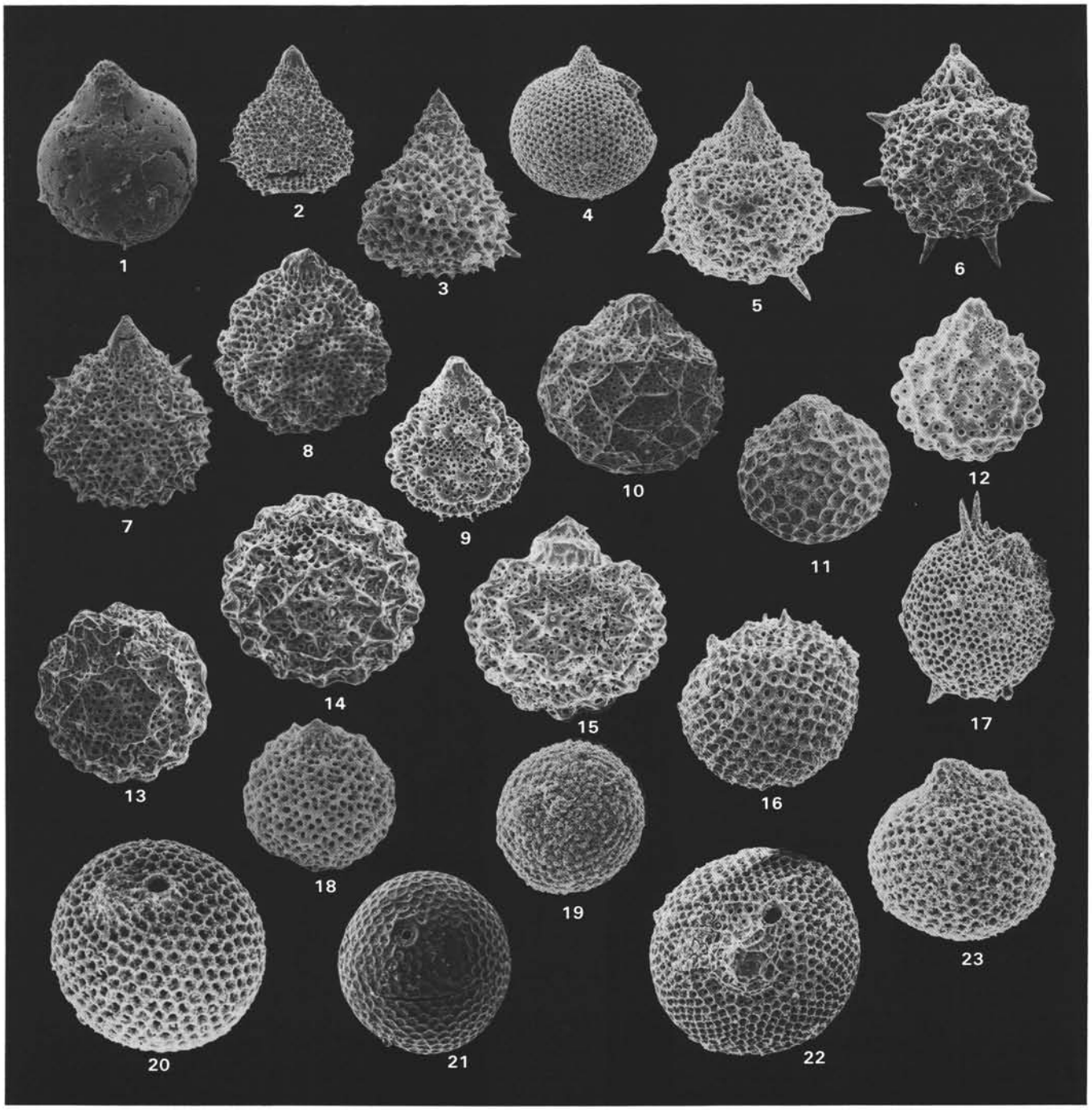


Plate 8. SEM micrographs. Specimens are characteristic of the upper Hauterivian to lower Aptian. If not otherwise indicated, specimens are from Sample 103-640A-3R-3, 138–142 cm, and are replaced by pyrite. **1.** *Theocorys renzae* Schaaf. **2 and 3.** *Cyrtocapsa* sp. cf. *C. grutterinki* Tan Sin Hok. **4.** *Sethocapsa orca* Foreman. Replaced by opal-CT. Sample 103-638-21R-5, 52–54 cm. **5–7.** *Sethocapsa trachyostraca* Foreman (Figure 5 has opal-CT replacement; Sample 103-638-21R-5, 52–54 cm). **8.** *Williriedellum peterschmittae* Schaaf (lateral view). **9.** *Williriedellum* sp. aff. *W. peterschmittae* Schaaf, this species is closely related to *W. peterschmittae*, but lacks the central pore on each node. **10.** *Williriedellum gilkeyi* Dumitrica. **11.** *Williriedellum* sp. aff. *W. carpathicum* Dumitrica. **12.** *Williriedellum* sp. A. **13.** *Williriedellum gilkeyi* Dumitrica, apical view—note prominent sutural pore. **14.** *Williriedellum gilkeyi* Dumitrica, antapical view—the aperture is not visible. **15.** *Zhamoidellum ornatum* (Zhamoida). **16.** *Cryptothoracic Nassellaria*, gen. et sp. indet. 14. Note spines surrounding sunken cephalis. **17.** Cryptocephalic and cryptothoracic Nassellaria, gen. et sp. indet. 8. Pyrite replacement. Sample 103-638B-21R-5, 52–54 cm. **18.** *Hemicryptocapsa*(?) sp. A. Replacement by opal-CT. Sample 103-638B-21R-5, 52–54 cm. **19.** Gen. et sp. indet. 9 aff. *Holocryptocanium* sp. A. Replaced by opal-CT. Sample 103-638B-21R-5, 52–54 cm. **20.** *Cryptamphorella* sp. cf. *C. conara* (Foreman). Replaced by opal-CT. Sample 103-638B-21R-5, 52–54 cm. **21.** *Holocryptocanium* sp. C, numerous in this interval. **22.** *Cryptamphorella* sp. B, apical view showing prominent sutural pore. **23.** *Cryptamphorella dumitricai* Schaaf. Replaced by opal-CT. Sample 103-638B-21R-5, 52–54 cm.

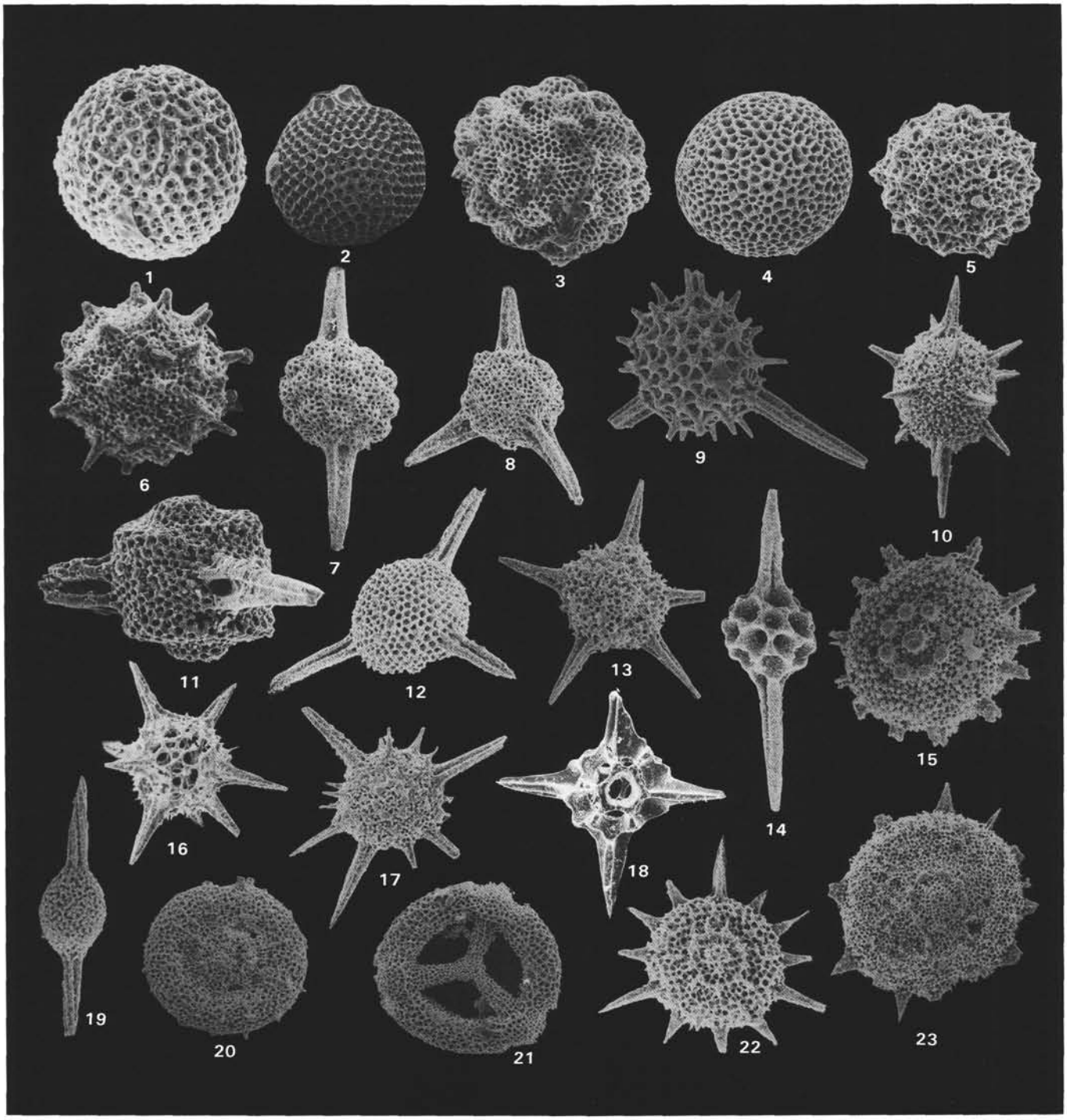


Plate 9. SEM micrographs. Specimens are characteristic of the upper Hauterivian lower Aptian. If not otherwise indicated, specimens are from Sample 103-638B-21R-5, 52–54 cm, and replaced by opal-CT. **1.** *Holocryptocanium* sp. B. **2.** *Cryptamphorella* sp. A, lateral view showing the prominent sutural pore. Pyrite replacement. Sample 103-640A-3R-3, 138–142 cm. **3.** *Conosphaera tuberosa* Tan Sin Hok. **4.** *Orosphaerid* gen. et sp. indet. 10. **5.** *Conocaryomma* sp. A (cf. *Praeconocaryomma* sp. A in Pessagno 1977b). **6.** *Conocaryomma* sp. B. **7.** *Acaeniotyle umbilicata* (Rüst). **8.** *Acaeniotyle diaphorogona* Foreman. **9.** *Alievium helenae* Schaaf. **10.** Spumellarids gen. et sp. indet. 11, numerous in this interval. **11.** *Triactoma hybum* Foreman. Pyrite replacement. Sample 103-641C- R, 38–41 cm. **12.** *Triactoma echoides* Foreman. **13.** Spumellarids gen. et sp. indet. 11, numerous in this interval. **14.** *Pantanellium lanceola* (Parona). **15.** *Godia*(?) sp. D. **16.** *Hexastylurus magnificus* (Squinabol). **17.** *Pseudoaulophacus*(?) sp. C. **18.** *Cecrops septemporata* (Parona). Sample 103-638B-25R, CC. **19.** *Archaeospongoprunum cortinaensis* Pessagno. **20.** *Orbiculiforma railensis* Pessagno. **21.** *Cyclastrum infundibuliforme* Rüst. **22.** *Godia*(?) sp. E. **23.** *Godia*(?) sp. F.

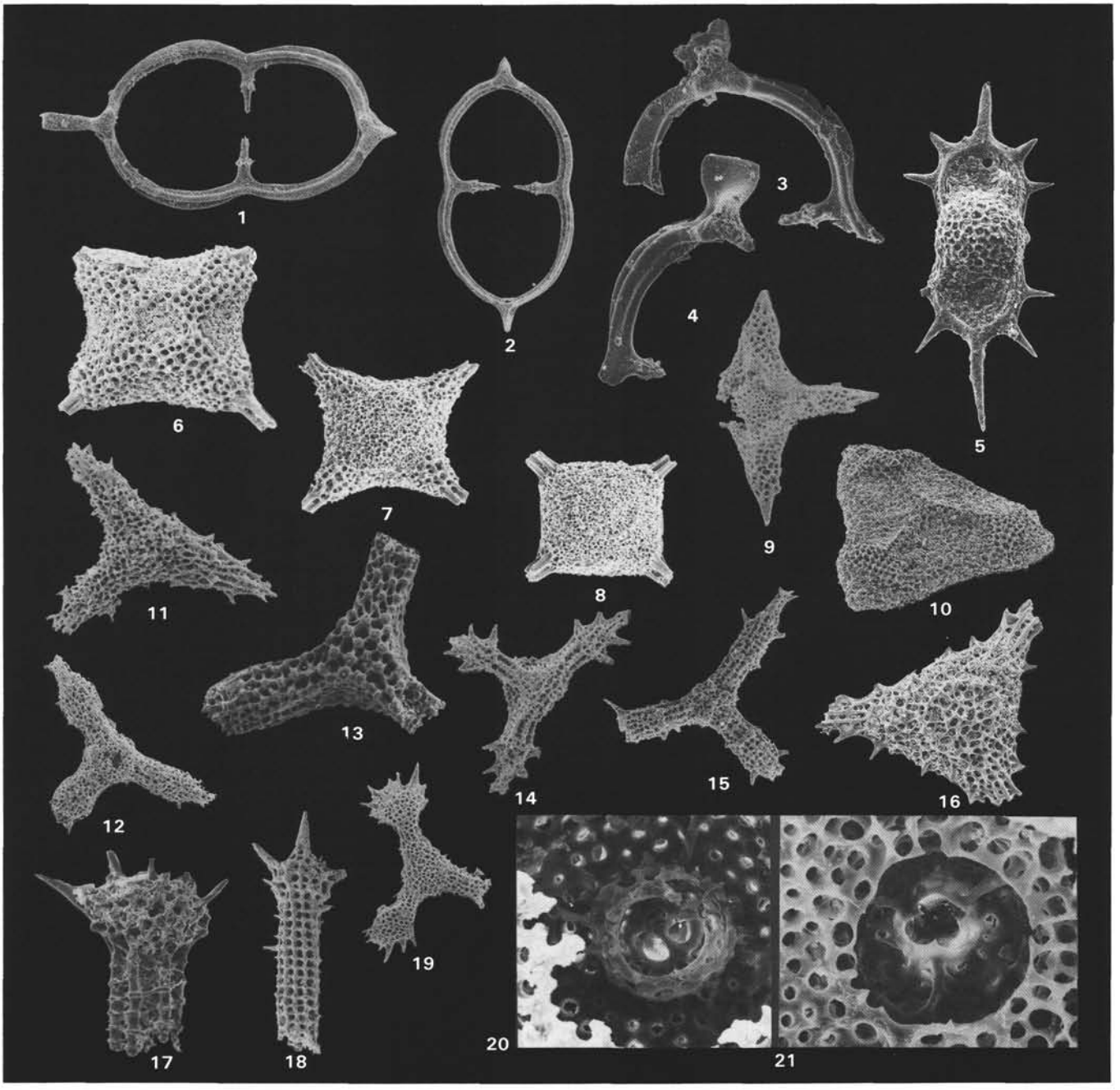


Plate 10. SEM micrographs. Specimens are characteristic of the upper Hauterivian to lower Aptian. **1.** *Acanthocircus* sp. Pyrite replacement. Sample 103-640A-3R-3, 138-142 cm. **2.** *Acanthocircus trizonalis* (Rüst). Pyrite replacement. Sample 103-640A-3R-3, 138-142 cm. **3.** *Acanthocircus dicranacanthos* (Squinabol). Pyrite replacement. Sample 103-640A-3R-3, 138-142 cm. **4.** *Acanthocircus* sp. cf. *A. dicranacanthos* (Squinabol), the characteristic dovelike shape of the spine is not clear. Pyrite replacement. Sample 103-640A-3R-3, 138-142 cm. **5.** *Vitorfusus campbelli* Pessagno. **6.** *Pseudocrucella*(?) sp. C. Pyrite replacement. Sample 103-638B-31R-2, 34-38 cm. **7.** *Pseudocrucella*(?) sp. B, numerous in this interval. Pyrite replacement. Sample 103-638B-31R-2, 34-38 cm. **8.** *Staurocyclia martini* Rüst. Pyrite replacement. Sample 103-638B-31R-2, 34-38 cm. **9.** *Pseudocrucella* sp. A. Replacement by opal-CT. Sample 103-638B-21R-5, 52-54 cm. **10.** *Homoeoparonaella* sp. A. Pyrite replacement. Sample 103-638B-31R-2, 34-38 cm. **11.** Gen. et sp. indet. 11, numerous in this interval (Schaaf, 1981, pl. 10, Figs. 1a and 1b). Replacement by opal-CT. Sample 103-638B-21R-5, 52-54 cm. **12.** *Paronaella* sp. cf. *P. bandyi* Baumgartner. Replacement by opal-CT (note bracchiopyle). Sample 103-638B-21R-5, 52-54 cm. **13.** *Angulobracchia*(?) *portmanni* Baumgartner, numerous if not fragmented. Pyrite replacement. Sample 103-640A-3R-3, 138-142 cm. **14.** *Tritrabs* sp. cf. *T. rhododactylus* (Baumgartner). Replacement by opal-CT. Sample 103-638B-21R-5, 52-54 cm. **15.** *Angulobracchia*(?) *portmanni* Baumgartner, numerous in this interval. Replacement by opal-CT. Sample 103-638B-21R-5, 52-54 cm. **16.** Gen. et sp. indet. 12, numerous in this interval. Pyrite replacement. Sample 103-638B-31R-2, 34-38 cm. **17.** *Tritrabs* sp. (fragment of one ray), fragments of *Tritrabs* sp. are numerous in this interval, but complete specimens have never been found. Pyrite replacement. Sample 103-640A-3R-3, 138-142 cm. **18.** *Hagiastrid* gen. et sp. indet. 13, numerous in this interval, but always fragmented. Replacement by opal-CT. Sample 103-638B-21R-5, 52-54 cm. **19.** *Paronaella* sp. B, numerous in this interval. Replacement by opal-CT. Sample 103-638B-21R-5, 52-54 cm. **20.** Cephalic-thoracic part of *Cryptamphorella dumitricai* Schaaf. Sample 103-638B-21R-5, 52-54 cm. **21.** Cephalic-thoracic part of *Hemicryptocapsa*(?) sp. A. Sample 103-638B-21R-5, 52-54 cm.